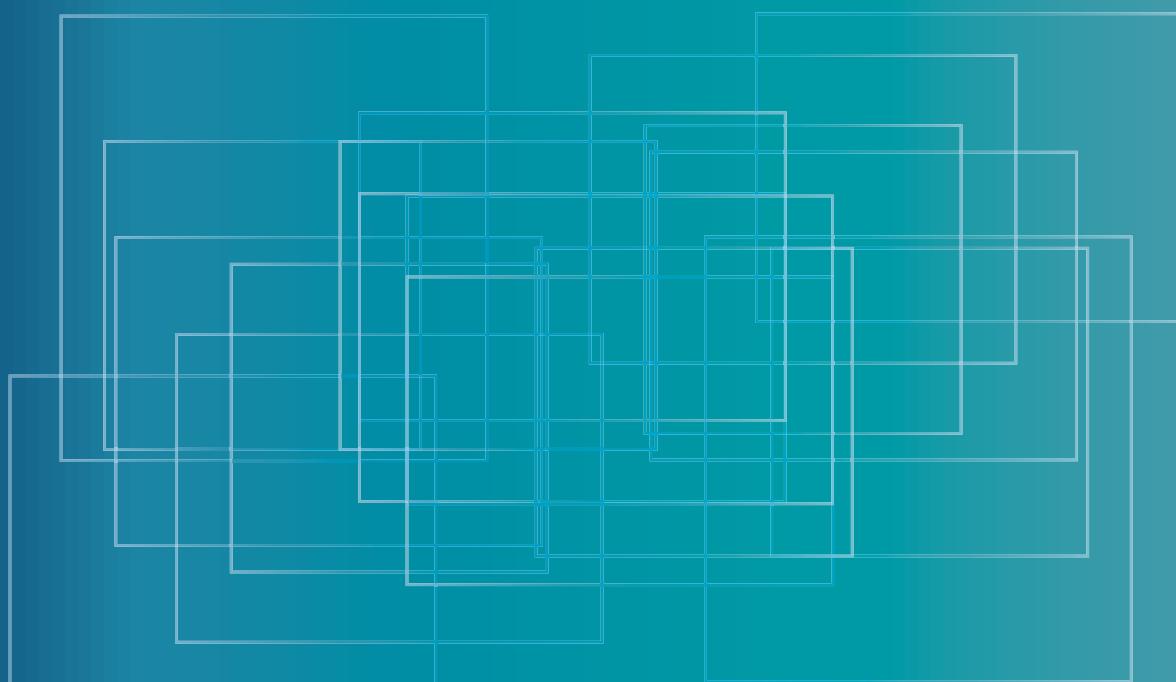


# Cyclotron Produced Radionuclides: Emerging Positron Emitters for Medical Applications: $^{64}\text{Cu}$ and $^{124}\text{I}$



**IAEA**

International Atomic Energy Agency

# IAEA RADIOISOTOPES AND RADIOPHARMACEUTICALS SERIES PUBLICATIONS

One of the main objectives of the IAEA Radioisotope Production and Radiation Technology programme is to enhance the expertise and capability of IAEA Member States in deploying emerging radioisotope products and generators for medical and industrial applications in order to meet national needs as well as to assimilate new developments in radiopharmaceuticals for diagnostic and therapeutic applications. This will ensure local availability of these applications within a framework of quality assurance.

Publications in the IAEA Radioisotopes and Radiopharmaceuticals Series provide information in the areas of: reactor and accelerator produced radioisotopes, generators and sealed sources development/production for medical and industrial uses; radiopharmaceutical sciences, including radiochemistry, radiotracer development, production methods and quality assurance/quality control (QA/QC). The publications have a broad readership and are aimed at meeting the needs of scientists, engineers, researchers, teachers and students, laboratory professionals, and instructors. International experts assist the IAEA Secretariat in drafting and reviewing these publications. Some of the publications in this series may also be endorsed or co-sponsored by international organizations and professional societies active in the relevant fields.

There are two categories of publications: the **IAEA Radioisotopes and Radiopharmaceuticals Series** and **IAEA Radioisotopes and Radiopharmaceuticals Reports**.

## IAEA RADIOISOTOPES AND RADIOPHARMACEUTICALS SERIES

Publications in this category present guidance information or methodologies and analyses of long term validity, for example protocols, guidelines, codes, standards, quality assurance manuals, best practices and high level technological and educational material.

## IAEA RADIOISOTOPES AND RADIOPHARMACEUTICALS REPORTS

In this category, publications complement information published in the IAEA Radioisotopes and Radiopharmaceuticals Series in areas of the: development and production of radioisotopes and generators for medical and industrial applications; and development, production and QA/QC of diagnostic and therapeutic radiopharmaceuticals. These publications include reports on current issues and activities such as technical meetings, the results of IAEA coordinated research projects, interim reports on IAEA projects, and educational material compiled for IAEA training courses dealing with radioisotope and radiopharmaceutical related subjects. In some cases, these reports may provide supporting material relating to publications issued in the IAEA Radioisotopes and Radiopharmaceuticals Series.

All of these publications can be downloaded cost free from the IAEA web site:

<http://www.iaea.org/Publications/index.html>

Further information is available from:

Marketing and Sales Unit  
International Atomic Energy Agency  
Vienna International Centre  
PO Box 100  
1400 Vienna, Austria

Readers are invited to provide feedback to the IAEA on these publications. Information may be provided through the IAEA web site, by mail at the address given above, or by email to:

[Official.Mail@iaea.org](mailto:Official.Mail@iaea.org)

CYCLOTRON PRODUCED  
RADIONUCLIDES:  
EMERGING POSITRON EMITTERS FOR  
MEDICAL APPLICATIONS:  $^{64}\text{Cu}$  AND  $^{124}\text{I}$

The following States are Members of the International Atomic Energy Agency:

AFGHANISTAN	GEORGIA	OMAN
ALBANIA	GERMANY	PAKISTAN
ALGERIA	GHANA	PALAU
ANGOLA	GREECE	PANAMA
ANTIGUA AND BARBUDA	GUATEMALA	PAPUA NEW GUINEA
ARGENTINA	GUYANA	PARAGUAY
ARMENIA	HAITI	PERU
AUSTRALIA	HOLY SEE	PHILIPPINES
AUSTRIA	HONDURAS	POLAND
AZERBAIJAN	HUNGARY	PORTUGAL
BAHAMAS	ICELAND	QATAR
BAHRAIN	INDIA	REPUBLIC OF MOLDOVA
BANGLADESH	INDONESIA	ROMANIA
BARBADOS	IRAN, ISLAMIC REPUBLIC OF	RUSSIAN FEDERATION
BELARUS	IRAQ	RWANDA
BELGIUM	IRELAND	SAN MARINO
BELIZE	ISRAEL	SAUDI ARABIA
BENIN	ITALY	SENEGAL
BOLIVIA, PLURINATIONAL STATE OF	JAMAICA	SERBIA
BOSNIA AND HERZEGOVINA	JAPAN	SEYCHELLES
BOTSWANA	JORDAN	SIERRA LEONE
BRAZIL	KAZAKHSTAN	SINGAPORE
BRUNEI DARUSSALAM	KENYA	SLOVAKIA
BULGARIA	KOREA, REPUBLIC OF	SLOVENIA
BURKINA FASO	KUWAIT	SOUTH AFRICA
BURUNDI	KYRGYZSTAN	SPAIN
CAMBODIA	LAO PEOPLE'S DEMOCRATIC REPUBLIC	SRI LANKA
CAMEROON	LATVIA	SUDAN
CANADA	LEBANON	SWAZILAND
CENTRAL AFRICAN REPUBLIC	LESOTHO	SWEDEN
CHAD	LIBERIA	SWITZERLAND
CHILE	LIBYA	SYRIAN ARAB REPUBLIC
CHINA	LIECHTENSTEIN	TAJIKISTAN
COLOMBIA	LITHUANIA	THAILAND
CONGO	LUXEMBOURG	THE FORMER YUGOSLAV REPUBLIC OF MACEDONIA
COSTA RICA	MADAGASCAR	TOGO
CÔTE D'IVOIRE	MALAWI	TRINIDAD AND TOBAGO
CROATIA	MALAYSIA	TUNISIA
CUBA	MALI	TURKEY
CYPRUS	MALTA	TURKMENISTAN
CZECH REPUBLIC	MARSHALL ISLANDS	UGANDA
DEMOCRATIC REPUBLIC OF THE CONGO	MAURITANIA	UKRAINE
DENMARK	MAURITIUS	UNITED ARAB EMIRATES
DJIBOUTI	MEXICO	UNITED KINGDOM OF GREAT BRITAIN AND NORTHERN IRELAND
DOMINICA	MONACO	UNITED REPUBLIC OF TANZANIA
DOMINICAN REPUBLIC	MONGOLIA	UNITED STATES OF AMERICA
ECUADOR	MONTENEGRO	URUGUAY
EGYPT	MOROCCO	UZBEKISTAN
EL SALVADOR	MOZAMBIQUE	VANUATU
ERITREA	MYANMAR	VENEZUELA, BOLIVARIAN REPUBLIC OF
ESTONIA	NAMIBIA	VIET NAM
ETHIOPIA	NEPAL	YEMEN
FIJI	NETHERLANDS	ZAMBIA
FINLAND	NEW ZEALAND	ZIMBABWE
FRANCE	NICARAGUA	
GABON	NIGER	
	NIGERIA	
	NORWAY	

The Agency's Statute was approved on 23 October 1956 by the Conference on the Statute of the IAEA held at United Nations Headquarters, New York; it entered into force on 29 July 1957. The Headquarters of the Agency are situated in Vienna. Its principal objective is "to accelerate and enlarge the contribution of atomic energy to peace, health and prosperity throughout the world".

CYCLOTRON PRODUCED  
RADIONUCLIDES:  
EMERGING POSITRON EMITTERS FOR  
MEDICAL APPLICATIONS:  $^{64}\text{Cu}$  AND  $^{124}\text{I}$

## COPYRIGHT NOTICE

All IAEA scientific and technical publications are protected by the terms of the Universal Copyright Convention as adopted in 1952 (Berne) and as revised in 1972 (Paris). The copyright has since been extended by the World Intellectual Property Organization (Geneva) to include electronic and virtual intellectual property. Permission to use whole or parts of texts contained in IAEA publications in printed or electronic form must be obtained and is usually subject to royalty agreements. Proposals for non-commercial reproductions and translations are welcomed and considered on a case-by-case basis. Enquiries should be addressed to the IAEA Publishing Section at:

Marketing and Sales Unit, Publishing Section  
International Atomic Energy Agency  
Vienna International Centre  
PO Box 100  
1400 Vienna, Austria  
fax: +43 1 2600 29302  
tel.: +43 1 2600 22417  
email: [sales.publications@iaea.org](mailto:sales.publications@iaea.org)  
<http://www.iaea.org/books>

© IAEA, 2016

Printed by the IAEA in Austria

March 2016

STI/PUB/1717

### IAEA Library Cataloguing in Publication Data

Names: International Atomic Energy Agency.

Title: Cyclotron produced radionuclides : emerging positron emitters for medical applications :  $^{64}\text{Cu}$  and  $^{124}\text{I}$  / International Atomic Energy Agency.

Description: Vienna : International Atomic Energy Agency, 2016. | Series: IAEA radioisotopes and radiopharmaceuticals reports, ISSN 2413-9556 ; no. 1 | Includes bibliographical references.

Identifiers: IAEAL 16-01022 | ISBN 978-92-0-109615-9 (paperback : alk. paper)

Subjects: LCSH: Radiopharmaceuticals. | Targets (Nuclear physics). | Copper — Isotopes. | Iodine — Isotopes.

Classification: UDC 621.039.574.5 | STI/PUB/1717

# FOREWORD

Advances in medical knowledge and better understanding of disease processes are driving the search for early diagnosis and screening methods, and for new therapy options. Diagnostic and therapeutic applications using radioisotopes and radiopharmaceuticals continue to be the key elements in this context, and demand for such nuclear based services is expected to expand. Radioisotope products that can be produced in greater quantities and in centres around the world are essential to ensure availability of these services when needed. There is also a trend towards reduced dependence on long distance transport of radioisotope products to minimize the scope for any malicious diversion of radioactive consignments. The ability to produce cost effective radiopharmaceuticals locally could have a significant impact in developing countries, leading to increased need for assistance regarding best production practices, quality assurance and regulatory aspects.

The IAEA has been assisting interested Member States in this context with the development of  $^{18}\text{F}$  products beyond 2- $^{18}\text{F}$ fluoro-2-deoxy-D-glucose ( $^{18}\text{F}$ -FDG), as well as in using generator produced  $^{68}\text{Ga}$  products for positron emission tomography (PET) imaging. The IAEA, in continuing with this approach and as a result of a recently completed coordinated research project (CRP) titled Production and Utilisation of Emerging Positron Emitters for Medical Applications with an Emphasis on  $^{64}\text{Cu}$  and  $^{124}\text{I}$ , decided to compile this publication as a guide to enhance the utilization of medical cyclotrons for production and application of other emerging positron emitters, in particular  $^{64}\text{Cu}$  and  $^{124}\text{I}$ . The CRP was intended to develop better production routes and better separation and purification of these PET radionuclides so as to achieve high specific activity and chemical purity suitable for labelling molecules of medical interest and to enable fruitful use of the spare capacity available in medical cyclotron centres.

This IAEA publication was compiled using inputs from experts in the field as well as the results of the CRP. It contains sections on production of  $^{64}\text{Cu}$  and  $^{124}\text{I}$ , techniques for preparation of targets, irradiation of targets under high beam currents, target processing, target recovery and other related topics. The accompanying CD-ROM supports the book, providing the participants' account of their work during the CRP demonstrating the successful application of the principles described in the book.

The IAEA wishes to thank all CRP participants and contributors to this publication for their valuable contributions. The IAEA officer responsible for this publication was M. Haji-Saeid of the Division of Physical and Chemical Sciences.

#### *EDITORIAL NOTE*

*Guidance provided here, describing good practices, represents expert opinion but does not constitute recommendations made on the basis of a consensus of Member States.*

*This report does not address questions of responsibility, legal or otherwise, for acts or omissions on the part of any person.*

*Although great care has been taken to maintain the accuracy of information contained in this publication, neither the IAEA nor its Member States assume any responsibility for consequences which may arise from its use.*

*The use of particular designations of countries or territories does not imply any judgments by the publisher, the IAEA, as to the legal status of such countries or territories, of their authorities and institutions or of the delimitation of their boundaries.*

*The mention of names of specific companies or products (whether or not indicated as registered) does not imply any intention to infringe proprietary rights, nor should it be construed as an endorsement or recommendation on the part of the IAEA.*

*The authors are responsible for having obtained the necessary permission for the IAEA to reproduce, translate or use material from sources already protected by copyrights.*

*This publication has been prepared from the original material as submitted by the authors (CRP participants). The views expressed do not necessarily reflect those of the IAEA, the governments of the nominating Member States or the nominating organizations.*

*The material on the accompanying CD-ROM has been prepared from the original materials as submitted by the authors.*



# CONTENTS

1.	INTRODUCTION .....	1
1.1.	Background .....	1
1.2.	Objective .....	2
1.3.	Scope .....	2
1.4.	Structure .....	2
2.	PRODUCTION OF $^{64}\text{Cu}$ .....	2
2.1.	Chemical and physical characteristics of $^{64}\text{Cu}$ .....	2
2.2.	Selection of nuclear production route .....	3
2.2.1.	$^{64}\text{Ni}(\text{p}, \text{n})$ .....	3
2.2.2.	$^{64}\text{Ni}(\text{d}, 2\text{n})$ .....	4
2.2.3.	$^{68}\text{Zn}(\text{p}, \alpha\text{n})$ .....	4
2.2.4.	Other routes .....	7
2.3.	Target preparation .....	7
2.3.1.	$^{64}\text{Ni}$ electroplating .....	7
2.3.2.	$^{68}\text{Zn}$ electroplating .....	12
2.4.	Target irradiation .....	13
2.4.1.	Cooling .....	13
2.4.2.	Geometry .....	13
2.4.3.	Beam scanners .....	14
2.4.4.	Target retrieval .....	14
2.4.5.	Irradiation of electroplated targets on Ag backing .....	14
2.4.6.	Detection of neutron flux during irradiation .....	15
2.4.7.	Degraders for beam energy adjustment .....	15
2.5.	Extraction of $^{64}\text{Cu}$ from irradiated target .....	16
2.5.1.	Purification of $^{64}\text{Cu}$ from Ni targets .....	16
2.5.2.	Purification of $^{64}\text{Cu}$ from Zn targets .....	19
2.6.	Quality control .....	19
2.6.1.	Radioactivity measurements .....	21
2.6.2.	Measurement of cold metal contaminants .....	29
2.6.3.	Identification of possible sources of metal contamination .....	31
2.7.	Radiolabelling methods .....	32
2.7.1.	$^{64}\text{Cu}$ -ATSM .....	32
2.7.2.	Proteins and peptides .....	32
2.7.3.	General labelling procedure .....	33
2.8.	Applications .....	34
2.8.1.	Considerations for local preparation of $^{64}\text{Cu}$ labelled radiopharmaceuticals .....	34
2.8.2.	Considerations for production under manufacturing conditions .....	36
2.9.	Preclinical studies .....	36
2.9.1.	Using $^{64}\text{Cu}$ labelled peptides in diabetes research .....	36
2.9.2.	$^{64}\text{Cu}$ -cyclam-RAFT-c(-RGDfK-) <sub>4</sub> for tumour $\alpha_v\beta_3$ integrin imaging .....	37
2.9.3.	$^{64}\text{Cu}$ radiolabelled antibodies (immuno-PET) .....	38
2.10.	Clinical studies .....	39
2.10.1.	$^{64}\text{Cu}$ -ATSM .....	39
2.10.2.	$^{64}\text{Cu}$ labelled DOTATATE in staging neuroendocrine tumours .....	40

3.	PRODUCTION OF $^{124}\text{I}$ .....	40
3.1.	Selection of nuclear production route .....	40
3.2.	Target preparation .....	43
3.2.1.	Target design .....	43
3.2.2.	Te targets .....	44
3.2.3.	Sb targets .....	48
3.3.	Development of radioiodinated synthons .....	48
3.3.1.	$^{124}\text{I}$ properties, chemistry and labelling methods .....	48
3.4.	Potential applications of $^{124}\text{I}$ .....	51
4.	CONCLUSIONS .....	52
4.1.	$^{64}\text{Cu}$ outlook .....	52
4.2.	$^{124}\text{I}$ outlook .....	53
	REFERENCES .....	55
	ANNEX: CONTENTS OF THE ATTACHED CD-ROM .....	59
	ABBREVIATIONS .....	61
	CONTRIBUTORS TO DRAFTING AND REVIEW .....	63

# 1. INTRODUCTION

## 1.1. BACKGROUND

The application of radionuclides in medicine has undergone significant growth in the last two decades, with the availability of a large number of cyclotrons exclusively dedicated to their production contributing to this growth. The widespread use of positron emission tomography (PET) in oncology and the rapid dissemination of PET-computed tomography (PET-CT) cameras throughout the world have revolutionized nuclear medicine. The rapidly growing fleet of modern cameras and the progress in molecular imaging signify that clinical PET will grow beyond present state of the art 2-[ $^{18}\text{F}$ ]fluoro-2-deoxy-D-glucose ( $^{18}\text{F}$ -FDG) imaging in diagnosis and staging in oncology. New  $^{18}\text{F}$  tracers will certainly drive some of this expansion, but there is a growing understanding that many physiological and biological uptake mechanisms in humans are slow when compared to the short half-life of  $^{18}\text{F}$ . An abundant positron emission and long half-life are in general not favoured for nuclear physics reasons, however a handful of such isotopes have been explored and reported on by researchers in the past. Among these, only two at present deserve to be raised to the level of being called ‘emerging PET isotopes’:  $^{64}\text{Cu}$  and  $^{124}\text{I}$ . A third isotope,  $^{89}\text{Zr}$ , might deserve to be added to this category, and could prove to be ideally suited for future use in PET labelled antibodies.

New radiopharmaceuticals which can be routinely used for diagnosis or for evaluation of cancer therapy would be valuable additions to the arsenal available to the nuclear medicine physician. There is great potential for production and development of new radiopharmaceuticals using PET radionuclides other than  $^{18}\text{F}$  and  $^{11}\text{C}$  at most of the present day medical cyclotron facilities with cyclotrons in the energy range of 10–20 MeV. Cyclotron time is usually available for research, but there are several other factors to be addressed in the development and use of new radiopharmaceuticals. More than 30 potentially useful cyclotron produced positron emitting radionuclides have been reported, and  $^{64}\text{Cu}$  and  $^{124}\text{I}$  in particular have received considerable attention. Because of low positron energy, low abundance of gamma radiation, suitable half-life and favourable coordination chemistry, these radionuclides are attracting widespread interest. There are two major challenges in wider production of these PET tracers:

- (1) The targets for the production of these radionuclides are not widely available or are considered too difficult to use.
- (2) The separation of the radionuclide from the target material requires ion exchange chromatography or thermal diffusion and the labelling efficiency of the resultant nuclide needs to be further developed.

There is a need to evaluate and compare the emerging radionuclides as imaging agents. The most widespread medical applications of these non-standard PET radionuclides are in oncology for labelling of proteins, particularly immunoglobulins (antibodies to tumour specific antigens), and of small peptides which recognize receptors expressed on tumours. Some examples of applications would be:

- (a) As diagnostic PET imaging agents (with greater biological specificity than  $^{18}\text{F}$ -FDG). Such a diagnostic tracer, for example, would differentiate between malignant tumours and benign conditions such as sarcoidosis. This currently is a problem when using  $^{18}\text{F}$ -FDG, which mimics increased anaerobic glucose metabolism in tumours but also inflammatory processes.
- (b) To identify patients with specific tumour phenotypes for novel targeted therapies (e.g. antibody therapies).
- (c) To provide improved dosimetry of therapeutic radionuclides based upon improved quantitation of tumour and normal tissue (organ) distribution using PET instrumentation. In particular, the use of PET radionuclides with a longer half-life than  $^{18}\text{F}$ , such as  $^{124}\text{I}$  or  $^{64}\text{Cu}$ , provides information required for optimal organ and tumour dosimetry.

Even though interest in the use of these radionuclides for clinical application is steadily increasing, support from the (radio)pharmaceutical industry is rather limited. The major reason is that large scale production for provision of a sufficient number of customers is technically not achievable, whereas local, small scale production, on the other hand, is economically not very attractive. In this respect, the IAEA’s role in fostering streamlined

research and production capacities in Member States is of great importance to further develop this field and in general for these health care applications where short lived radionuclides are being used.

## 1.2. OBJECTIVE

This IAEA publication was initiated following a coordinated research project (CRP) on Production and Utilisation of Emerging Positron Emitters for Medical Applications with an Emphasis on  $^{64}\text{Cu}$  and  $^{124}\text{I}$  with participation of 15 institutions worldwide and with the aim to enhance the capability of Member States in production of emerging positron emitters for medical applications in order to meet the demand for new PET based diagnostic agents for specific diseases and provide improved dosimetry of therapeutic radionuclides. This publication is intended to provide broad information (with ample references for those who wish to go deeper) on better production routes and better separation and purification of these PET radionuclides so as to achieve high specific activity and chemical purity suitable for labelling molecules of medical interest and also enable fruitful use of the spare capacity available in medical cyclotron centres.

Guidance provided here, describing good practices, represents expert opinion but does not constitute recommendations made on the basis of a consensus of Member States.

## 1.3. SCOPE

This publication provides methods and guidelines on development of targets (making use of standardized nuclear data) capable of producing sufficient quantities of  $^{64}\text{Cu}$  and  $^{124}\text{I}$  for clinical investigations, chemistry for the separation of radionuclides from target materials to improve extraction and purity of the radionuclides and to minimize metal contaminants which might reduce the labelling efficiency, and development of new radiopharmaceuticals labelled with these non-standard PET radionuclides.

## 1.4. STRUCTURE

This publication contains sections on production of  $^{64}\text{Cu}$  and  $^{124}\text{I}$ ; techniques for preparation of targets, irradiation of targets under high beam currents, target processing and target recovery; and conclusions. The accompanying CD-ROM, which supports the book, contains accounts of the participants' work during the CRP demonstrating the successful application of the principles described in the publication. These are the unedited reports of the CRP participants as presented at the final research coordination meeting.

# 2. PRODUCTION OF $^{64}\text{Cu}$

## 2.1. CHEMICAL AND PHYSICAL CHARACTERISTICS OF $^{64}\text{Cu}$

The element Cu, with a normal content of 1.4–2.1 mg/kg in the human body, is the third most abundant metal after Fe and Zn. It is an essential trace element and a cofactor in various enzymes, with dysregulation implicated in a number of diseases. A number of Cu radionuclides exist with physical decay rates well matched to probe a sequence of increasingly selective physiological processes:

- Short lived  $^{62}\text{Cu}$  and  $^{60}\text{Cu}$  to follow the rapid uptake of simple agents measuring myocardial and renal perfusion (ethylglyoxal bis(thiosemicarbazone) (ETS), pyruvaldehyde-bis(N4-methylthiosemicarbazone) (PTSM), diacetyl-bis(N4-methylthiosemicarbazone) (ATSM); half-life in the range of minutes);
- Longer lived  $^{61}\text{Cu}$  and  $^{64}\text{Cu}$  suited for the slower accumulation of other targeting agents (ATSM, peptides; half-life in the range of hours);

- The protracted decay of  $^{64}\text{Cu}$  and  $^{67}\text{Cu}$  needed for the imaging and therapeutic applications of the slower kinetics of larger molecules (antibodies) targeting specific receptors or other targets on the cell surface over the course of days.

The nuclear decay characteristics of these five Cu radioisotopes are listed in Table 1.

TABLE 1. COMPARISON OF CHARACTERISTICS OF Cu RADIONUCLIDES [1, 2]

Radionuclide	Half-life	Decay mode	Gammas (keV)	Production reaction
Cu-60	23 min	beta+ (93%), EC (7%)	511, 1332 (88%)	Ni-60(p, n)
Cu-61	3.4 h	beta+, EC	511, 283 (13%)	Ni-61(p, n); Ni-60(d, n); Zn-64(p, $\alpha$ )
Cu-62	10 min	beta+	511, 1173 (0.4%)	Cu-63(p, 2n)Zn-62(EC)Cu-62
Cu-64	12.7 h	beta+ (19%), beta-, EC (41%)	511, 1346 (0.6%)	Ni-64(p, n); Zn-68(p, $\alpha$ n)
Cu-67	62 h	beta-	185 (48%)	Zn-68(p, 2p); Zn-70(p, $\alpha$ )

The dosimetric consequences have been well documented in the literature [3], with a general trend that, aside from the obvious advantage of matching the decay rate to the physiological process in question, a penalty results from the increasing beta end-point energies and branching ratios. The actual calculation of organ dose primarily depends on the biodistribution and kinetics (residence time) of the agent being administered, data which must be entered into such computational programs as OLINDA (Organ Level Internal Dose Assessment) or MIRD (Medical Internal Radiation Dose). However, a quick inspection of the particle emissions and half-lives of  $^{61}\text{Cu}$ ,  $^{64}\text{Cu}$  and  $^{67}\text{Cu}$  suggests that the liver, which is the key to Cu metabolism, will be the critical organ in most clinical applications of Cu labelled small molecules.

The low positron energy (650 keV end point), and subsequent short average range in tissue, of  $^{64}\text{Cu}$  is unique among the Cu candidates. This results in a marked improvement in the spatial resolution observed in modern PET scanners, now capable of several mm (full width at half maximum) in spatial detail. At the same time, the absence of significant additional decay gammas similarly makes  $^{64}\text{Cu}$  ideal for high resolution preclinical PET imaging of small animals. It should be noted that the branching ratio of  $^{64}\text{Cu}$  is somewhat lower than for the more conventional radionuclides ( $^{18}\text{F}$  and  $^{11}\text{C}$ ) and thus higher amounts of radioactivity may need to be injected to obtain images of similar quality.

## 2.2. SELECTION OF NUCLEAR PRODUCTION ROUTE

### 2.2.1. $^{64}\text{Ni}(\text{p}, \text{n})$

Several routes to produce  $^{64}\text{Cu}$  have been reported in the literature [4–8], among which  $^{64}\text{Ni}(\text{p}, \text{n})$  is used most often. Typically, incident proton energies of 11–14 MeV are used on an electroplated enriched  $^{64}\text{Ni}$  target. As with most other (p, n) reactions, the production cross-sections are high (Fig. 1), with a maximum of 600 millibarns (1 millibarn =  $10^{-31} \text{ m}^2$ ), at 11 MeV. This production route is compatible with the low energy cyclotrons that are commonly used for production of  $^{18}\text{F}$  and  $^{11}\text{C}$ . The disadvantage is the low natural abundance of  $^{64}\text{Ni}$ , making the target material expensive and local  $^{64}\text{Ni}$  recycling warranted.

Cobalt-61 (half-life = 1.65 h) is produced as a contaminant with this reaction via the (p,  $\alpha$ ) reaction, which has a high cross-section value. During the ion chromatography separation process, this isotope typically ends up in the  $^{64}\text{Ni}$  recovery vessel and thus can be left to decay before replating of the target material.

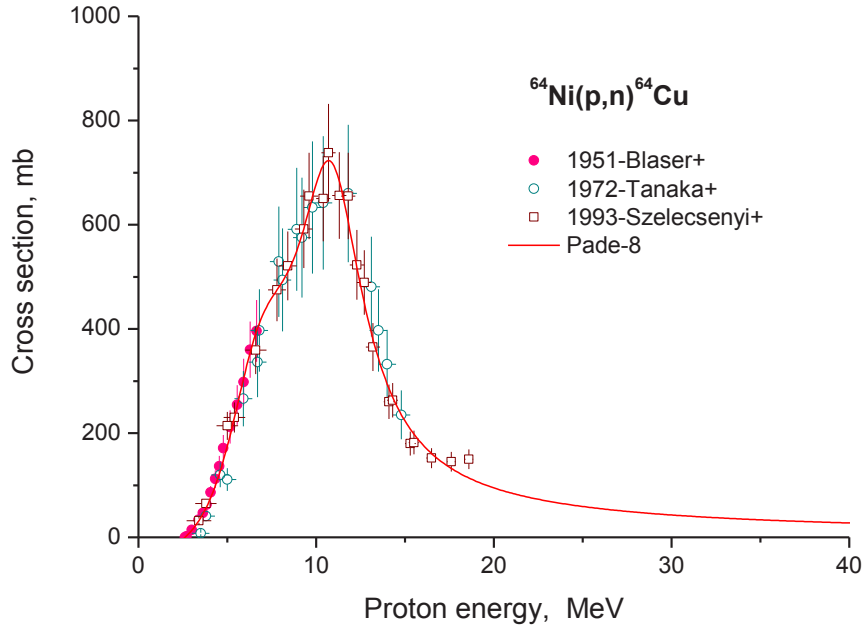


FIG. 1. Excitation function of  $^{64}\text{Ni}(p, n)^{64}\text{Cu}$  (reproduced from Ref. [9]).

### 2.2.2. $^{64}\text{Ni}(d, 2n)$

At facilities with higher energy cyclotrons, low energy protons are not available without substantial energy degradation, which often increases beam spot size and causes significant spread in the particle energy. Such higher energy cyclotrons often have deuterons available at half the proton energy, and for such cases a deuteron production route has been investigated. Figure 2 illustrates the excitation function of the  $(d, 2n)$  reaction as a function of the incident energy. The maximum cross-section for  $(d, 2n)$  is higher than for  $(p, n)$ , reaching 800 millibarns at 14 MeV.

A deuteron beam of 16 MeV has been used to take full advantage of the maximum cross-section. Moreover, it has been found that using the  $^{64}\text{Ni}(d, 2n)$  reaction makes it possible to get the same production yield as  $^{64}\text{Ni}(p, n)$  with a thinner deposit of  $^{64}\text{Ni}$ , which means a lower initial cost for  $^{64}\text{Ni}$ . Calculations for production routes from these two reactions are given in Table 2, illustrating that high yields are possible from both routes.

This deuteron reaction route inevitably produces  $^{65}\text{Ni}$  (half-life = 2.52 h) as a contaminant; however, it can be left to decay after the radiochemical separation of the  $^{64}\text{Cu}$  and before renewed use of the Ni for new target plating.

### 2.2.3. $^{68}\text{Zn}(p, \alpha n)$

Several cyclotron facilities currently produce  $^{67}\text{Ga}$  via the  $^{68}\text{Zn}(p, pn)$  reaction. In this case,  $^{64}\text{Cu}$  is produced as a byproduct via the  $^{68}\text{Zn}(p, \alpha n)$  reaction. This nuclear reaction produces lower amounts of  $^{64}\text{Cu}$  than the  $^{64}\text{Ni}(p, n)^{64}\text{Cu}$  reaction, depending on the incident energy. At 23.5 MeV, the calculated yield is 17 MBq/ $\mu\text{A}\cdot\text{h}$  (13 times lower), and at 29 MeV the yield is 35 MBq/ $\mu\text{A}\cdot\text{h}$  (6.5 times lower). For this approach, it is necessary to modify the target backing from the conventional  $^{67}\text{Ga}$  method by electroplating Au on the Cu backing prior to electroplating the enriched Zn target material. This prevents the stable backing Cu being dissolved during the target processing. Silver can be also used for target backing; however, this may also require electroplating Au on Ag prior to electroplating the enriched Zn to prevent the dissolution of Ag or any radioisotopes which may be coproduced during the irradiation process.

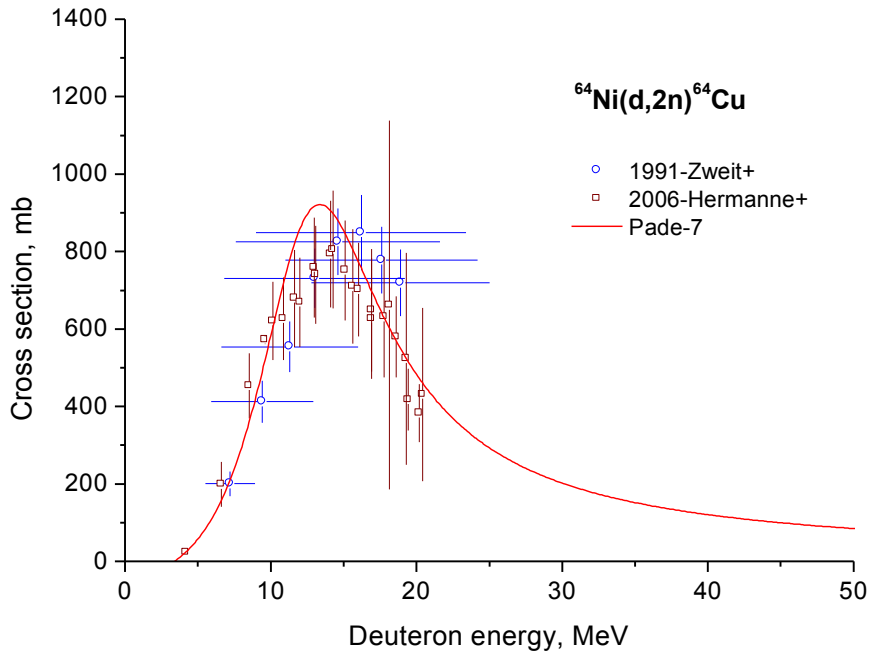


FIG. 2. Excitation function of  $^{64}\text{Ni}(d, 2n)^{64}\text{Cu}$  (reproduced from Ref. [9]).

TABLE 2.  $^{64}\text{Cu}$  CALCULATED YIELDS FOR (p, n) AND (d, 2n) PRODUCTION ROUTES

Nuclear reaction	Energy range (MeV)	Calculated yield (MBq/ $\mu\text{A}\cdot\text{h}$ )	Target thickness ( $\mu\text{m}$ )	Target thickness at $15^\circ$ ( $\mu\text{m}$ )
Ni-64(p, n)Cu-64	12–9	228	120	31.05
Ni-64(d, 2n)Cu-64	16–13	206	90	23.29

When choosing the target backing material, radiation safety issues should be considered in addition to chemistry constraints due to the activation of the target backing material during the irradiation, which may yield high radiation doses during operation.

Natural Cu contains 30.83%  $^{65}\text{Cu}$  and 69.17%  $^{63}\text{Cu}$  and when irradiated with protons produces different isotopes of Zn:  $^{65}\text{Cu}(p, n)^{65}\text{Zn}$ ,  $^{65}\text{Cu}(p, 2n)^{64}\text{Zn}$ ,  $^{63}\text{Cu}(p, n)^{63}\text{Zn}$ ,  $^{63}\text{Cu}(p, 2n)^{62}\text{Zn}$ . Between them,  $^{65}\text{Zn}$  (half-life = 244 d) has the longest half-life and decays by electron capture to the 1115 keV excited state and by electron capture and beta plus emission to the ground state level of  $^{65}\text{Cu}$ . The maximum cross-section for the reaction  $^{65}\text{Cu}(p, n)^{65}\text{Zn}$  is around 11 MeV; at 23.5 MeV of incident energy used for the  $^{68}\text{Zn}(p, \alpha n)$  reaction, depending on the target thickness, the cross-section for the  $^{65}\text{Cu}(p, n)^{65}\text{Zn}$  reaction will be high enough to produce  $^{65}\text{Zn}$ . This radioisotope will produce high radiation doses for a longer period of time; therefore, safety concerns might require a more careful design of target processing.

Natural Ag may be used as a backing material composed of 48.17%  $^{109}\text{Ag}$  and 51.83%  $^{107}\text{Ag}$ , and when irradiated with protons produces different isotopes of Cd:  $^{109}\text{Ag}(p, n)^{109}\text{Cd}$ ,  $^{109}\text{Ag}(p, 2n)^{108}\text{Cd}$ ,  $^{107}\text{Ag}(p, n)^{107}\text{Cd}$ ,  $^{107}\text{Ag}(p, 2n)^{106}\text{Cd}$ . Cadmium-108 and 106 are stable isotopes. At the energy range used to jointly produce  $^{67}\text{Ga}$  and  $^{64}\text{Cu}$  ( $< 23.5$  MeV), the nuclear reactions on the Ag backing will produce  $^{107}\text{Cd}$  and  $^{109}\text{Cd}$ . Cadmium-107 has a short half-life of 6.5 h, whereas  $^{109}\text{Cd}$  has a long half-life of 453 d but has no gamma emission and decays by electron capture to the isomeric state (88 keV) of  $^{109}\text{Ag}$ , which has an extremely short half-life of 39.6 s. Therefore, handling of irradiated target backings is easier for Ag than for Cu. Silver also has a higher thermal conductivity than Cu ( $429 \text{ W} \cdot \text{m}^{-1} \cdot \text{K}^{-1}$ ) and a high melting point of  $961.78^\circ\text{C}$ , which makes it suitable. Silver target backings can be reused after several weeks ( $>9$  weeks). Therefore, it is possible to sustain weekly production by recycling at least 10 target backings made with Ag.

The co-production of  $^{64}\text{Cu}$  from  $^{67}\text{Ga}$  production presents several advantages. The price of the target material,  $^{68}\text{Zn}$ , which can be obtained at a high enrichment level ( $>97\%$ ), is typically 10 to 40 times lower than that of  $^{64}\text{Ni}$ . However, recycling of enriched  $^{68}\text{Zn}$  is still deemed necessary. The experimental cross-section [10] presented in Fig. 3 as black points, shows two components: one coming from the  $(p, \alpha n)$  reaction and the other starting at 36.6 MeV and coming from the  $(p, 2n)$  reaction.

With this method, it is important to limit the production of other radioactive Cu isotopes as well as  $^{66}\text{Ga}$  to ensure high purity for both isotopes. On the one hand, for  $^{64}\text{Cu}$ , the two main potential contaminating radioisotopes are  $^{67}\text{Cu}$ , which starts to be produced at 10 MeV but only becomes significant above 35 MeV, as shown by the red squares in Fig. 3 [10], and  $^{61}\text{Cu}$ , which is produced above 36 MeV [2]. Gallium-66, which is a potential contaminant for  $^{67}\text{Ga}$ , starts to be produced at 23.5 MeV. Thus, the optimal proton beam energy for this dual production is 23.5 MeV, just below the  $^{68}\text{Zn}(p, 3n)^{66}\text{Ga}$  threshold of 23.55 MeV. If only  $^{64}\text{Cu}$  is desired and the Ga activity is dismissed, higher energies can be used in order to increase yields. Copper-64 production increases from 17 to 35 MBq/ $\mu\text{A} \cdot \text{h}$  when using 29 MeV as incident proton energy instead of 23.5 MeV [11]. Higher incident energies produce increasing amounts of  $^{66}\text{Ga}$ , requiring more lead shielding and a higher degree of remote handling and automation. However, all Ga radioisotopes can be efficiently separated in the radiochemical purification process using exchange methods, as shown later in this report.

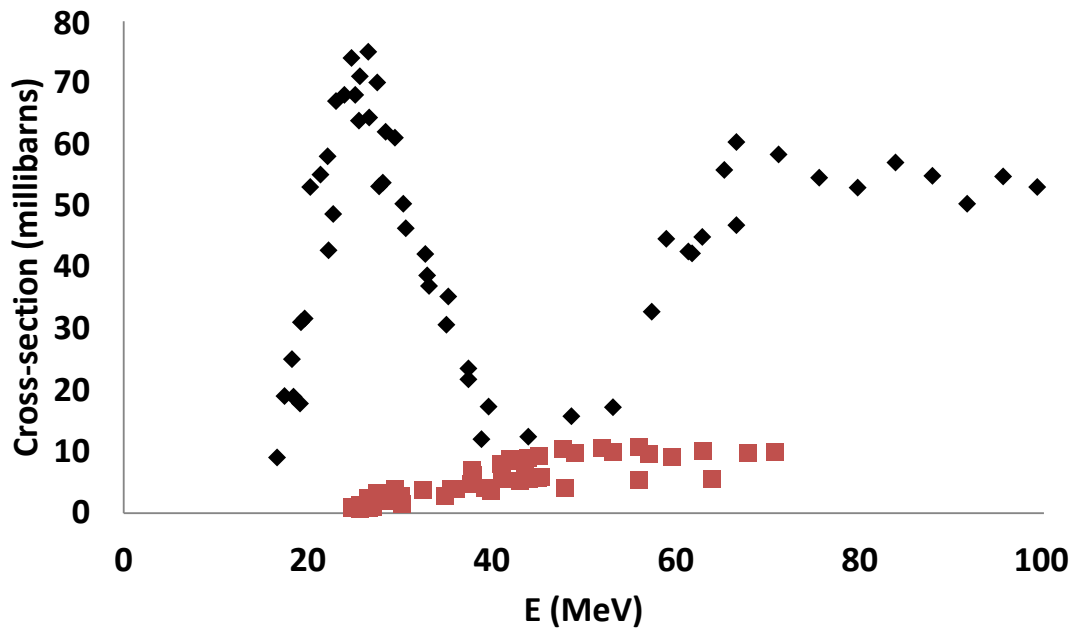


FIG. 3. Excitation function of  $^{68}\text{Zn}(p, \alpha n)$  (black) and  $^{68}\text{Zn}(p, 2n)^{67}\text{Cu}$  (red).



#### 2.2.4. Other routes

Copper-64 can also be produced in research reactors by thermal neutron capture on  $^{63}\text{Cu}$ . While this route can be used for calibration purposes, it is typically not useful for medical applications due to the inherent low specific activity; Szilard–Chalmers methods have been used in the past to somewhat enhance the specific activity, but not to the level presently available from charged particle reactions.

### 2.3. TARGET PREPARATION

#### 2.3.1. $^{64}\text{Ni}$ electroplating

Normally, electroplating methods are used universally for target production. The main variation seen is in the choice of target size and thickness. The optimal plating thickness for achieving the highest yield depends critically on the energy of the incoming protons [12].

##### 2.3.1.1. Target requirements

The general physical requirements for a solid cyclotron target for production of  $^{64}\text{Cu}$  are the same as for Ni targets: uniform, well adherent plating on a metal with high thermal conductivity and chemical resistance to the acid chosen for dissolution of the irradiated target. Generally, the same principles and practices developed for high current solid targets for the production of single photon emission computed tomography (SPECT) isotopes may also be used for the low energy targets [13].

Electroplated solid targets should meet a series of quality requirements that may be summarized as follows. The Ni layer should adhere strongly to the backing material and be smooth, dense (no craters, no cracks) and homogeneous, and show a well-defined thickness. A good adhesion of the Ni metallic layer to the backing support is necessary in order to avoid the loss of expensive enriched target material during the irradiation. The electroplating can be accomplished with standard, commercially available electrodes, galvanostat and electrolytic cell, or with inexpensive in-house components.

##### (a) Quality requirements for Ni plating

For Ni plating, intact glassware of good quality or clean and well wrapped disposable plastic should always be used. All glass components (beakers, vials, stoppers etc.) should always be washed in acid ( $\text{HCl}$  or  $\text{HNO}_3$ ) and rinsed in clean water prior to use. Handling of the backing and the plated target should be done avoiding metal tweezers.

##### (b) Dissolution of metallic Ni

Hydrochloric, nitric and sulphuric acids are used for dissolution of  $^{64}\text{Ni}$  and for the preparation of the plating bath. Very pure grades of acid with high grade specifications are suggested. Prices for these may be considerably higher than for low grade acids. All water should be metal free. Enriched Ni may contain metallic impurities and thus purchased Ni may need to be purified in order to reduce the presence of contaminants.

##### (c) Ni target backing materials

During the CRP, different materials were investigated as backing supports. The target backing materials Au, Ag, Au plated on Cu, Ag plated on Cu, Nb and graphite were evaluated in terms of beam tolerance, ease of plating, resistance to release of contaminating metals, activation and price. The target backing should be free from Cu. This is normally not a problem when using Au, but users of Ag backings should only use material known to be free of Cu. When Cu substrate is used as backing material, a layer of inert metal material (Au or Ag) should be electroplated on the Cu before the Ni plating to prevent stable Cu leakage when dissolving the irradiated Ni target material (Table 3).

TABLE 3. POTENTIAL TARGET BACKING MATERIALS

Backing material	Advantage	Disadvantage
Au	Reusable for many years Low activation	Expensive
Ag	High thermal conductivity Inexpensive	Presence of metallic contaminants High activation
Ag on Cu	Inexpensive High thermal conductivity	Presence of metallic contaminants Cu leakage
Au on Cu	Inexpensive Good adhesion	Cu leakage
Graphite	High purity No activation Inexpensive High fusion temperature	Limit on the deposit thickness Lower thermal conductivity and limited target current
Nb	None	Poor adhesion

## (d) Electrodes

Either a graphite rod or Pt wire or foil is used as the anode. The purity of the anode material has been shown to have influence on target content of Cu when using graphite. Very high purity graphite is available and should be used.

## (e) Quality control of Ni target

During the development of the electroplating procedure the following tests are suggested for quality control of a Ni target:

- (i) Scanning electron microscopy (SEM) at  $\sim 500$  to  $\sim 1000\times$  magnification is suggested to determine the uniformity of target surface and adherence to backing of a Ni target. A typical SEM image is shown in Fig. 4.
- (ii) In some cases, stability evaluation of the Ni target may be necessary. One way to perform such an evaluation is to heat the Ni target to over  $350^\circ\text{C}$ , then bend the target by force and check if the Au and Ni layer separates from the Cu backing.

For routine electroplating, it is best to perform a visual inspection of the Ni layer in order to verify good adhesion of the Ni layer and to check for the presence of craters or cracks. Laboratories have reported different set-ups for the electroplating procedure and the preparation of the electroplating bath. The main characteristics of different electroplating methods are reported in Table 4.

Three electroplating procedures with different set-ups are given below as examples.

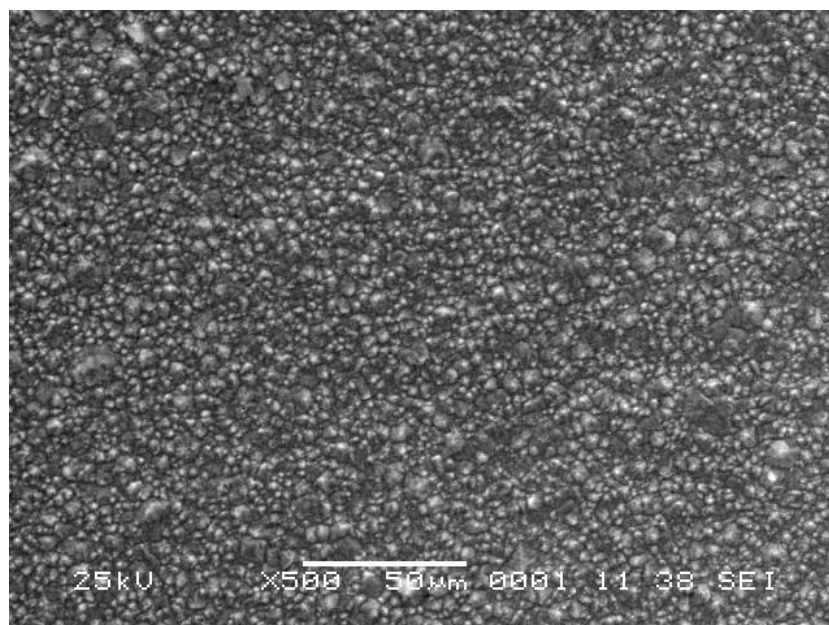


FIG. 4. SEM image of Ni target surface at 500 $\times$ .

TABLE 4. SUMMARY OF ELECTROPLATING CONDITIONS USED IN THIS CRP

Country	Plating bath (aqueous solution)	pH	Backing material	Electrode	Volume (mL)	Voltage (V)	Electrode distance (mm)	Stirring	Temperature ( $^{\circ}$ C)
Italy	$(\text{NH}_4)_2\text{Ni}(\text{SO}_4)_2$	9	Au	Pt	15	2.2	5	Rotating	Room
Japan	$(\text{NH}_4)_2\text{Ni}(\text{SO}_4)_2$	9	Au	Graphite	5–7	2.6	5	Syringe	Room
Finland	$(\text{NH}_4)_2\text{Ni}(\text{SO}_4)_2$	9	Au	Graphite	10	2.5	8	No	Room
Rep. of Korea	$(\text{NH}_4)_2\text{Ni}(\text{SO}_4)_2$	9	Au	Pt	10	3.0	5	Rotating	Room
China	$\text{NiCl}_2$	2	Au	Pt	50	3.8	20	Rotating	Room
Denmark	$\text{Ni}(\text{SO}_4)_2$	6	Ag	Pt	6.5	3.2	20	No	Room
USA (Washington)	$(\text{NH}_4)_2\text{Ni}(\text{SO}_4)_2$	9	Au	Graphite	10	2.5	5	Rotating	Room
USA (Wisconsin)	$(\text{NH}_4)_2\text{Ni}(\text{SO}_4)_2$	9	Au	Pt	5	2.5	10	No	Room
France	$(\text{NH}_4)_2\text{Ni}(\text{SO}_4)_2$	9.8	Au	Pt	100	1.1	10	Rotating	30
Syrian Arab Republic	$\text{Ni}(\text{NO}_3)_2$ , $\text{Na}_2\text{SO}_4$ , $\text{NH}_4\text{Cl}$ and $\text{H}_3\text{BO}_4$	9	Ag	Pt	250	6	30	Rotating	Room

(f) Ni electroplating: Method 1

Metallic Ni was dissolved in 9M concentrated HCl solution with several drops of H<sub>2</sub>O<sub>2</sub> solution and the mixture was evaporated to dryness. After cooling to room temperature, the residue was treated with 0.05M HCl and transferred to the plating cell for electrodeposition. High purity Cu substrate was employed as backing material. Gold (18 mm × 110 mm, ~18 μm thickness) was electroplated on the Cu backing to prevent cold Cu leakage. The Ni target (10 mm × 100 mm) was made by electrodeposition on the Au layer. Platinum was used as the anode, rotated at about 250 rev./min during electrodeposition. The distance between the electrodes was 2.0 cm.

(g) Ni electroplating: Method 2

<sup>64</sup>NiCl<sub>2</sub> salt was dissolved in 3 mL of 6.0M HNO<sub>3</sub>. The solution was then evaporated to dryness under air flow. This step was completed in 60 min at 180°C. The residue was dissolved in 1 mL of concentrated H<sub>2</sub>SO<sub>4</sub>. The resulting solution was diluted in 4 mL of deionized water. The pH was then adjusted to 9 with concentrated NH<sub>4</sub>OH (25%). The final solution was adjusted to 15 mL with deionized water. This solution was filtered through a 0.22 μm filter and transferred to an electrolytic cell with a Pt electrode as anode and the Au disk of the target backing as cathode. The cathode was cleaned with 6N HNO<sub>3</sub> and acetone to remove any metal residue on the surface. The cell was operated at 2.2 V with a starting current of 70–80 mA/cm<sup>2</sup>. The solution was mixed by a mechanical stirrer. The distance between the electrodes was 5 mm. The deposit diameter was 14 mm.

(h) Ni electroplating: Method 3

From fresh Ni:

- Dissolve the Ni metal in 5 mL of warm 6N HNO<sub>3</sub> (clear green solution).
- After the dissolution is completed, evaporate the acidic solution under a stream of N (hot block, 130 °C), bubbling the acidic waste vapours into water.
- After the complete evaporation of the acidic solution, remove the cap of the evaporation vessel and keep it overnight at 90°C.
- Treat the residue with 300 μL of concentrated H<sub>2</sub>SO<sub>4</sub> and dilute with 2 mL of water. Gently mix until the complete dissolution of the residue (clear green solution).
- Add concentrate NH<sub>4</sub>OH (~1.5 mL) until a pH of 9.05 ± 0.05 is reached (clear blue solution).  
(Use a clean and calibrated pH meter (check the calibration of the pH meter). After you add the NH<sub>4</sub>OH, the solution will warm up; be sure to measure the pH when the solution is at room temperature. If the pH is >9.10, adjust to the desired pH using concentrated H<sub>2</sub>SO<sub>4</sub>.)
- Add 270–300 mg of (NH<sub>4</sub>)<sub>2</sub>SO<sub>4</sub> to the electrolyte solution. Now it is ready for the electrodeposition process as outlined below.

Starting from recovered target material:

- The HCL (~30 mL) containing the recovered Ni is evaporated to complete dryness (2 stages) under a stream of N (hot block, 130°C), bubbling the acidic waste in water.
- Treat the residue with 3 mL (×2) of 6N HNO<sub>3</sub> and evaporate the acidic solution under a stream of N.
- After the complete evaporation of the acidic solution, remove the cap of the evaporation vessel and keep it overnight at 90°C.
- Treat the residue with 300 μL of concentrate H<sub>2</sub>SO<sub>4</sub> and dilute with 2 mL of water. Gently mix until the complete dissolution of the residue (clear green solution).
- Add concentrate NH<sub>4</sub>OH (~1.5 mL) until a pH of 9.05 ± 0.05 is reached (clear blue solution).  
(Use a clean and calibrated pH meter (check the calibration of the pH meter). After you add the NH<sub>4</sub>OH, the solution will warm up; be sure to measure the pH when the solution is at room temperature. If the pH is >9.10, adjust to the desired pH using concentrated H<sub>2</sub>SO<sub>4</sub>.)
- Add 270–300 mg of (NH<sub>4</sub>)<sub>2</sub>SO<sub>4</sub> to the electrolyte solution. Now it is ready for the electrodeposition process.

- Record the weight of the Au disk (e.g. 2.738 g) and place it (centred) on the base of the electrolytic cell. (The Au disk needs to be washed with detergent using a heavy duty scour pad, treated with 6N HNO<sub>3</sub> for a few hours and rinsed with 18 MΩ·cm water.)
- Add the electrolyte solution to the cell and rinse the vessel with 1–2 mL of clean water.
- Place the graphite anode at a distance of ~0.5 cm from the face of Au disk.
- Perform electrodeposition at 2.4–2.6 V (15–25 mA). This process takes 24–48 h.  
(If after 24–48 h the electrodeposition is not working (no change in the color of the electrolyte), the pH of the solution should be checked and adjusted to  $9.05 \pm 0.05$  if needed. The graphite anode should also be checked for degradation. If degradation is found, polish the anode with a piece of paper, rinse it with clean water and clean it with a lint free wipe. The graphite anode must be replaced after 5–7 electrodeposition processes.)
- After the blue colour is gone, stop the electrodeposition process when the concentration of Ni is below 25 ppm (Ni<sup>2+</sup> test strip).
- Remove the Au disk from the cell, rinse the plated area with clean water, and dry with a heat gun. (When using the heat gun to dry the Au disk, cover the plated area with a lint free wipe.)
- Weigh and determine the mass of Ni. The plated area is ~0.5 cm<sup>2</sup>.

### 2.3.1.2. Target support for electroplating on Ag

Another example of a method used to electroplate Ni on a backing consisting of Ag electroplated on Cu is as follows.

The surface of the Cu target support (2 × 10 cm) was cleaned with fine abrasive wool and acetone. This surface was electroplated with Ag using a AgNO<sub>3</sub>, NaCN and Na<sub>2</sub>CO<sub>3</sub> bath with a pH ≥ 12 at room temperature. The voltage and current density used for Ag electroplating were 4 V and 4 mA/cm<sup>2</sup>, respectively. The thickness of the electroplated Ag layer was calculated to be 35 μm.

The purpose of the electroplated Ag layer is to prevent the dissolution of the Cu target support in order to produce no-carrier-added <sup>64</sup>Cu.

On the Ag layer, natural Ni was electroplated on a smaller surface (1 × 10 cm) using a Ni(NO<sub>3</sub>)<sub>2</sub>, Na<sub>2</sub>SO<sub>4</sub>, NH<sub>4</sub>Cl and H<sub>3</sub>BO<sub>4</sub> bath with a pH ≈ 9 at room temperature. The voltage and current density for Ni electroplating was 6 V and 50 mA/cm<sup>2</sup>, and the electroplated thickness was about 12 μm. Figures 5–7 show the electroplated target and target surface.



FIG. 5. Target support: (right) without electroplating, (middle) Ag electroplated and (left) Ni electroplated on the Ag layer.



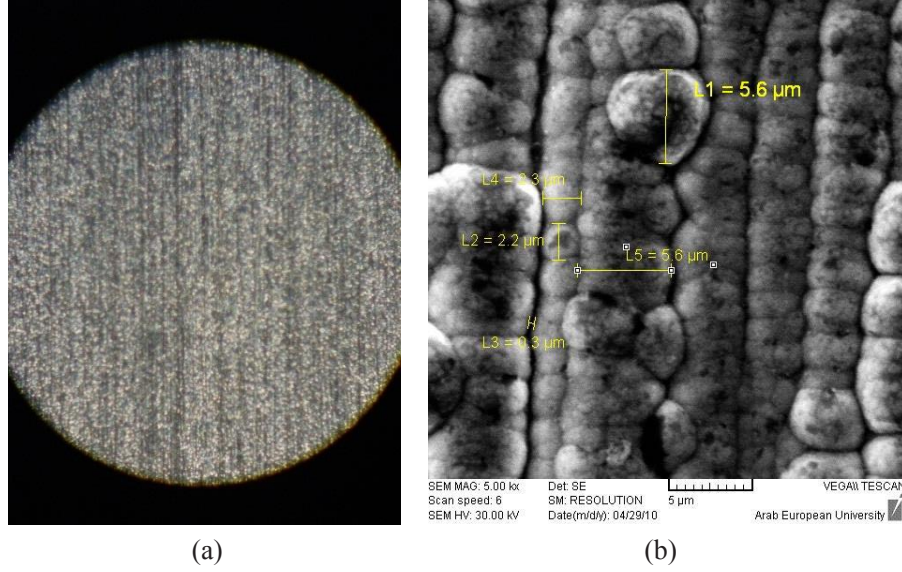


FIG. 6. Nickel electroplated target surface: (a) optical micrograph (magnification: 50 $\times$ ); (b) SEM micrograph.

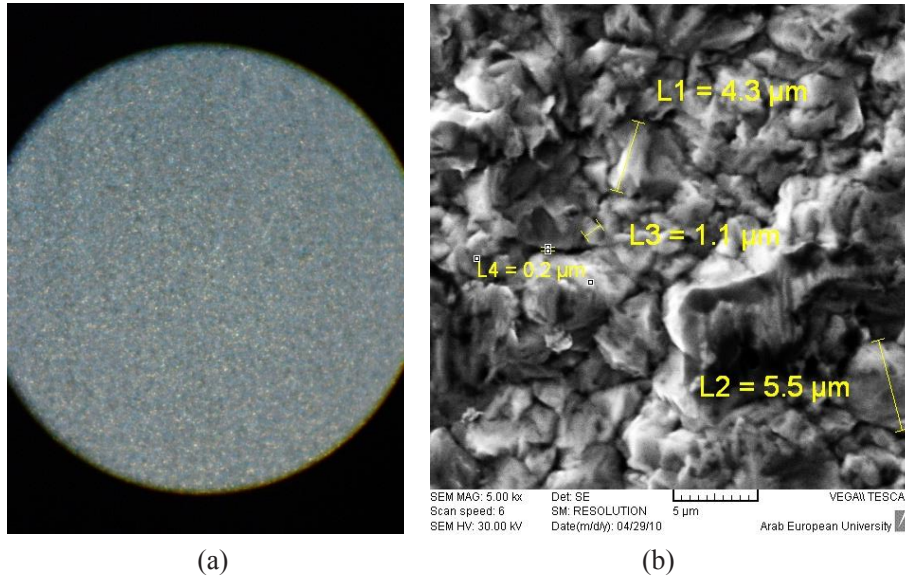


FIG. 7. Silver electroplated target surface: (a) optical micrograph (magnification 50 $\times$ ); (b) SEM micrograph.

### 2.3.2. $^{68}\text{Zn}$ electroplating

Enriched  $^{68}\text{Zn}$  (enrichment >97%) is used to electroplate targets for the  $^{68}\text{Zn}(p, \alpha n)$  reaction. The surface of the Cu target support ( $2 \times 10$  cm) is cleaned with fine abrasive wool and acetone. This surface is electroplated with a Au layer using an alkaline Au cyanide bath. The voltage and current density used for Au electroplating are 100 mV and 1 mA/cm<sup>2</sup>, respectively. The purpose of the electroplated Au layer is to prevent the dissolution of the Cu target support in order to produce no-carrier-added  $^{64}\text{Cu}$  via the  $^{68}\text{Zn}$  target. The enriched  $^{68}\text{Zn}$  is electroplated on the Au layer on a smaller surface ( $1 \times 10$  cm) using a slightly acidic (pH  $\approx$  2.5) electrolytic solution containing hydrazine hydrate as anodic depolarizer. The current density is 20 mA/cm<sup>2</sup> and the electroplated quantity is about 0.8 g.

When using a Cu target support only once, the thickness of the electroplated Au layer should be 3–5  $\mu\text{m}$  for economic reasons. In one example, the target is electroplated with a Au layer of 2.3  $\mu\text{m}$  thickness, then with a  $^{68}\text{Zn}$  layer of 115  $\mu\text{m}$  thickness. The angle between the incident proton beam and the target is  $6^\circ$ ; thus the effective thickness of the  $^{68}\text{Zn}$  layer is 1100  $\mu\text{m}$  and the exit energy of the proton beam is 10 MeV.

Electroplated targets created using this method can be irradiated by a 250  $\mu\text{A}$ , 23.5 MeV proton beam for 6 h. The back side of the target is cooled with very high speed stream of deionized water using a commercial irradiation station. Considering that for irradiations at 23.5 MeV, 23.5 W/ $\mu\text{A}$  will be delivered into the target, it is important to take into account the heat generation for irradiations at high beam current ( $>200 \mu\text{A}$ ). The quality of the electroplated target layer, the flow rate and temperature of the coolant are critical factors to be considered.

## 2.4. TARGET IRRADIATION

Production of  $^{64}\text{Cu}$  requires optimization in order to maximize  $^{64}\text{Cu}$  activity and minimize side reactions. Optimization of a production process means choosing a production route that is economical and fulfils the requirement of producing high quality  $^{64}\text{Cu}$ . Based on the excitation function of the contributing reactions, an optimization calculation can be performed. It is always suggested that a preliminary calculation be made to determine the best target and irradiation parameters, bombarding particle and energy, target thickness and irradiation time. For these calculations, there are databases [2] containing the relevant information about the nuclear reactions (main and side reactions) involved in the production process. The required basic information includes the excitation function of the reactions and the stopping parameters of the target material in the irradiation energy range, which can be found using the freely available Stopping and Range of Ions in Matter (SRIM) code.

A typical structure of a target for  $^{64}\text{Cu}$  production is shown in Fig. 8.

### 2.4.1. Cooling

The efficiency of the cooling and the particle beam quality are as important as the quality of the electroplated target layer. The efficiency of the cooling is determined by both the target carrier geometry and the flow rate of the coolant, while the beam quality relates to the current density distribution on the irradiated surface area, which contributes to the heat deposition in the target.

### 2.4.2. Geometry

Two different irradiation geometries are common: the target can be set perpendicular to the beam axis or slanted. Placing it perpendicular to the beam axis has the advantage of making beam alignment easy; however, it has limitations in beam current. Slanted geometry typically allows the use of higher beam current, but the alignment of the beam becomes more complicated. For these reasons, a dedicated external beam line with beam scanning should be used for a slanted target. Neutron monitoring during the irradiation can be used to investigate beam alignment.

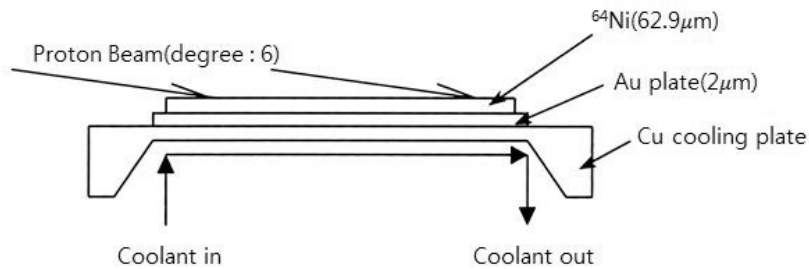


FIG. 8. Enriched  $^{64}\text{Ni}$  target design layout (beam angle:  $6^\circ$ ,  $^{64}\text{Ni}/\text{Au}$  electroplating, Cu plate for cooling).

#### 2.4.3. Beam scanners

Using accelerators with a beam line, it is possible to manipulate the beam profile on the target. Accelerator beam profile scanners are used to determine particle beam dimensions and intensity distribution. In many cases, the goal is to achieve uniformity of the beam intensity distribution for radionuclide production.

#### 2.4.4. Target retrieval

Pneumatic or mechanical automatic target retrieval systems have been developed in order to reduce the dose to the operators. These systems could be a potential source of metal contamination. Particular attention should be paid to the materials used and the procedures for cleaning of transport systems.

In a typical experiment,  $^{64}\text{Cu}$  can be produced by bombarding an enriched  $^{64}\text{Ni}$  target in a  $6^\circ$  beam/target geometry with a  $\sim 9$  to  $\sim 12$  MeV proton beam using the  $^{64}\text{Ni}(p, n)^{64}\text{Cu}$  nuclear reaction. The applied current could be in the range of  $\sim 20$  to  $\sim 200$   $\mu\text{A}$  and the irradiation time  $\sim 2$  to  $\sim 5$  h.

In a case study, the Ni target was fixed on the solid target system on a Cyclone 30 accelerator and irradiated with 15.6 MeV protons. The solid target station is equipped with a beam port for the target tilted  $6^\circ$  compared to the beam line. Hence the proton angle of incidence to the target was  $6^\circ$ . Routine production runs of  $^{64}\text{Cu}$  were performed at currents of 30–70  $\mu\text{A}$  lasting for 2–3 h.

#### 2.4.5. Irradiation of electroplated targets on Ag backing

In an example, the Ag electroplated target was irradiated by a 15 MeV proton beam at 200  $\mu\text{A}$  using a 30 MeV cyclotron for 3 h. The back side of the target was cooled with a very high speed stream of deionized water using a commercial irradiation station. No damage was observed on the electroplated target, which illustrated that the two electroplated layers adhere very well on the Cu substrate, as shown in Fig. 9.



FIG. 9. Irradiated  $^{64}\text{Ni}$  target (200  $\mu\text{A}$ , 3 h).



#### 2.4.6. Detection of neutron flux during irradiation

The detection and logging (1 Hz) of the neutron flux during the course of irradiation provides a real-time indicator of possible pitfalls:

- Target degradation at high beam currents;
- Beam wander;
- Other subtle cyclotron instabilities (e.g. radio frequency) that would otherwise go unnoticed by any other means.

Integrating the flux with decay correction ('leaky integration') will accurately predict the activity expected at the end of bombardment. The correspondence between the observed neutron flux and the  $^{64}\text{Cu}$  production rate must be offset by the blank rate at zero thickness of  $^{64}\text{Ni}$ , which is low (20%) at 11 MeV proton energy on cyclotrons designed with careful attention to avoiding beam loss on low-Z structures (collimators and neutral beam baffles). In particular, two detectors are commercially available, based on:

- A miniaturized  $^{10}\text{B}$  trifluoride proportional counter;
- A  $^6\text{Li}$  fluoride / AgS scintillator.

Both of these detectors offer virtually quantitative n/gamma discrimination.

The gamma flux within the cyclotron vault provides less discriminating information, being prone to the influence of the high energy photons coming from neutron absorption in the shielding walls. Nonetheless, a distant, well collimated  $\text{LaBr}_3$  scintillator can be similarly logged, reinforcing the information on the progress of the irradiation. Finally, the gamma flux can be observed by a very simple current mode, namely an uncollimated detector consisting of a commercially available  $\text{CaWO}_4$  scintillator screen/photomultiplier tube, which provides a final confirmatory signal.

#### 2.4.7. Degradors for beam energy adjustment

Not all cyclotrons have variable energy or capability to deliver particle beams at the optimal energy. Especially in the case of the (p, n) reactions, the standard energy of some of the medical cyclotrons is too high (16.5–19 MeV) for efficient utilization of the plated target material. For the  $^{64}\text{Ni}(\text{p}, \text{n})$  reaction, optimal activity after bombardment with orthogonal beam strike from relatively thick targets ( $100 \text{ mg/cm}^2$ ) is obtained at an incident energy around 10 MeV.

Insertion of metal degrader foil(s) of appropriate thickness in front of the target is a common and simple solution. In the case of  $^{64}\text{Cu}$  production, the degrader deserves some special attention:

- Production of  $^{64}\text{Cu}$  often relies on high current (20–100  $\mu\text{A}$ ) on the target. A substantial fraction of the total beam power is deposited in the degrader, and this calls for efficient water cooling. Degrader materials (metals) of high thermal conductivity and low stopping power are preferred. The standard choice has been Al, which has been used with success by many groups. Beryllium has been tested but found unsuitable because of instances of mechanical failure under high current bombardment.
- Cooling of the degrader is normally obtained by radial thermal conduction into a water cooled support. Additional cooling can be obtained with He cooling, but care should be taken that this does not contribute metal impurities to the target surface.
- With direct contact between the degrader and the primary target material (Ni layer) there is risk of metal contamination of the target, either by direct contact and diffusion, or by sputtering effects. Standard mechanical grade Al plates contain unacceptably high levels of Cu and should be avoided for 'in contact' degraders.
- There is a substantial amount of beam scattering from any degrader. If the target is separated from the degrader by just 10–20 mm, the size of the beam spot will grow, perhaps exceeding the Ni plated area. In this case, the activity output will be lower than predicted by the calculation of the accumulated current on the target. The freely available SRIM code can predict the amount of scatter and number of protons lost out of the target area.

## 2.5. EXTRACTION OF $^{64}\text{Cu}$ FROM IRRADIATED TARGET

### 2.5.1. Purification of $^{64}\text{Cu}$ from Ni targets

After the bombardment, the  $^{64}\text{Ni}$  should be dissolved from the backing material in order to separate the  $^{64}\text{Cu}$  from other metals, and the expensive  $^{64}\text{Ni}$  should be recovered for later recycling (Fig. 10). This dissolution step is typically performed with high concentrations of HCl, and care should be taken to collect the corrosive fumes using water, sodium hydrogen carbonate ( $\text{NaHCO}_3$ ) or sodium hydroxide (NaOH) traps. Many types of hot cells and commercially available lab equipment will not tarnish after short exposure to HCl fumes, but will gradually develop rust after repeated exposure.

The separation of the different metals is best achieved using the well known chromatography of chloro-complexes on an anion exchange resin column. This approach allows for a selective elution of metals with different HCl concentrations [14]. The resins widely used for the chemical separation are AG 1-X8 ( $\text{Cl}^-$  form) and Dowex 1X8. Before use, the resin should be washed to remove metal contaminants and regenerated with concentrated or 6–8N HCl. To ensure high specific activity in the  $^{64}\text{Cu}$  product it is important that all solvents and reagents are of ultra-pure quality. Special attention should be paid to the cleaning of all tools and glassware. The cleaning can include washing with  $\text{HNO}_3$  or HCl followed by careful rinsing with high purity water. The column material can be reused many times (>20). Between each round of production, the column should be washed as described above and regenerated.

The dissolution of the  $^{64}\text{Ni}$ , depending of the type of target backing material, can be done using concentrated or 6–8M HCl. Care must be taken to collect the acid vapours. To speed up the dissolution process, a few  $\mu\text{L}$  of  $\text{H}_2\text{O}_2$  can be added to the vessel and the solution can be heated; however if a Ag backing is used,  $\text{H}_2\text{O}_2$  should be avoided. In many production set-ups, the cooling water is in direct contact with the target backing. Cooling water is normally not metal free, and metal contents can plate on the back of the target during irradiation. Drying of the target backing is not necessarily adequate to eliminate this, and thus so called ‘one sided deplating’ (etching) procedures are preferred when high specific activity is sought. After cooling of the dissolved target solution, it can be transferred directly to the column for chemical separation. Several factors, such as amount of resin, flow rate of eluent and size of column, can influence the elution profile of metals. The following sections outline two methods for the purification step.

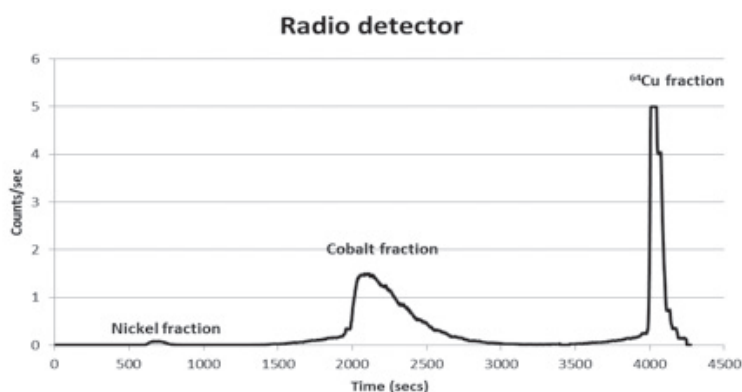


FIG. 10. Typical  $^{64}\text{Cu}$  separation profile.

### 2.5.1.1. Method 1

After the irradiation the target was transferred into a glass cell for the dissolution of the target material. Only the Ni electroplated surface was in contact with 4 mL of 9N HCl used for dissolution. The dissolution step was performed at 90°C under He flow. Dissolution of the target material was completed in about 20 min. Then the reactor was cooled by compressed air for 12 min. The HCl solution containing  $^{64}\text{Cu}$  and  $^{64}\text{Ni}$  was transferred (flow rate 1 mL/min) into a  $20 \times 0.8$  cm column filled with anion exchange resin AG 1-X8 (5 g,  $\text{Cl}^-$  form). Nickel-64 was completely eluted with 45 mL of 6N HCl at a flow rate of 1 mL/min. Only the first 20 mL of 6N HCl were collected for the recovery of Ni in order to reduce the volume to be evaporated for the preparation of the electroplated solution. The remaining 25 mL were collected in the Co waste. Copper-64 retained on the column was then eluted with 20 mL of 0.1N HCl. The  $^{64}\text{Cu}$  was recovered in about 3 mL of HCl solution. The final acid concentration was about 1.5N.

### 2.5.1.2. Method 2

After the irradiation, the target was manually transferred to the laboratory and placed in a Teflon cell for the dissolution of the target material. A small quantity (1.5 mL) of 30% HCl was added and the target backing was heated to 60°C. After approximately 30 min, the  $^{64}\text{Ni}$  metal was dissolved. A few  $\mu\text{L}$  of  $\text{H}_2\text{O}_2$  can be added to speed up the process. This should only be done if the target seems difficult to dissolve and if a Au backing is used. The target solution was automatically transferred to the column packed with Dowex 1X8 mesh 200–400 resin (length 17 cm  $\times$   $\varnothing$ 1 cm). Before production, the resin was carefully washed with water (250 mL) and regenerated with 30 mL of 6M HCl. The column material can be used up to 20 times. The  $^{64}\text{Ni}$  fraction was eluted with 23 mL of 6M HCl at a speed of 1.7 mL/min. Cobalt radioisotopes were eluted with 40 mL of 5M HCl and finally the  $^{64}\text{Cu}$  fraction was collected in 8 mL of 1M HCl.

In all methods, elution of the Ni can also be followed by measurement of the radioactivity of the coproduced  $^{57}\text{Ni}$ , as shown in Fig. 11.

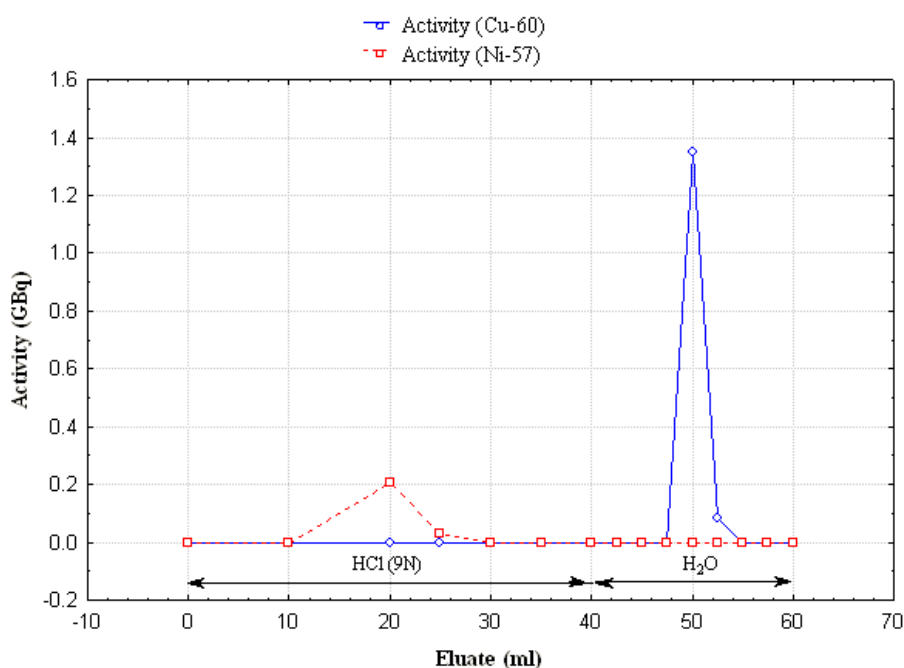


FIG. 11. Elution profile of  $^{60}\text{Cu}$  and  $^{57}\text{Ni}$ .

### 2.5.1.3. Automation

Because of the dose rates involved with processing of large amounts of  $^{64}\text{Cu}$ , several groups have automated the purification process as shown in Fig. 12 [15].

In order to reduce the  $^{64}\text{Cu}$  fraction volume while minimizing impurities, the  $^{64}\text{Cu}$  fraction should be collected at the end of the column. At the end of the purification step, the  $^{64}\text{Cu}$  fraction should be evaporated in order to reduce the high HCl concentration and collect the  $^{64}\text{Cu}$  in the smallest volume. The gas used during this step is also a potential source of metallic contamination; thus it should be as pure as possible.

### 2.5.1.4. Cation purification

The amount of metal contamination in the  $^{64}\text{Cu}$  fraction is a crucial parameter for the utility of the final product. In order to reduce the quantity of metallic contaminants, an additional purification step with cation exchange resin AG 50W-X8 can be performed. This approach allows for a selective elution of metals with different acetone/HCl concentrations.

This method is widely used for the cationic exchange post-processing purification for  $^{68}\text{Ga}$  eluted from a  $^{68}\text{Ge}/^{68}\text{Ga}$  generator [16]. Preliminary results demonstrate that quantitative trapping of all metals on the column is strongly dependent on the acid concentration as increasing acid concentration dramatically decreases the amount of metals trapped on the column. A concentration of 0.1N HCl seems to be the most favourable. After loading the column with the 0.1N HCl  $^{64}\text{Cu}$  fraction, the  $^{64}\text{Cu}$  can be selectively and quantitatively eluted by means of a 90% acetone/0.2N HCl solution while the Co and Ni remain trapped on the column (Table 5).

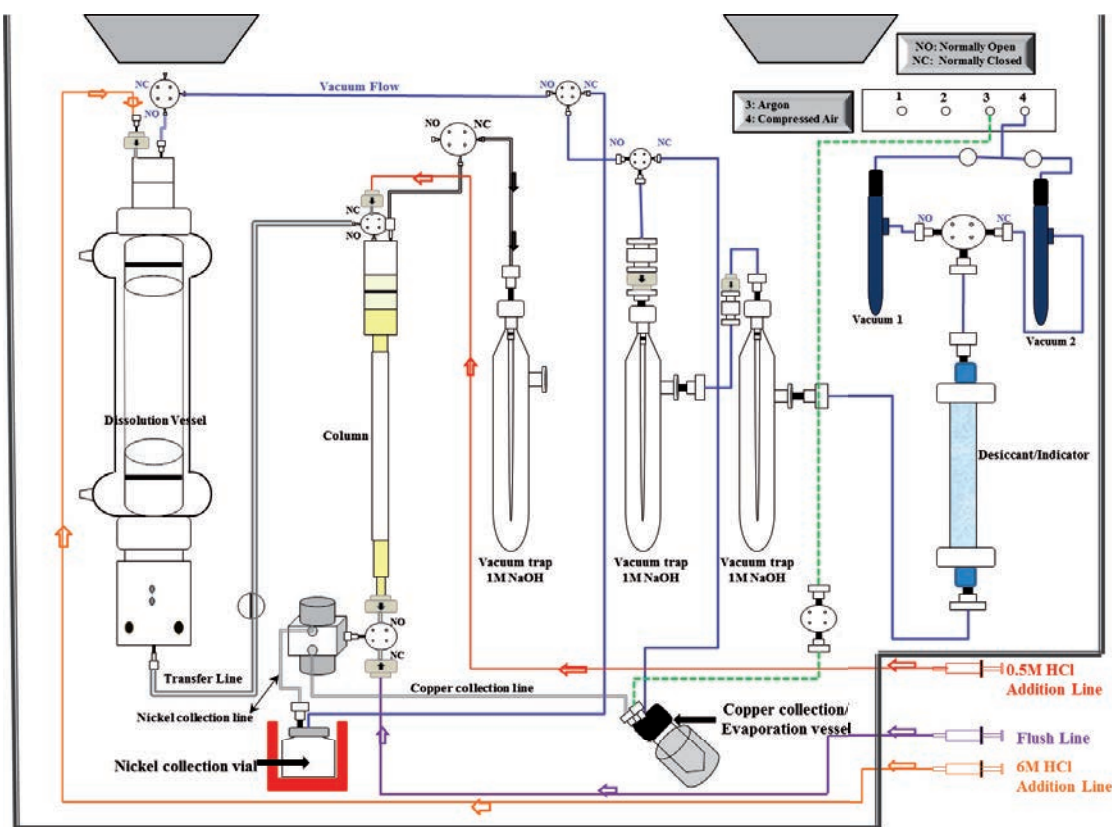


FIG. 12. Schematic of the automated Cu processing module (reproduced from Ref. [15] with permission from Elsevier).

TABLE 5. RELATIVE DISTRIBUTION OF  $^{64}\text{Cu}$ ,  $^{55}\text{Co}$ ,  $^{57}\text{Ni}$  ON CHROMATOGRAPHIC COLUMN (80 mg OF BIO-RAD AG 50W-X8 RESIN, 200–400 MESH) IN HYDROCHLORIC ACID/ACETONE MEDIA

Step	Eluent (concentration)	Relative distribution (%)		
		Cu-64	Co-55	Ni-57
Column waste	0.1N HCl	0.03	0.03	0.02
Column elution	90% acetone 0.2N HCl	97.26	0.87	0.10
Washing	4N HCl	2.70	99.10	99.87

Copper-64 can be obtained with 0.6 mL of acetone/HCl solution. Copper-64 solution is ready for labelling after a short evaporation step to eliminate the acetone. HCl can be neutralized by synthesis buffer.

### 2.5.2. Purification of $^{64}\text{Cu}$ from Zn targets

The production of  $^{64}\text{Cu}$  from Zn targets is performed in three steps.

The first step is related to the  $^{67}\text{Ga}$  production process and involves dissolving the irradiated  $^{68}\text{Zn}$  target layer gradually with 10N HCl. In a typical separation method: a plexiglas chromatographic column (1.2 cm inner diameter and 6.0 cm long) packed with ion exchange resin (Dowex 50W-X4, 200 mesh) is used to separate enriched  $^{68}\text{Zn}$  and  $^{64}\text{Cu}$  from  $^{67}\text{Ga}$  using 9N HCl with flow rate of 1 mL/min using a peristaltic pump.

Alternatively, 12 mL of 12N HCl plus 10 mL 10N HCl (for washout) can be used for complete dissolution of the target; when only 10N HCl was used, occasional incomplete dissolution was observed. The first separation step can also be carried out using a stronger cation exchange resin (Dowex 50W-X8). Using this resin, the amounts of Ga radioisotopes co-eluted with  $^{64}\text{Cu}$  were observed to be reduced. Lower amounts of Ga radioisotopes in the  $^{64}\text{Cu}$  solution from the onset are preferred, and resulted in a cleaner gamma spectrum during the quantification of  $^{64}\text{Cu}$ . When using cation exchange resin Dowex 50W-X8 in the first step, the elution of  $^{67}\text{Ga}$  must be with 3.5N HCl.

In the second step of the  $^{64}\text{Cu}$  production process, the eluted fraction from the first step containing  $^{68}\text{Zn}$  and  $^{64}\text{Cu}$  is loaded on a second chromatographic column ( $2.0 \times 12$  cm) packed with ion exchange resin (Dowex 1X8). Before loading, the column is preconditioned with 6N HCl. After loading, the elution of  $^{64}\text{Cu}$  from the column is performed using 2N HCl, then  $^{68}\text{Zn}$  is eluted from the column by 0.05N HCl. The elution flow rate is 3 mL/min. The volume of the obtained solution containing  $^{64}\text{Cu}$  is 18 mL, whereas the solution containing  $^{68}\text{Zn}$ , to be reused in electroplating of enriched Zn on a new target support, is 150 mL. Figure 13 shows the steps for production of  $^{64}\text{Cu}$  via the reaction  $^{68}\text{Zn}(p, \alpha n)^{64}\text{Cu}$ , and a schematic of the system is shown in Fig. 14.

The  $^{64}\text{Cu}$  solution volume may be too large to be used in typical labelling processes. For this reason, the  $^{64}\text{Cu}$  solution is concentrated in the third step using a semimanual unit. All  $^{64}\text{Cu}$  activity is obtained through this unit in 2 mL of 0.05N HCl. A small  $3 \times 10$  mm column, filled with ion exchange resin (Dowex 1X8) is used for this purpose. Figure 15 shows the concentration unit for  $^{64}\text{Cu}$ .

## 2.6. QUALITY CONTROL

Quality control of  $[^{64}\text{Cu}]\text{CuCl}_2$  after the separation from the target material is necessary to determine the quality of the product. The radioactivity, the radionuclidic purity and the chemical purity are important parameters to be measured [3, 14].

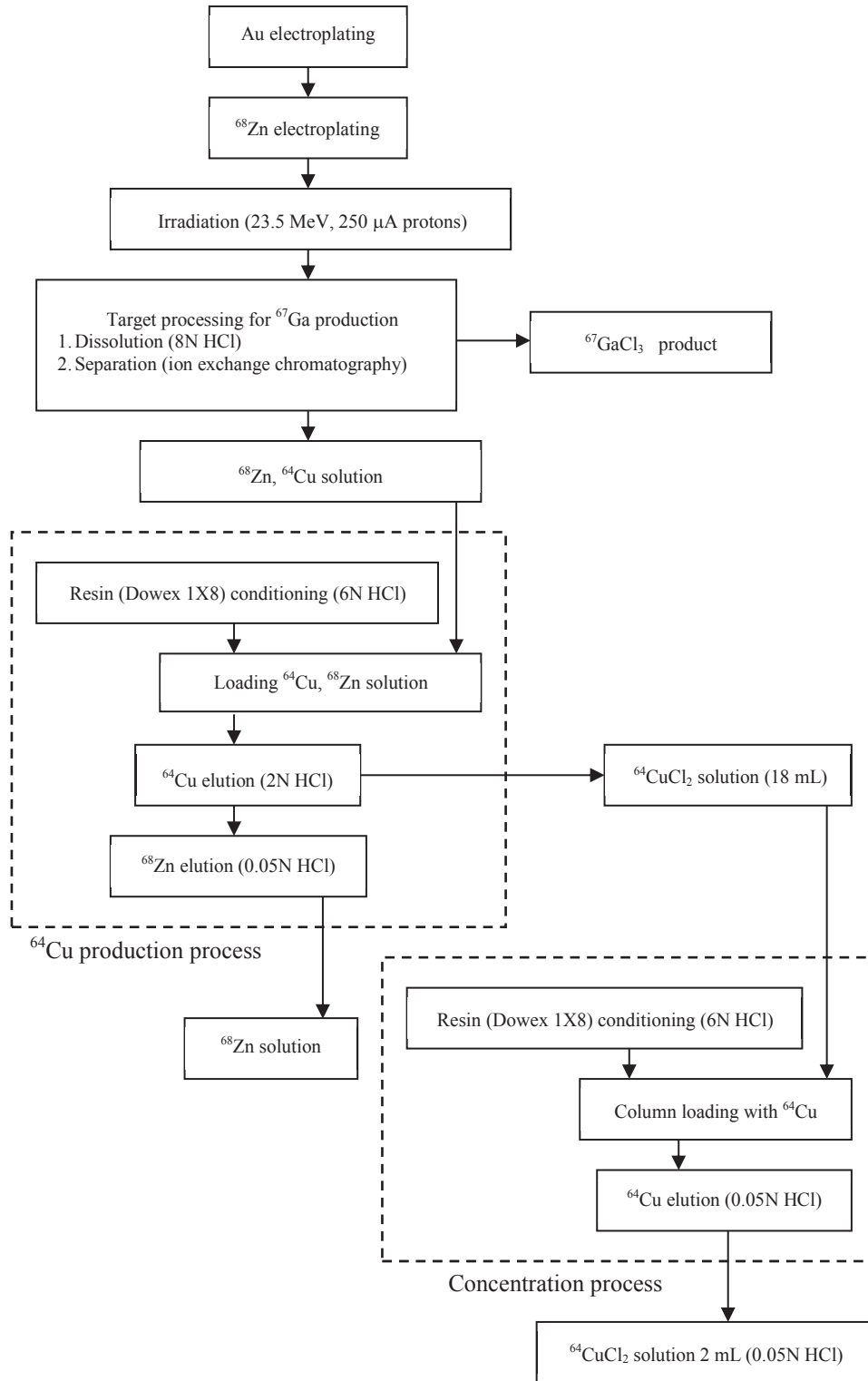


FIG. 13. Purification of  $^{64}\text{Cu}$  produced via the reaction  $^{68}\text{Zn}(p, an)^{64}\text{Cu}$ .

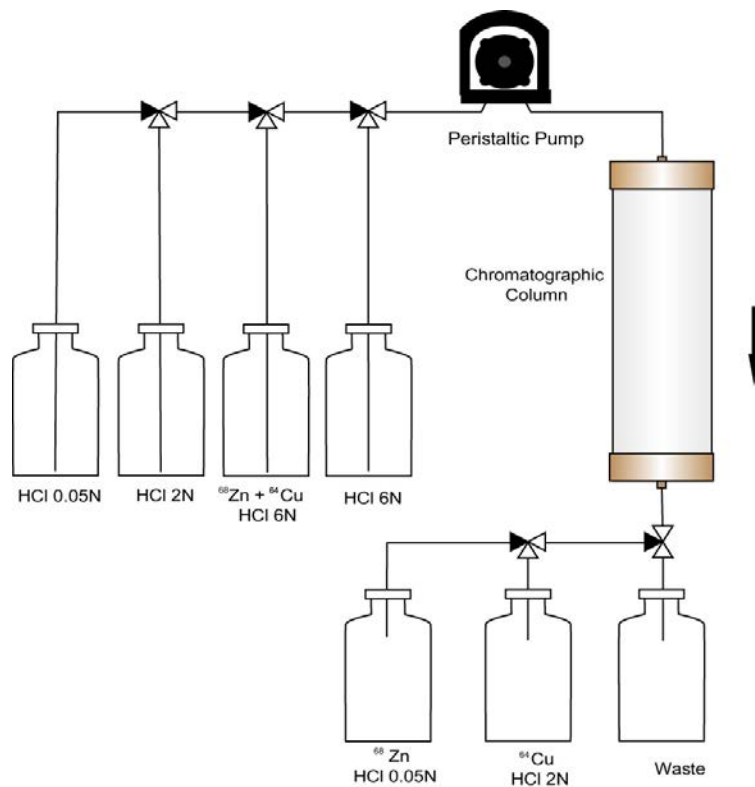


FIG. 14. Scheme of the apparatus for the  $^{64}\text{Cu}$  production process.

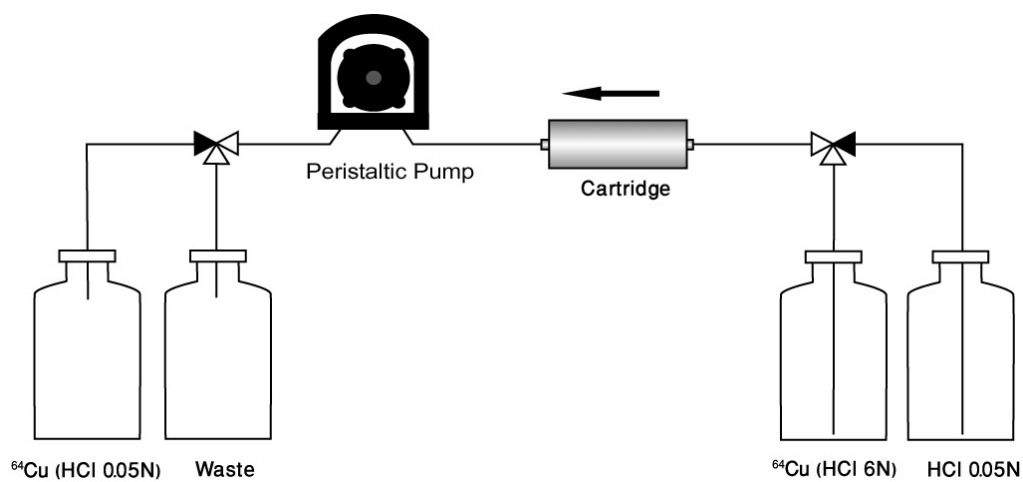


FIG. 15.  $^{64}\text{Cu}$  concentration unit.

### 2.6.1. Radioactivity measurements

The radioactivity measurements are usually performed with a dose calibrator. An initial cross-calibration with a high purity Ge detector (if available) for the accuracy of the dose calibrator for  $^{64}\text{Cu}$  is suggested.

### 2.6.1.1. Radionuclidic purity

The radionuclidic purity should be measured with a  $\gamma$  ray spectrometer. Figure 16 shows a clean  $\gamma$  ray spectrum of  $^{64}\text{Cu}$ .

Because all production routes produce radionuclidic impurities (isotopes of Co, Zn and Ga for example) that must be removed by chemical separation before use, a final gamma spectroscopy measurement is needed. Under well explored and validated conditions, this can be done by the simpler means of sodium iodide and lanthanum bromide scintillation counters, but in general, solid state Ge detectors are best. If the  $^{64}\text{Cu}$  is produced via  $^{68}\text{Zn}$  targets with the risk of the presence of contaminant  $^{67}\text{Cu}$ , the precise quantification of  $^{67}\text{Cu}$  and the exclusion of  $^{67}\text{Ga}$  become tricky, as they rely on careful evaluation of line area ratios in the low energy region with strong Compton background.

When pursuing the  $^{68}\text{Zn}$  route, 23.5 MeV can be considered the optimum energy to maximize the  $^{67}\text{Ga}$  and  $^{64}\text{Cu}$  yield and minimize the quantities of  $^{67}\text{Cu}$  and  $^{66}\text{Ga}$  produced. In this case, the quantification of  $^{64}\text{Cu}$  should be made using the information coming from the peak at 1346 keV (Fig. 17). Its measurement presents challenges because of the lower efficiency at this energy range; however, this peak is specific and is the one to be used for quantification. The peak at 511 keV cannot be used for quantification because it has several contributions, including  $^{64}\text{Cu}$  but also  $^{66}\text{Ga}$ .

The three main impurities to identify and quantify are  $^{67}\text{Ga}$ ,  $^{67}\text{Cu}$  and  $^{66}\text{Ga}$ . The last of these does not present any particular challenge; it can be measured at the 1039 keV peak, which is specific for  $^{66}\text{Ga}$ . However,  $^{67}\text{Ga}$  and  $^{67}\text{Cu}$  are more complicated to measure because both radioisotopes share all the principal  $\gamma$  ray emissions, as can be seen in Table 6.

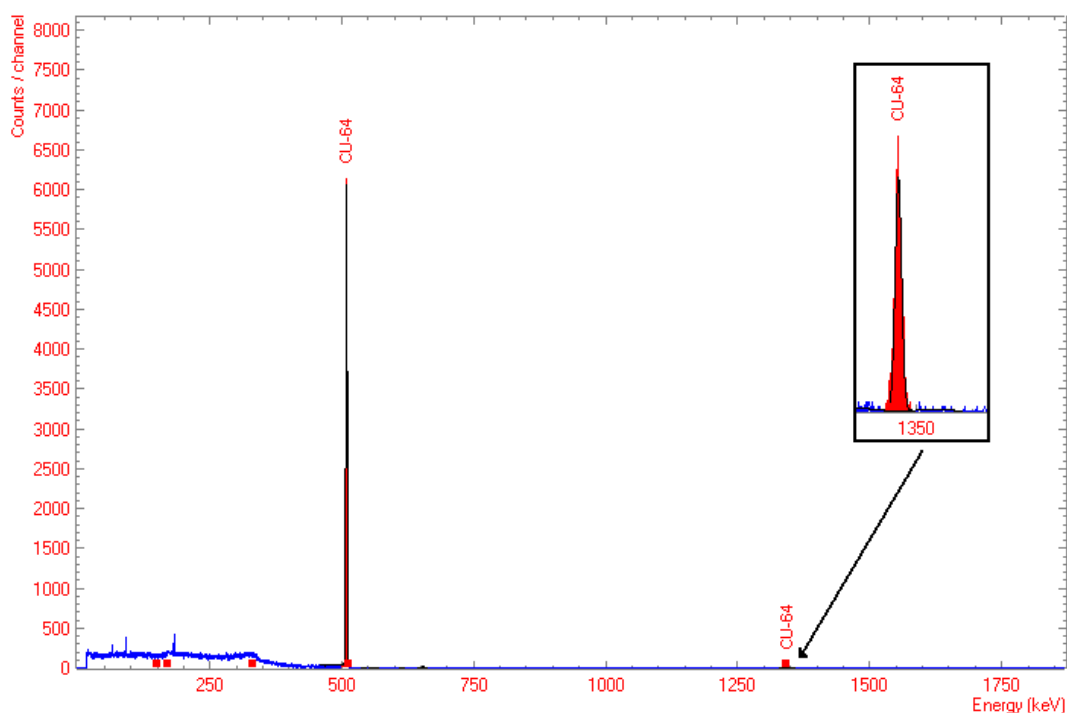


FIG. 16. Gamma spectrum of the produced  $[^{64}\text{Cu}]\text{CuCl}_2$  solution with no major radionuclidic contaminants. It should be noted that the 511 keV peak by itself is not a sure sign of  $^{64}\text{Cu}$ , but only indicates the presence of some relatively pure positron emitter. More important is the absence of other gamma lines except the 1346 keV line from  $^{64}\text{Cu}$ .



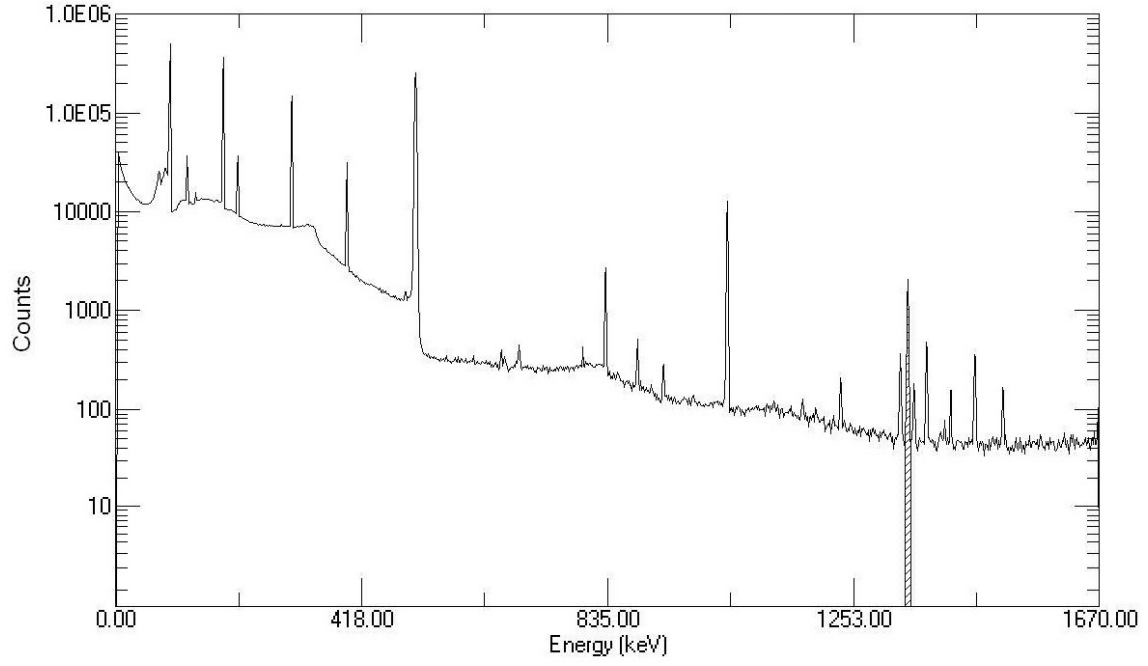


FIG. 17. Gamma spectra data of  $^{64}\text{Cu}$  purified fraction.

TABLE 6. COMPARISON OF  $\gamma$  RAY EMISSIONS FROM  $^{67}\text{Ga}$  AND  $^{67}\text{Cu}$

Gamma energy (keV)	Ga-67	Cu-67
	I%	I%
91.265	3.11	7.00
93.310	38.81	16.10
184.576	21.410	48.7
208.950	2.460	0.115
300.217	16.64	0.797
393.527	4.56	0.220
494.166	0.0684	—
703.106	0.0105	—
794.381	0.0540	—
887.688	0.148	—

Considering the cross-section for the reaction  $^{68}\text{Zn}(p, 2p)^{67}\text{Cu}$ , the determination of  $^{67}\text{Cu}$  becomes important only if the incident energy of the protons is close to, or higher than, 40 MeV. At 23.5 MeV, the production rate of  $^{67}\text{Cu}$  is quite low ( $<0.01\%$ ) [11].

### 2.6.1.2. Measurements of the effective specific activity

The theoretical obtainable maximum specific activity (radioactivity per unit mass) for  $^{64}\text{Cu}$  is 9.4 TBq/ $\mu\text{mol}$  (254 Ci/ $\mu\text{mol}$ ). However, this theoretical value is never obtained in practice, because some contents of inactive Cu always leak into the production process.

For use as a radiolabel in PET tracers,  $^{64}\text{Cu}$  is chelated by a bifunctional macrocyclic (2,2',2'',2'''-(1,4,8,11-tetraazacyclotetradecane-1,4,8,11-tetrayl)tetraacetic acid (TETA), 1,4,7,10-tetraazacyclododecane-1,4,7,10-tetraacetic acid (DOTA), 2,2',2'''-(1,4,7-triazanone-1,4,7-triyl)triacetic acid (NOTA), etc.), which itself has been complexed to peptides, proteins, liposomes, nanoparticles and antibodies. In order to reach high specific activities for the tracers, it is important to not only have  $^{64}\text{Cu}$  with high specific activity, but also to ensure that the labelling solution is free of competitive metals that might occupy chelation sites.

When producing the labelling solution, it is useful to measure the amount of competitive metals it contains. This is known as the effective specific activity (ESA), and represents the amount of the radiometal relative to the non-radioactive competitive metals, typically expressed in units of Ci/ $\mu\text{mol}$  or GBq/ $\mu\text{mol}$ .

The ESA of  $^{64}\text{Cu}$  is determined by titration of  $[\text{}^{64}\text{Cu}]\text{Cu}^{2+}$  against a suitable chelator. The most commonly used chelators are TETA and NOTA.

### 2.6.1.3. TETA titration

The ESA of  $^{64}\text{Cu}$  can be determined by titration of  $[\text{}^{64}\text{Cu}]\text{CuCl}_2$  with the macrocycle TETA as shown in Fig. 18. This involves adding 30 mL aliquots of diluted  $^{64}\text{Cu}$  stock solution (11–18 GBq at end of bombardment) to vessels containing 100  $\mu\text{L}$  of 0.04M  $\text{NH}_4\text{OAc}$  buffer solution. Additional volumes of  $10^{-6}$ – $10^{-7}\text{M}$  TETA solution (25–200  $\mu\text{L}$ ) are added to the vessels, which are then vortexed and incubated for 20 min at 80°C. The percentage of the radionuclide chelated in each aliquot is determined when the yield of  $^{64}\text{Cu}$ -TETA is higher than 95%. Alternatively, the 50% complexation point may be determined and doubled to calculate the total metals present in the solution that form a complex with the chelator used.

The method for measuring ESA is by titration with the chelator (e.g. TETA), wherein the radiometal is added to buffered chelator solutions of various concentrations under favourable conditions (pH, temperature, time) for chelation. The amount of complexed radiometal relative to unbound radiometal as a function of chelator concentration gives the ESA. Therefore, the ESA measurement can also be considered a quantification of the reactivity of the labelling solution.

While these measurements show what the end user wants to know regarding how much activity to add to a precursor, they provide little guidance to the producer of  $^{64}\text{Cu}$  labelling solution. If labelling yields are poor, is there a problem with the reaction conditions or the precursor, or is there a cold metal contaminant, and if so, which metal(s) should be removed?

The aim of one study was to give some resolution in this area. In particular, it attempted to answer the following questions: How does the ESA measurement correlate with the total non-radioactive metal concentration? Which metals are the most competitive at standard conditions? Does this picture change when moving from the free chelator to the bifunctionalized chelator, which has one less carboxyl group available for facilitating and stabilizing chelation?

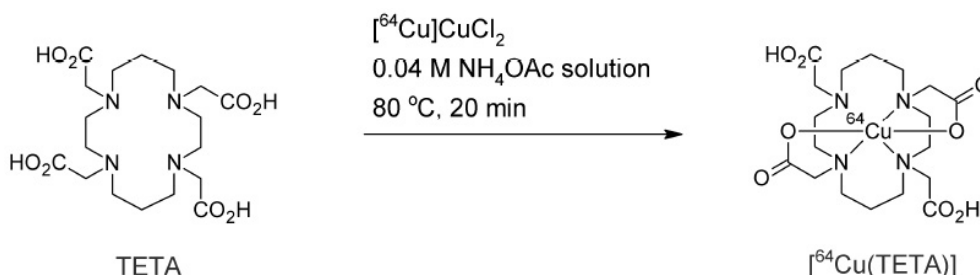


FIG. 18. Formation of the  $^{64}\text{Cu}$ -TETA complex by complexation of  $^{64}\text{Cu}^{2+}$  with TETA.

In principle, theoretical considerations should be able to address these questions. However, trace chemistry often varies from bulk behaviour, and with many metals in possible competition, theory becomes difficult to implement. Thus, questions can be addressed purely experimentally: by performing TETA and DOTA-octreotate (DOTATATE) titrations on  $^{64}\text{Cu}$  solutions which contain known amounts of added non-radioactive metals, and independently determining the concentrations of each metal by inductively coupled plasma optical emission spectrometry (ICP-OES).

In an experiment, samples of  $[\text{}^{64}\text{Cu}]\text{CuCl}_2$  were taken from weekly batches of good manufacturing practices (GMP) grade  $^{64}\text{Cu}$  produced at the Hevesy Laboratory in Denmark. (The procedure for production and purification of GMP  $^{64}\text{Cu}$  is outlined in the previous sections.) ICP-OES was used to determine the amounts of competitive metals in the solution, particularly the concentrations of Cu, Ni, Zn and Fe. The  $^{64}\text{Cu}$  was buffered in 0.1M  $\text{NH}_4\text{OAc}$ , pH5.5, that had been stored over chelex resin and was determined by ICP-OES to be metal free below the detection limits (typically 0.5–5 ppb depending upon the metal).

In separate experiments, the effect of common metal impurities on TETA and DOTATATE labelling were tested by reacting a fixed solution of TETA (200  $\mu\text{L}$ , 370 nM) or DOTATATE (200  $\mu\text{L}$ , 1.7  $\mu\text{M}$ ) with 200  $\mu\text{L}$  of solutions containing varying concentrations of metals. TETA containing solutions were incubated for 1 h at 35°C, and DOTA containing solutions were reacted at 90°C for 10 min. The metal solutions were prepared by dissolution of metal chloride salts in buffer, followed by serial dilution with more buffers. The concentration of each metal in the solutions was determined by ICP-OES in order to verify the dilutions. In the case of Fe(III), stable solutions against hydrolysis could not be achieved, and no agreement was found between the dilution and ICP-OES analyses. Therefore, Fe(II) was used instead because it offered enhanced solubility. Small (1  $\mu\text{L}$ ) samples of the reacted solutions were then spotted onto Al-backed silica gel thin-layer chromatography (TLC) plates and run with 1:1 v/v MeOH:buffer (0.1M  $\text{NH}_4\text{OAc}$  as described above) as the mobile phase. The  $^{64}\text{Cu}$ -TETA complex moved to a retardation factor ( $R_f$ ) of roughly 0.55, while uncomplexed  $^{64}\text{Cu}$  remained at the origin. The numbers of nmol of the metals in each sample are shown in Table 7 along with the percentage of labelled tracer versus 37 pmol TETA or 334 pmol DOTATATE, and these results are shown graphically in Figs 19 and 20.

TABLE 7. NANOMOLES OF METAL IONS IN SOLUTION AND THEIR EFFECT ON  $^{64}\text{Cu}$  LABELLING OF 37 pmol TETA AND 334 pmol DOTATATE (IN SEPARATE EXPERIMENTS)

Sample name	$\text{Cu}^{2+}$	$\text{Zn}^{2+}$	$\text{Ni}^{2+}$	$\text{Fe}^{2+}$	%Cu-64-TETA	%Cu-64-DOTATATE
Ø	3.0E-02				89.74	99.3
Cu1	4.3E-02				83.3	94.3
Cu2	7.0E-02				58.2	99.4
Cu3	1.5E-01				18.1	97.4
Cu4	4.4E-01				3.2	50.5
Zn1		4.3E-02			100	99.5
Zn2		1.1E-01			100	97.7
Zn3		3.9E-01			100.00	72.0
Zn4		6.3E-01			99.76	53.9
Zn5		1.7E+01			96.3	
Zn6		2.2E+02			76.97	
Zn7		8.9E+02			54.81	

TABLE 7. NANOMOLES OF METAL IONS IN SOLUTION AND THEIR EFFECT ON  $^{64}\text{Cu}$  LABELLING OF 37 pmol TETA AND 334 pmol DOTATATE (IN SEPARATE EXPERIMENTS) (cont.)

Sample name	$\text{Cu}^{2+}$	$\text{Zn}^{2+}$	$\text{Ni}^{2+}$	$\text{Fe}^{2+}$	%Cu-64-TETA	%Cu-64-DOTATATE
Ni1			6.2E-01		99.74	
Ni2			6.8E+00		95.72	
Ni3			4.2E+01		84.31	
Ni4			2.6E+02		40.15	
Fe1				3.7E-02	97.76	
Fe2				1.8E-01	97.4	
Fe3				3.7E-01	97.26	
Fe4				7.5E-01	96.46	

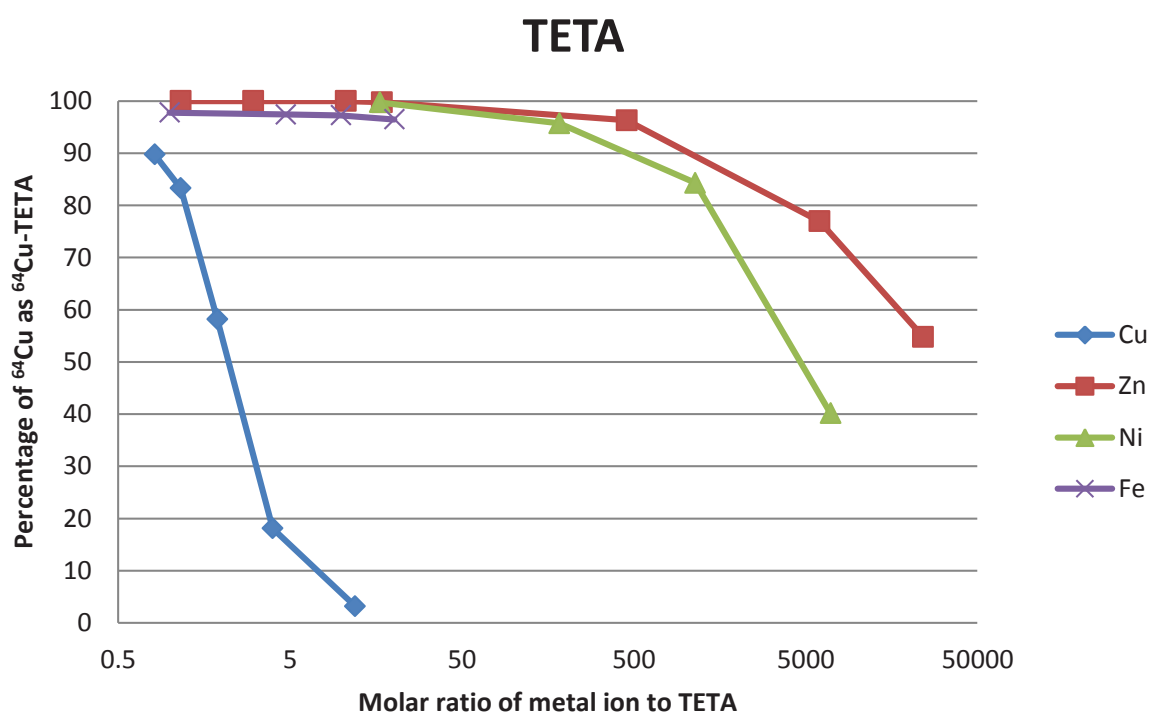


FIG. 19. A plot of results from Table 7 for TETA labelling.

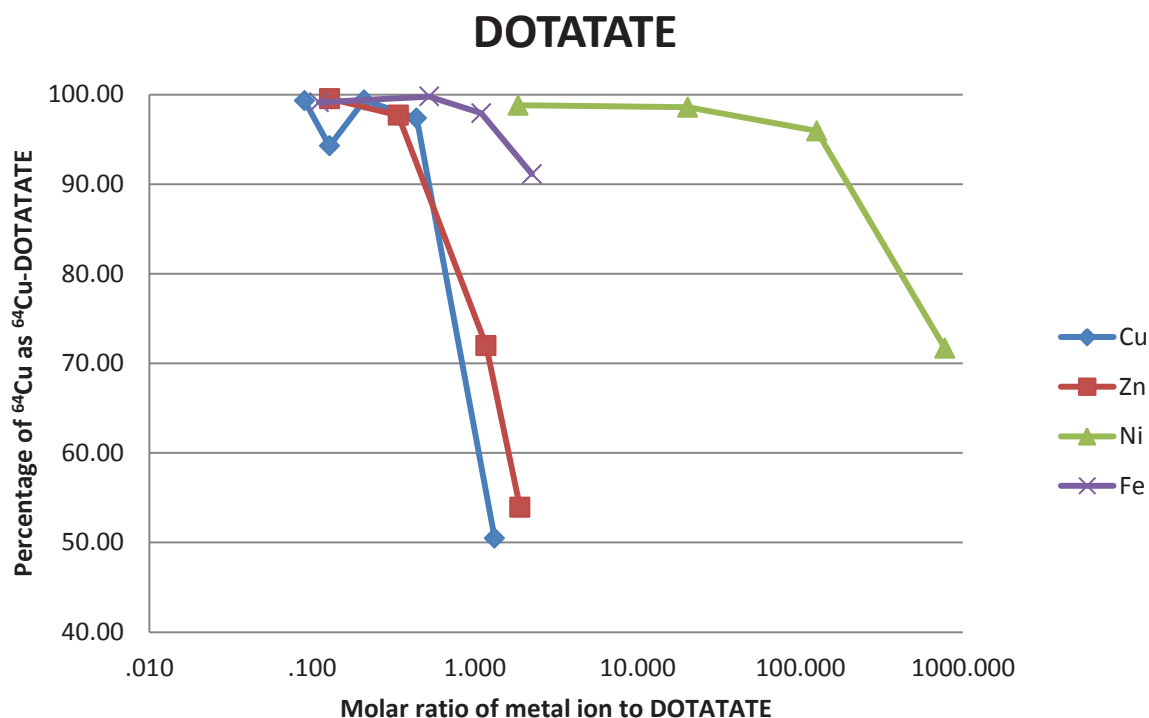


FIG. 20. A plot of results from Table 7 for DOTATATE labelling.

The results show quite clearly that Cu(II) is selectively labelled into TETA without influence from the other metal ions until they reach significantly higher concentrations. For DOTATATE, the labelling is less selective towards Cu, with a comparable rate of binding observed for Zn(II).

Based upon these results, when assessing the literal specific activity, TETA chelation seems to be a good choice because it selectively binds Cu over common metal ions. In order to investigate its efficacy as a metric, titrations were next performed of Cu containing solutions with known concentrations of TETA, and the results compared with ICP-OES.

Titrations of various solutions were performed with TETA solutions in  $\text{NH}_4\text{OAc}$  buffer of the following concentrations: 0, 80 nM, 370 nM, 920 nM and 3.6  $\mu\text{M}$ . Then 100  $\mu\text{L}$  of each of these solutions was added to 400  $\mu\text{L}$  of buffered  $^{64}\text{Cu}$  solution, mixed, and incubated for 10 min at 35°C according to the procedure outlined above. Small (1  $\mu\text{L}$ ) samples of the solutions were spotted onto Al-backed silica gel TLC plates and run with 1:1 v/v MeOH:buffer (0.1M  $\text{NH}_4\text{OAc}$  as described above) as the mobile phase. The  $^{64}\text{Cu}$ -TETA complex moved to roughly  $R_f = 0.55$ , while uncomplexed  $^{64}\text{Cu}$  remained at the origin. The percentage of complexed  $^{64}\text{Cu}$  versus TETA mass is shown in Fig. 21. The Cu(II) concentration ranged from 5 to 20 ppb and was tested by ICP-OES (Table 8). In this table, the TETA numbers are given without an uncertainty, because the precision is not determined. A rough estimate assumes 5% uncertainty from counting statistics and pipetting precision, but systematics may play a larger role. The ICP-OES precision is the standard deviation of three measurements.

The amount of Cu in each sample was calculated by taking a data point with labelling between 15 and 85% (assume linearity in this region) and dividing the quantity of TETA by the fraction of  $^{64}\text{Cu}$  as  $^{64}\text{Cu}$ -TETA. Division by the volume of the sample (200  $\mu\text{L}$  in this case) and multiplication by the molar mass of Cu gives the concentration in ppb, shown in Table 8. The column labelled Dilution indicates the amount of Cu in each solution determined by mixing solutions with concentrations determined by ICP-OES (with about 20% precision at such low concentrations).

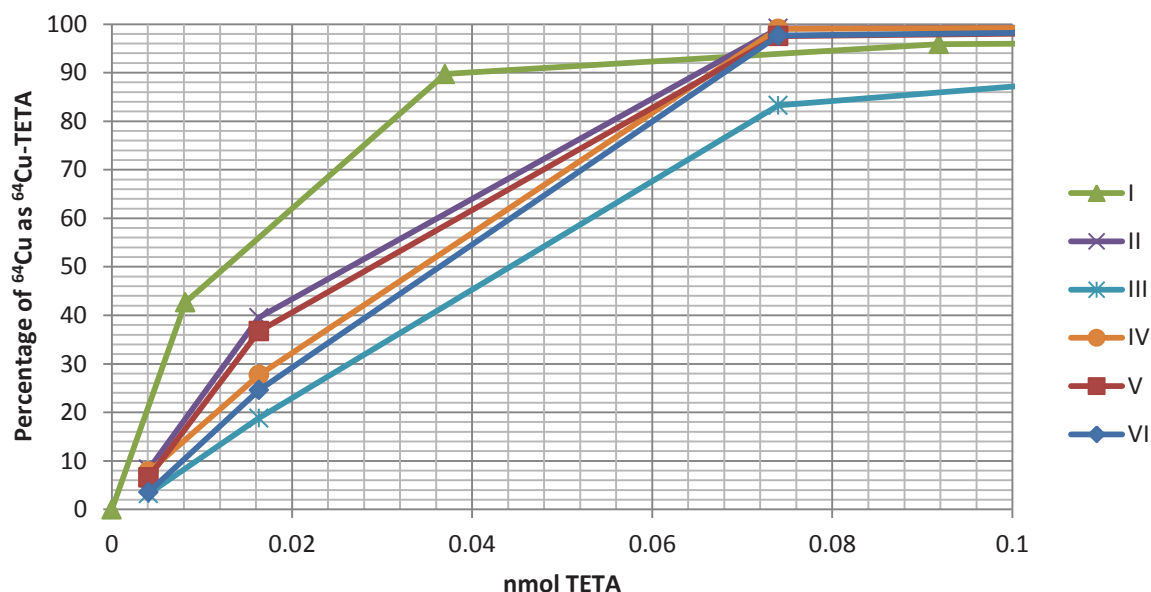


FIG. 21. TETA titration results, showing the percentage of  $^{64}\text{Cu}$  as  $^{64}\text{Cu}$ -TETA for 200  $\mu\text{L}$  samples of different Cu containing solutions.

TABLE 8. A COMPARISON OF TETA TITRATION AND ICP-OES FOR DETERMINING THE CONCENTRATION OF Cu(II) IN SOLUTION

Sample	Dilution	TETA titration	ICP-OES precision
I	—	6	$10 \pm 2$
II	$7 \pm 1$	13	$11 \pm 2$
III	$13 \pm 3$	28	$19 \pm 3$
IV	$9 \pm 2$	19	$14 \pm 3$
V	$7 \pm 1$	14	$17 \pm 5$
VI	$10 \pm 2$	21	$11 \pm 1$

The results indicate that TETA titration will give an estimate of specific activity comparable to that given by ICP-OES, always within a factor of two. The precision with which the titration can be performed is yet to be determined.

TETA titration creates a fair measure of the amount of cold Cu in a solution without interference from common metal impurities. Thus, it is a good metric for the determination of true specific activity. The reactivity, however, may be influenced by competitive metals (e.g. Zn(II) with DOTATATE); therefore the chemical purification of  $^{64}\text{Cu}$  should still be as metal free as possible. Also, a TETA titration is not necessarily the right method to determine if the labelling solution will achieve a high labelling yield. Rather, the precursor should be tested in a titration with  $^{64}\text{Cu}$  prior to committing large amounts of either  $^{64}\text{Cu}$  or precursor to a reaction.

#### 2.6.1.4. Competing metals

For quality control with radioactive samples, titration against a chelator is the normal procedure to determine the amount of competing metals in the solution. In some cases, other metals will also bind to the chelators to a different degree. The most harmful contaminants are the stable Cu isotopes  $^{63}\text{Cu}$  and  $^{65}\text{Cu}$ . These compete directly

with  $^{64}\text{Cu}$  for complexation to the chelator. Other metals that can be found in the  $^{64}\text{Cu}$  solution in quantities of  $\mu\text{g/L}$  are Ni, Zn, Fe, Al and Pb. Metals with high affinity for the chelator will compete with the Cu. Stability constants of metal complexes of several common chelators are listed by Anderegg et al. [17].

## 2.6.2. Measurement of cold metal contaminants

The producers of  $^{64}\text{Cu}$  face a dilemma when they are occasionally asked for a broadband elemental analysis of their outgoing  $^{64}\text{Cu}$  solution. Commercial analytical laboratories using inductively coupled plasma mass spectrometry refuse to accept radioactive samples, and waiting for six orders of magnitude decay to the level of background radiation would entail a delay of several weeks, meaning the service would be of no use to the user. This would suggest that dedicated equipment would be needed, at a considerable cost for the initial purchase and operation. The current use of titration with various chelators will act as a 'go/no go' gate to alert the end user, but the question remains whether to use TETA (Cu specific) or NOTA (generally preferred by the labelling community) as the indicator of true or effective specific activity. For a broadband assay, four alternatives (with ppb sensitivity) have been identified to the prohibitively expensive technique of inductively coupled plasma mass spectrometry. These are listed in Table 9.

While the X ray fluorescence technique appears not to be well suited for the task of elemental analysis of radioactive samples, it does provide ppm signals if the  $^{64}\text{Cu}$  activity is less than 1  $\mu\text{Ci}$  (37 kBq) on the planchette, holding a dried residue from a 10  $\mu\text{L}$  aliquot. The betas (plus and minus) contribute a broad (MeV) background under the keV  $K_{\alpha}$  peaks of the transition metals, but the electron capture decay (41%) of  $^{64}\text{Cu}$  results in an intense  $K_{\alpha}$  background overwhelming any analysis of Ni levels. For all of its drawbacks with radioactive samples, the X ray fluorescence instrument is ideal for rapidly searching for the source of confounding metals in the cold reagents and blank runs, allowing tens of samples to be analysed unattended in a few hours, with minimal preparation of the sample matrix.

### 2.6.2.1. Ion chromatography

A high performance liquid chromatography (HPLC) method (Dionex) that measures trace amounts of metals (ppb) has been used to measure the transition metal contaminants in  $^{64}\text{Cu}$  lots. Ion chromatography is simple, fast (<25 min) and practical for routine measurement of the specific activity of  $^{64}\text{Cu}$ .

Copper-64 samples are diluted with trace metal free water. Then 1 mL of each sample is injected into the metal free ion chromatography system. The eluent (1.4 mM pyridine-2,6-dicarboxylate/13.2 mM potassium hydroxide/1.12 mM potassium sulphate/14.8 mM formic acid) is passed through the column at 0.30 mL/min. As the metals elute from the column, they pass through a mixing loop where they are mixed with 1.0M 2-dimethylaminoethanol/0.50M ammonium hydroxide/0.30M sodium bicarbonate containing 0.06 g/L 4-(2-pyridylazo)resorcinol (PAR) flowing at 0.15 mL/min. During this time, the metals complex with the PAR dye and then they are passed through a detector and measured at 530 nm. A typical chromatogram for calibration is shown in Fig. 22.

TABLE 9. COMPARISON OF TECHNIQUES USED TO ANALYSE NON-RADIOACTIVE CONTAMINANTS IN  $^{64}\text{Cu}$  SOLUTIONS

Technique	Elemental range	Advantages	Disadvantages
Ion exchange HPLC <sup>a</sup> with post-column dye	3-d shells	Lower instrument cost	Reagent cost
ICP-OES	Almost all except As, Se	Very sensitive, rapid analysis	Ar cost
X ray	Al–U except Mo, Nb	No sample preparation	No radioactivity
Voltammetry		Low cost	Potential low sensitivity

<sup>a</sup> HPLC = high performance liquid chromatography.



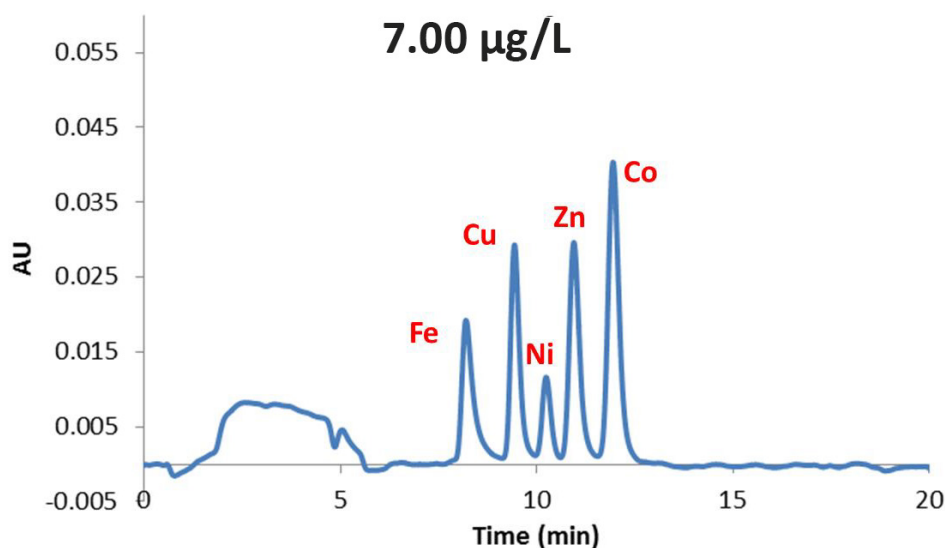


FIG. 22. Typical ion chromatogram. AU — absorbance unit.

Calibration curves were made for Fe, Cu, Ni, Zn and Co. The  $R^2$  values for these curves are all 0.989 or better. The lower limit of detection for Cu and Co is 1 µg/L, for Fe and Ni it is 2 µg/L, and for Zn it is 3 µg/L. All samples were brought between the lower limits and 10 µg/L for analysis.

#### 2.6.2.2. Anodic stripping voltammetry

The chemical purity of  $[^{64}\text{Cu}]\text{CuCl}_2$  produced can be determined by anodic stripping voltammetry. The concentration of Zn and Cu were 0.1 and 0.05 µg/mL, respectively, in  $^{64}\text{Cu}$  produced by irradiation of a Zn target.

#### 2.6.2.3. Optimization of specific activity and elimination of foreign metal contaminants from the labelling solution

High specific activity and, equivalently, the absence of other metals in the labelling solution are critical quality parameters defining the  $^{64}\text{Cu}$  product. In most cases and for most known  $^{64}\text{Cu}$  labelled radiopharmaceuticals, other divalent transition metal cations might interfere or compete with the Cu radiotracer for labelling into the limited amount of chelator in the pharmaceutical substrate. The only recognized exception is  $^{64}\text{Cu}$ -ATSM, which is seen as very Cu specific. The ATSM labelling can normally be carried out even with some foreign metals present. Consequently, it should be observed that apparent success in  $^{64}\text{Cu}$  labelling does not guarantee that other pharmaceuticals will be labelled with equal success.

The  $^{64}\text{Cu}$  specific activity has to be high to allow for efficient labelling of small amounts of the substrate. The exact requirements for specific activity will depend on the application at hand, but substoichiometric labelling conditions will always be necessary for high labelling yields (the ratio  $[\text{Cu}]/[\text{chelator}]$  must be  $<1$ ).

The most demanding applications of  $^{64}\text{Cu}$  for labelling are at present found when used for nanoparticles or intact antibodies, but high specific activity could also be demanded for peptide labelling.

The theoretical obtainable maximum specific activity for  $^{64}\text{Cu}$  is 9.4 TBq/µmol (254 Ci/µmol). However, this theoretical value is never obtained in practice, because some inactive Cu will always leak into the production process.

During the course of the CRP, the  $^{64}\text{Cu}$  production groups reported specific activities in the range of 200–7000 GBq/µmol. Unfortunately, it is common for the specific activity to be highly variable. Much effort has already been devoted to development of Cu free target preparation and target/activity separation procedures, but it is recognized that further work is warranted.

During the same period, an attempt was made to identify possible sources of the confounding Cu. Similar attempts have been made over the years concerning the sources of cold C in the production of  $^{11}\text{C}$  pharmaceuticals, but the present situation with  $^{64}\text{Cu}$  (and other transition metals) is more complicated, with a much more open loop of target/activity handling and with widespread use of strong mineral acids in the vicinity of inevitable metallic parts. Automation and mandated radiation protection measures (like automated target loading, unloading and hot



cell transfer) may well add to the metal contamination problem unless addressed deliberately from the beginning of the system design.

### 2.6.3. Identification of possible sources of metal contamination

The following paragraphs describe possible sources of contaminant metals.

- (a) Original supplied  $^{64}\text{Ni}$  metal powder: The chemical impurities should always be stated in the compulsory certificate of analysis along with the relevant isotopic abundance factors for Ni isotopes. Unless further purified, Cu contents in the original target material batch will always limit the obtainable specific activity. Many impurities stated in the certificate of analysis will have no relevant influence on the radionuclidic purity of the product, but may well prevent any successful labelling with activity derived from such target material. Direct ways for undertaking relevant chemical analysis of the target material upon reception require sophisticated and expensive equipment, which is not generally justifiable within a PET isotope facility, and the certificate of analysis limit values for relevant metals should normally be trusted. Recycling  $^{64}\text{Ni}$  (when carefully handled) will improve the specific activity.
- (b) Acids for  $^{64}\text{Ni}$  dissolution, plating bath composition and purification ( $\text{HCl}$ ,  $\text{HNO}_3$ ,  $\text{H}_2\text{SO}_4$ ): These acids may all contribute a metal load to the  $^{64}\text{Cu}$  preparation. Very pure grades of acids are available, with acceptable specifications, however at a considerable price given the large quantities of acids necessary. Lower grades might be acceptable at some process steps; however, a careful analysis of the impact on the overall metal load is warranted.
- (c) Glassware and disposables: Intact glassware of good quality or clean and well wrapped disposable plastic should always be used. All components (beakers, vials, stoppers, etc.) should always be washed in acid ( $\text{HCl}$  or  $\text{HNO}_3$ ) and rinsed in clean water prior to use.
- (d) Water: Process water and water for rinsing should be metal free. Observation of the conductivity of the water is not in itself sufficient guarantee that the water is of sufficient quality. Most commercial laboratory water purifiers do reduce metal contents of water, but such systems need regular maintenance, cartridge replacements and quality control.
- (e) Ion exchange resin: New resin material should always be rinsed carefully before use. It has been observed that some metal ion impurities are only removed after repeated cycles of washing with 6M  $\text{HCl}$  and 0.1M  $\text{HCl}$ . Due to the detrimental effects of resin swelling and contraction, it is normally not advisable to wash columns with acid concentrations below 0.1M. Some laboratories reported improvement with multiple uses of the resins.
- (f) Anode, either a graphite rod or Pt wire or foil: The purity of the anode material has been shown to have influence on target content of Cu when using graphite. Very high purity graphite is available and should be used.
- (g) Metal parts near plating bath: The corrosive plating bath and the acids used for leaching and cleaning will attack most metals nearby. Any metal debris falling into the bath will contaminate the target. Glass, plastic or Teflon parts are preferable for the plating cell. Special attention should be paid to the Cu wires and plugs used for electrical connection to anode and cathode.
- (h) Instruments: Handling of the backing and the plated target should be done avoiding the use of metal tweezers.
- (i) Target backing: The target backing should be free from Cu. This is normally not a problem when using Au, but users of Ag backings should only use material known to be free of Cu.
- (j) Cooling water on back of target: In many production set-ups, the cooling water is in direct contact with the target backing. Cooling water is normally not metal free, and metal contents might even plate on the back of the target. Drying of the target back is not necessarily sufficient to eliminate this, and so called one sided deplating (etching) procedures should be preferred when high specific activity is sought.
- (k) Degradar: The degrader can contaminate the target, even when not in contact with the Ni surface. Sputtering can transport metal out of the degrader back. Aluminium is often used as degrader material, but care should be taken to avoid contamination from Cu contained in the Al.
- (l) Transport containers and systems: These systems can easily contaminate the target unless well cleaned and maintained.

- (m) Compressed air: Compressed air is often used for drying off cooling water and for moving the target in automated processes. When the air comes in direct contact with the target, the air should be well filtered.
- (n)  $\text{H}_2\text{O}_2$ : Normally,  $\text{H}_2\text{O}_2$  is only added in minute amounts if it is used, and the usual analytical quality should be sufficient. However, when using Ag backings, the addition of  $\text{H}_2\text{O}_2$  increases the leaching of Ag into the target solution.
- (o) Pipette tips, tubing, transfer line and valves: The use of valves without metal parts in contact with solution is important. Many valves are sensitive to prolonged exposure to strong mineral acids.
- (p) Column Pyrex/plastic frit: The column and the support should be free of metals.
- (q) Glassware for collection (V-Vial): The glass used for collection and evaporation of the Cu fraction should of course be capable of withstanding the boiling of HCL without the release of metals.
- (r) Drying Ar: Gases used for evaporation and drying should be filtered just in front of the point of application. Pressure reduction and metering valves occasionally shed metal particles into the gas stream.

## 2.7. RADIOLABELLING METHODS

### 2.7.1. $^{64}\text{Cu}$ -ATSM

Kits to be used for the production of  $^{64}\text{Cu}$ -ATSM are:

- Reconstitution solution (10% propylene glycol and 25 mM sodium acetate);
- A vial with the lyophilized ligand and some sucrose.

To make the lyophilized ligand mixture, dissolve the ATSM in a small amount of dimethyl sulfoxide and aliquot it into vials, add the sucrose and 1 mL water, then lyophilize. To prepare the dose, the reconstitution solution and  $^{64}\text{Cu}$  are added to the vial containing the lyophilized ligand. The compound is purified via a C18 Sep-Pak.

In another formulation, no-carrier-added  $^{64}\text{Cu}$  in 200 mM Gly solution is mixed with 0.2 mL of ATSM solution (0.4 mM ATSM in dimethyl sulfoxide, stored at  $-20^\circ\text{C}$ ). The radiochemical purity of  $^{64}\text{Cu}$ -ATSM can be confirmed with isocratic  $^{18}\text{C}$  HPLC in combination with spiked authentic non-radioactive Cu-ATSM and the compound used without further purification [18].

### 2.7.2. Proteins and peptides

Stable attachment of a radiometal to a biologically active molecule (e.g. peptide, protein) requires a bifunctional chelating agent [19–24]. Many different (macro)cyclic chelators are available or in development for the complexation of  $^{64}\text{Cu}$  with different complexation kinetics and thermodynamic stability (Fig. 23). Generally, two different labelling protocols are used, pre-labelling (wherein the chelating agent is first complexed with the radiometal and subsequently conjugated to the targeting ligand) and direct labelling (wherein the targeting ligand is first conjugated to the chelating agent and subsequently radiolabelled), with the latter protocol being predominant.

In general, fast and efficient radiolabelling is performed in an aqueous buffer solution at elevated temperatures (from room temperature up to  $90^\circ\text{C}$ ) within a reaction time between 15 min and 1 h. Structural integrity of most proteins, however, is compromised at high temperatures ( $>60^\circ\text{C}$ ). It is necessary to take into account the immunoreactivity and receptor affinity of the resulting radiotracer.

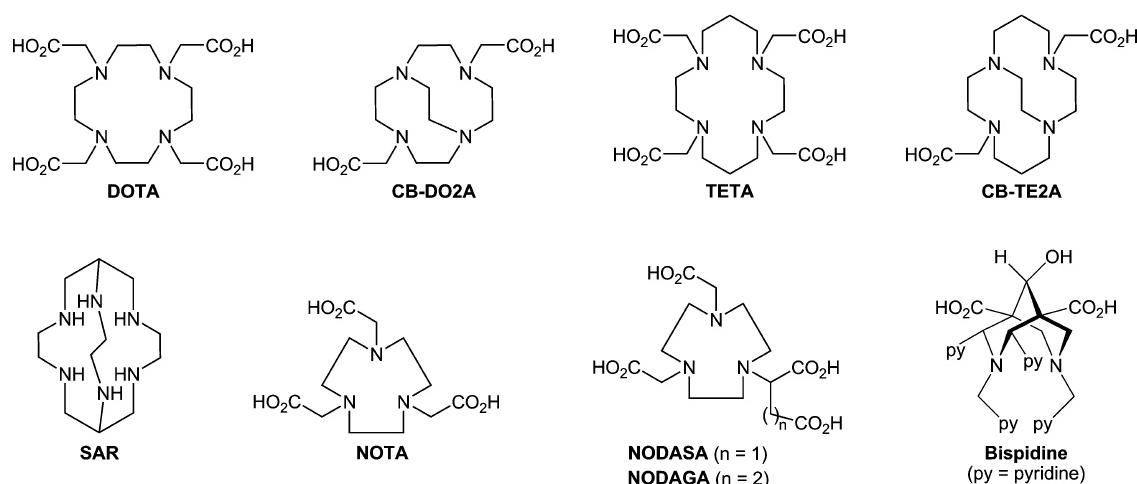


FIG. 23. Overview of different macrocyclic chelators for  $\text{Cu}^{2+}$  and other (radio)metals.

### 2.7.3. General labelling procedure

A typical  $^{64}\text{Cu}$  labelling procedure for peptides/proteins is as follows:

- (1) The ligand is dissolved in a buffered ( $\text{NH}_4\text{OAc}$ , MES, HEPES) solution (ultrapure quality, filtered 0.22  $\mu\text{m}$ , pH6–7), in an Eppendorf (Protein LoBind) tube.
- (2) An aliquot of  $[\text{}^{64}\text{Cu}]\text{CuCl}_2$  solution (0.04N HCl) is added to the peptide solution.
- (3) The pH of the reaction solution is checked and when necessary adjusted to 6–7 by adding more  $\text{NH}_4\text{OAc}$  solution. Usually a volume of  $\text{NH}_4\text{OAc}$  solution 4 or 5 times the volume of  $[\text{}^{64}\text{Cu}]\text{CuCl}_2$  solution will be sufficient.
- (4) Under (vigorous) stirring/shaking, the reaction is allowed to proceed at room or elevated temperature.
- (5) Afterwards, the reaction is allowed to cool down to room temperature.
- (6) Samples are prepared for quality control (e.g. HPLC, TLC and electrophoresis).
- (7) The protein concentration is determined using commercially available kits.

Two examples below describe practical labelling procedures and quality control set-up. Any new compound may require some variations.

Example 1: 1,4,7-triazacyclononane,1-glutaric acid-4,7-acetic acid (NODAGA)-exendin-4 peptide (1–2 nmol per synthesis) is labelled in a  $\text{NH}_4\text{OAc}$  solution (100–200  $\mu\text{L}$ ) at 90°C for 15 min, with a specific activity as high as 150 GBq/ $\mu\text{mol}$  (4 Ci/ $\mu\text{mol}$ ). Quality control is performed through reverse phase HPLC with in-line radiodetector. The radiotracer is eluted over a C18 column (250 x 10 mm) with a linear gradient from  $\text{H}_2\text{O}$  (0.1% trifluoroacetic acid (TFA)) to  $\text{CH}_3\text{CN}$  (0.1% TFA) in 20 min. Figure 24 shows a typical elution profile.

Example 2:  $^{64}\text{Cu}$  was dissolved in  $\text{NH}_4\text{OAc}$  pH5.5 to be used as  $[\text{}^{64}\text{Cu}]\text{-acetate}$  pH5.5 for radiolabelling purposes. Anti-CA 125 (cancer antigen 125) monoclonal antibody (MAb)-NOTA (420  $\mu\text{g}$ ) was mixed with ~85 MBq of  $^{64}\text{Cu}$  and allowed to react at 30°C and 450 rev./min in a thermomixer for 1 h. The reaction was terminated by addition of a 1mM final concentration of ethylene diamine tetraacetic acid (EDTA) to chelate any excess  $^{64}\text{Cu}$ . Size exclusion chromatography was performed using Econo-Pac 10DG columns equilibrated with chelex treated sodium acetate buffer pH5.5 to isolate  $^{64}\text{Cu}$  labelled anti-CA 125 MAb, which was obtained in radiochemical yield of  $69 \pm 3\%$ . Figure 25 shows an image of the results of sodium dodecyl sulphate–polyacrylamide gel electrophoresis (SDS–PAGE) analysis of the final product. The effective specific activity was determined to be 200 MBq/mg.

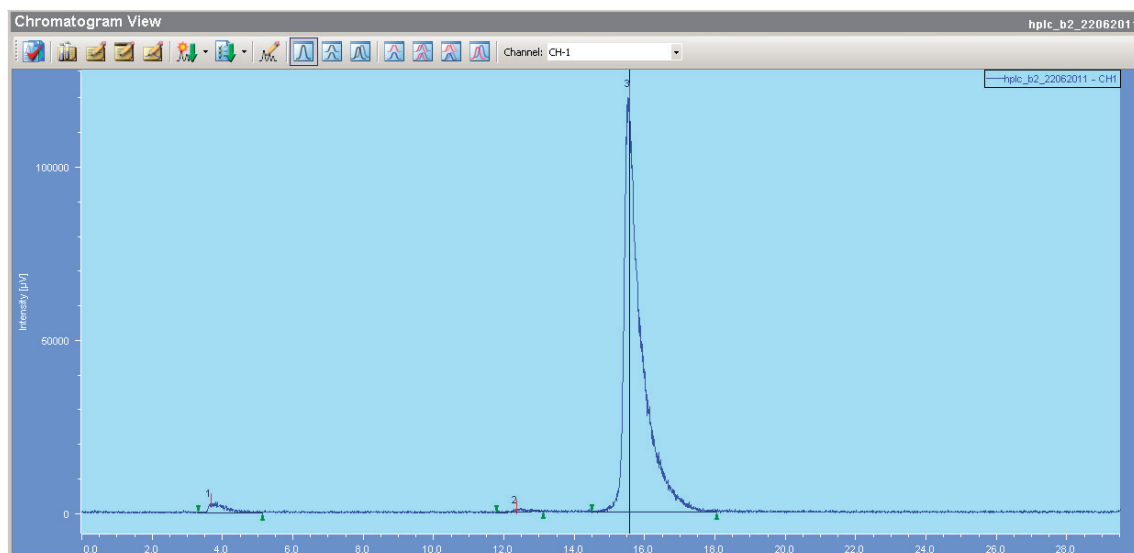


FIG. 24. Chromatogram of [ $^{64}\text{Cu}$ -NODAGA]-exendin-4 (reaction time: 15.6 min, 97% radiochemical purity) over a C18 column.

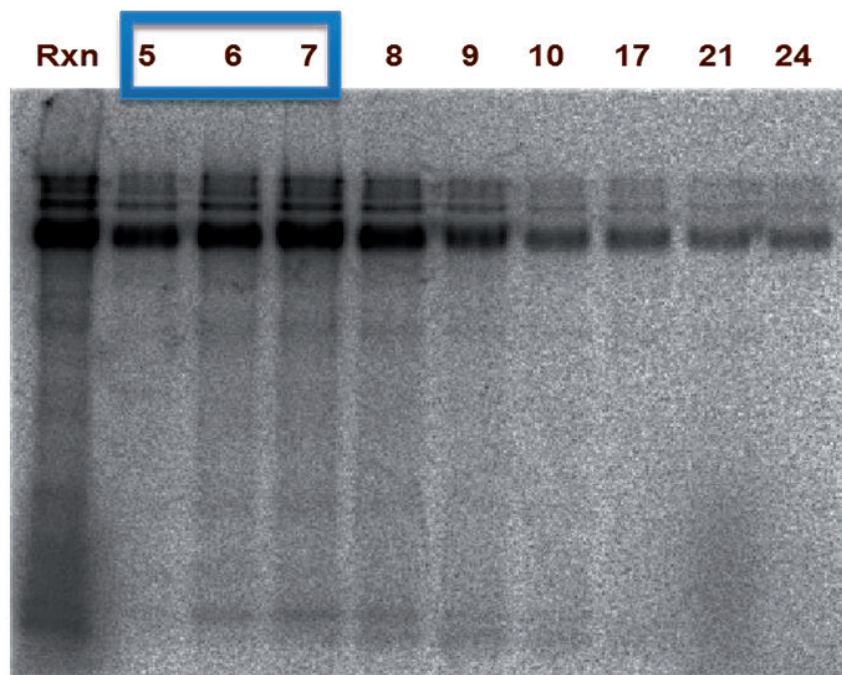


FIG. 25. Results of SDS-PAGE analysis of reaction mixture and isolated fraction containing radiolabelled anti-CA 125 MAb. Fractions 5, 6 and 7 were used for radiopharmacological evaluation.

## 2.8. APPLICATIONS

### 2.8.1. Considerations for local preparation of $^{64}\text{Cu}$ labelled radiopharmaceuticals

Any product which is intended to be injected into humans must comply with the requirements stated in the regional pharmacopoeias for injectable materials. Preparation of  $^{64}\text{Cu}$  labelled radiopharmaceuticals involves the following steps under the assumption that radioactive Cu and the bioactive agent are provided to the user and that the user has the responsibility of compounding and injecting the final drug product into the patient:

- (a) Preparation of the target (electroplating);
- (b) Irradiation;
- (c) Transfer to the extraction and recovery system;
- (d) Dispensing;
- (e) Quality control;
- (f) Transport;
- (g) Compounding;
- (h) Quality control;
- (i) Injection.

Each step has to follow certain regulations, but only a subset of them have to obey GMP regulations. Target preparation, irradiation, dispensing and transportation to the user are not required to be GMP compliant because [ $^{64}\text{Cu}$ ] $\text{CuCl}$  is supplied dry or in dilute  $\text{HCl}$  as a radiochemical. It must be kept in mind, however, that all these processes should be in accordance with quality assurance measures (documentation, method validation etc.).

The user, a hospital clinic or centralized radiopharmacy, is responsible for labelling the molecule of interest (antibody, peptide or other chemical entity attached to a chelator for binding) with  $^{64}\text{Cu}$  under GMP conditions and preparing a radiopharmaceutical which meets predefined specifications and is also pyrogen free and sterile.

The requirements may vary by region; as an example in the United States of America (USA) the end user manufactures the final drug product which is injected into the patient and which is classified as a PET drug and can be manufactured according to Title 21 of the Code of Federal Regulations (21 CFR), Part 212, Current good manufacturing practice for positron emission tomography drugs, or under the guidance in United States Pharmacopeia (USP) Chapter 823. USP Chapter 823 sets forth requirements for PET drug production, including control of components, materials and supplies; verification of procedures; stability testing and expiration dating; quality control; and sterilization and sterility assurance. Because most US PET drug producers are very familiar with the requirements in Chapter 823, allowing producers to meet the current GMP requirements for investigational and research PET drugs by following Chapter 823 should greatly facilitate producers' compliance with the current GMP requirements. Although the provisions in Chapter 823, including those on documentation, are generally less specific and explicit than the requirements in 21 CFR Part 212, the Food and Drug Administration believes that they are adequate to ensure that investigational and research PET drugs are produced safely under appropriate conditions and are appropriate current GMP requirements for the investigational and research stage of development.

In the USA, studies for human use are conducted according to regulations governing investigational new drugs sponsored by a physician, an institution or a commercial entity.

The radiolabelling and final dose dispensing should occur in a classified area as required by the guidance documents for aseptic processing. The air quality in the production and laboratory areas should be controlled to minimize the level of contamination (particulate and microbial) that may affect analyses or the quality, purity and strength of the PET drug.

The use of air filtered with high efficiency particulate air (HEPA) filters is suggested for this environment when the product is being sampled or diluted to reduce the possibility of microbial contamination.

Typically, a filter integrity test should be conducted after final filtration.

US manufacturers of  $^{64}\text{Cu}$  may choose to file a Type II drug master file, which describes the chemistry, manufacturing and controls (CMC) of their process so that investigators may easily reference the appropriate CMC data. As clinical trials progress to Phase III, full current GMP controls will be required for  $^{64}\text{Cu}$ , which will be then treated as an active pharmaceutical ingredient for the new drug. Information about the operating parameters for cyclotron operation (e.g. the make of cyclotron used, bombardment times, information on the target and the target material) should be submitted at that stage.

In the USA, human research using a PET tracer may also be approved by the Radioactive Drug Research Committee of the Food and Drug Administration if it is basic scientific research and not investigation that is intended for immediate therapeutic, diagnostic or similar purposes, or research to determine the safety and effectiveness of the radioactive drug or biological product for such purposes.



## 2.8.2. Considerations for production under manufacturing conditions

In some cases and for some products, it may be possible to manufacture and release the  $^{64}\text{Cu}$  labelled and formulated substance as a finished radiopharmaceutical. While this does take some GMP and radiochemistry considerations away from the end user, it requires closer attention to product formulation and stability, as storage and transit time can easily reach several times the half-life of  $^{64}\text{Cu}$ . When using this approach in the European Union, the manufacturer has to comply with the full set of GMP requirements set forth in Volume 4 of the rules governing medicinal products in the European Union (EudraLex), with special attention to annex 3 on radiopharmaceuticals. These rules carefully delineate where GMP starts during the manufacturing process and thereby exempt the target manufacturing and cyclotron itself from GMP coverage. However, later stages of manufacturing do require strict adherence to GMP rules, including use of clean rooms and laminar air flow environments for the last stages of manufacture and dispensing. The European Pharmacopoeia does not yet contain monographs on  $^{64}\text{Cu}$  or its compounds, but many important starting materials and general procedures may be drawn from this source, and these should be followed when working in the European Union.<sup>1</sup>

## 2.9. PRECLINICAL STUDIES

### 2.9.1. Using $^{64}\text{Cu}$ labelled peptides in diabetes research

Diabetes is a chronic disease that occurs either when the pancreas does not produce enough insulin or when the body cannot effectively use the insulin it produces. The development of diabetes is attributed to the decrease in pancreatic beta cell mass. However, determination of beta cell mass is a major challenge, because the beta cell mass represents only 1–2% of the total pancreatic mass and beta cells are highly dispersed throughout the pancreas. Therefore, a suitable imaging agent must have very high affinity for beta cells and very high specific activity.

Within this framework, some research efforts have focused on the development of exendin-4 based tracers. Exendin-4 is a stabilized analog of the glucagon-like peptide 1 (GLP-1) with increased enzymatic resistance. The tracer [ $^{64}\text{Cu}$ -NODAGA]-exendin-4 was evaluated for the preclinical imaging of beta cells using PET-CT. For more details and a full description of the materials and methods used, please read the full country report of Finland.

In summary, autoradiography studies showed specific and prolonged uptake of [ $^{64}\text{Cu}$ -NODAGA]-exendin-4 in pancreatic islets (Fig. 26). However, pancreatic uptake at 1 h post-injection was  $0.09 \pm 0.02\%$  injected dose per gram of tissue (ID/g) and declined to  $0.04 \pm 0.02\%$  ID/g at 40 h after injection. In contrast, at all investigated time intervals, the highest radioactivity levels were observed in the kidneys, peaking at approximately 30% ID/g at 1 h after tracer injection. Pancreatic islets could not be visualized via PET-CT due to this high kidney dose.

Efforts are underway to limit kidney radioactivity with the introduction of metabolically cleavable linkages, and to further increase the specific activity of the tracer via new chelation strategies and radiolabelling methods.

---

<sup>1</sup> For further information refer to these documents from the United States of America and the European Union:

FOOD AND DRUG ADMINISTRATION, CENTER FOR DRUG EVALUATION AND RESEARCH, Guidance: PET Drugs — Current Good Manufacturing Practice (CGMP), FDA, Silver Spring, MD (2009).

FOOD AND DRUG ADMINISTRATION, CENTER FOR DRUG EVALUATION AND RESEARCH, Guidance: Media Fills for Validation of Aseptic Preparations for PET Drugs, FDA, Silver Spring, MD (2012).

FOOD AND DRUG ADMINISTRATION, CENTER FOR DRUG EVALUATION AND RESEARCH, Guidance: Investigational New Drug Applications for Positron Emission Tomography (PET) Drugs, FDA, Silver Spring, MD (2012).

EUROPEAN PHARMACOPOEIA COMMISSION, European Pharmacopoeia, 8th Edition, European Directorate for the Quality of Medicines and Health Care, Strasbourg, France (2014).

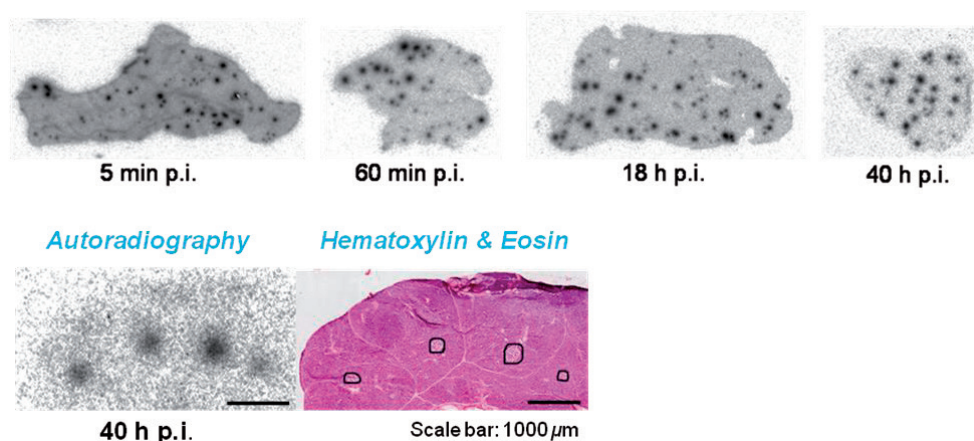


FIG. 26. Autoradiographic images of pancreatic slices of Sprague Dawley rats developed after intravenous injection of [ $^{64}\text{Cu}$ -NODAGA]-exendin-4.

### 2.9.2. $^{64}\text{Cu}$ -cyclam-RAFT-c(-RGDfK-) $_4$ for tumour $\alpha_v\beta_3$ integrin imaging

Integrins are a family of heterodimeric transmembrane glycoprotein receptors frequently overexpressed on many types of tumour cells. The structure of a cyclic pentapeptide containing a tripeptide sequence, Arg-Gly-Asp (RGD) (cRGD), was optimized to provide a high affinity and selectivity for the  $\alpha_v\beta_3$  integrin. To improve the affinity of cRGD to  $\alpha_v\beta_3$  integrin, cyclam-RAFT-c(-RGDfK-) $_4$  (Fig. 27) with a bifunctional chelator, 1,4,8,11-tetraazacyclotetradecane, for  $^{64}\text{Cu}$  labelling has been developed [24]. Results from small animal modelling are shown in Fig. 28 [25].

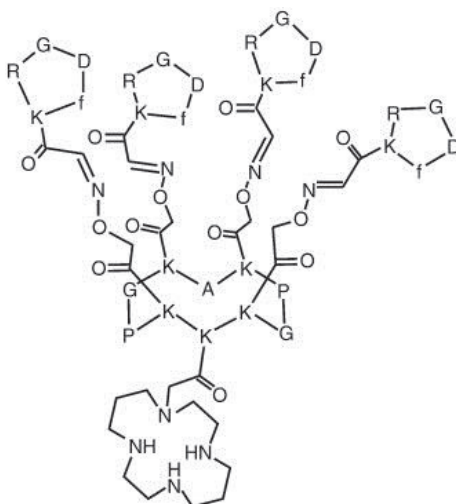


FIG. 27. Structure of cyclam-RAFT-c(-RGDfK-) $_4$  (reproduced from Ref. [25] with permission from Elsevier).



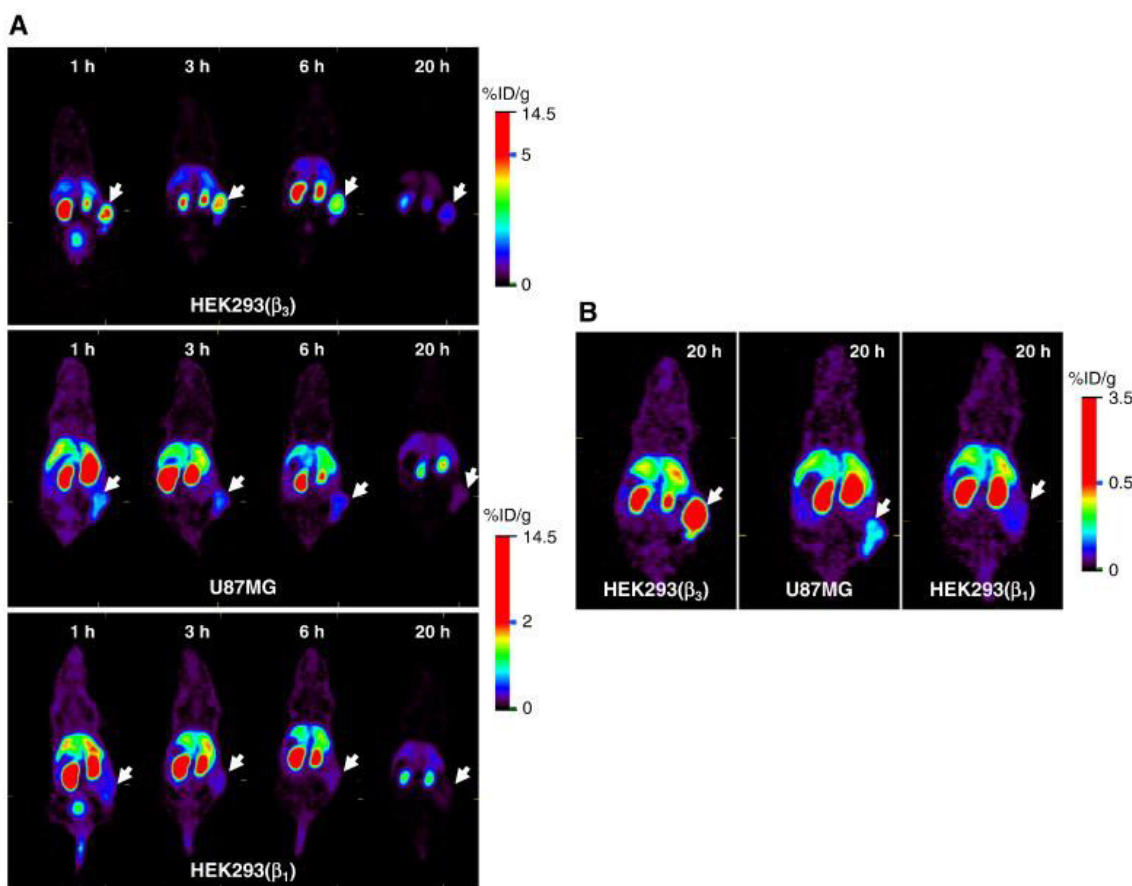


FIG. 28. Representative whole-body coronal PET images of nude mice bearing SC HEK293( $\beta_1$ ), HEK293( $\beta_3$ ) or U87MG tumours at 1, 3, 6 and 20 h post-injection of 11.1 MBq (15 nmol)  $\text{Cu}^{64}$ -cyclam-RAFT-c(-RGDfK-)<sub>4</sub> (reproduced from Ref. [25] with permission from Elsevier).

As a PET probe to evaluate the therapeutic effects of angiogenesis inhibitors,  $\text{Cu}^{64}$ -cyclam-RAFT-c(-RGDfK-)<sub>4</sub> exhibited binding affinity and specificity for the  $\alpha_v\beta_3$  integrin [25].

### 2.9.3. $\text{Cu}^{64}$ radiolabelled antibodies (immuno-PET)

The half-life of  $\text{Cu}^{64}$  makes long imaging timepoints possible, and thus studies investigating the use of intact antibodies as imaging agents (immuno-PET) have been conducted. High quality images are possible with this technique due to the high specificity of these agents for their targets. A recent preclinical study using  $\text{Cu}^{64}$ -bevacizumab illustrates this concept [26].

The importance of the growth of new blood vessels (angiogenesis) for primary and metastatic tumours has led to numerous clinical trials of angiogenesis inhibitors either alone or in combination with conventional therapies. One challenge with the use of molecularly targeted agents has been the disconnection between size reduction and tumour biological behaviour, either when the drug is efficacious or when tumour resistance emerges. One study reports the synthesis and characterization of  $\text{Cu}^{64}$ -NOTA-bevacizumab as a PET imaging agent for imaging intratumoural vascular endothelial growth factor (VEGF) content in vivo [26]. The imaging agent  $\text{Cu}^{64}$ -NOTA-bevacizumab avidly accumulated in 786-O renal carcinoma xenografts, with lower levels in host organs. RAD001 (everolimus) markedly attenuated  $\text{Cu}^{64}$ -NOTA-bevacizumab accumulation within 786-O renal carcinoma xenografts as shown in Fig. 29.

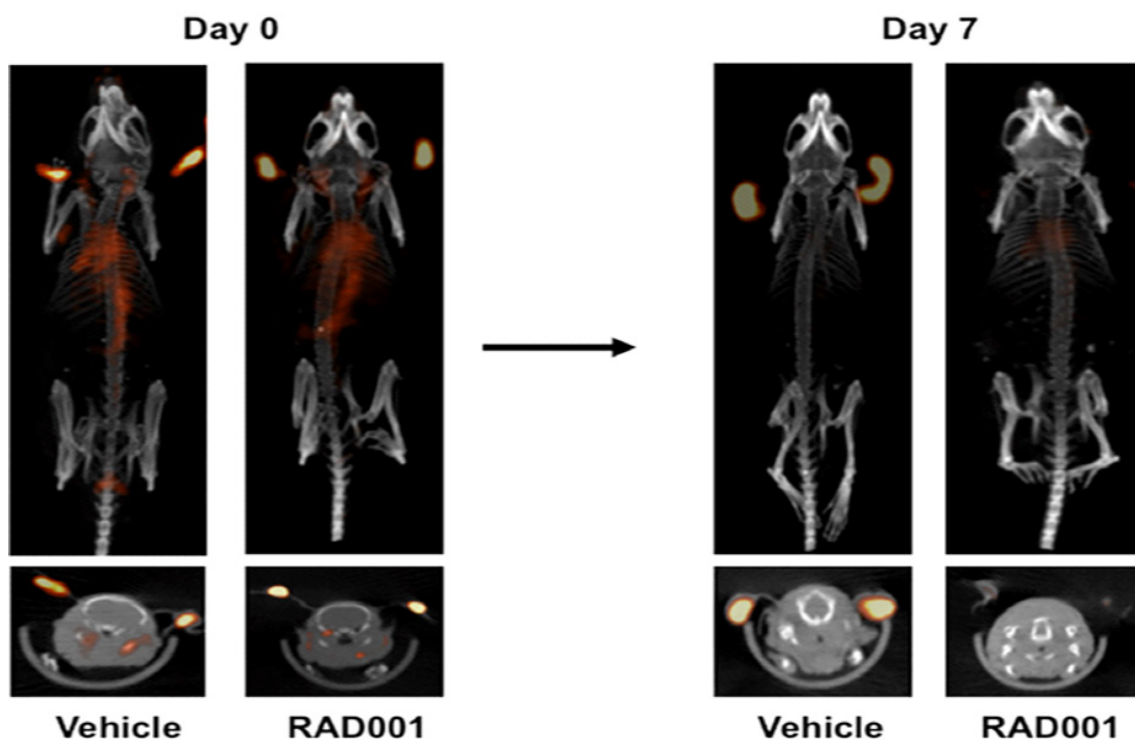


FIG. 29. MicroPET-CT study of  $^{64}\text{Cu}$ -NOTA-bevacizumab in mice bearing 786-O renal cell carcinoma tumours before and after treatment with RAD001 or vehicle (reproduced from Ref. [26]).

Tumour tissue and cellular molecular analysis validated PET imaging, demonstrating decreases in total and secreted VEGF content and VEGF receptor 2 (VEGFR2) activation. Notably,  $^{64}\text{Cu}$ -NOTA-bevacizumab PET imaging was concordant with the growth arrest of RAD001 tumours. These data suggest that immuno-PET targeting of angiogenic factors such as VEGF could be a mechanism for a new class of surrogate markers complementing currently used criteria in patients receiving molecularly targeted therapies [26].

## 2.10. CLINICAL STUDIES

### 2.10.1. $^{64}\text{Cu}$ -ATSM

Radiolabelled Cu-diacetyl-bis(N4-methylthiosemicarbazone) ( $^{64}\text{Cu}$ -ATSM) shows selective retention in cells with abnormal reducing conditions like hypoxia [27]. It visualizes this condition in unstable angina (heart), stroke sites for MELAS (mitochondrial encephalomyopathy, lactic acidosis and strokelike episodes) patients (brain) [28], striatum for Parkinson's disease patients (brain) [29], and tumours with hypoxic metabolism [18]. Strictly speaking,  $^{64}\text{Cu}$ -ATSM is not an ideal oxygen tension marker, but a marker of over-reduced conditions, in other words, oxidative stress.

In tumours,  $^{64}\text{Cu}$ -ATSM accumulates in 'cancer stem cell'-rich regions, a possible indication of high therapeutic tolerance and metastatic ability [30]. Moreover, the combination of the therapeutic properties of  $^{64}\text{Cu}$  and ATSM brings a new internal radiation therapy selective to 'cancer stem cell'-rich regions [31]. Several studies are also going on which illustrate the predictive potential of  $^{64}\text{Cu}$  in patients undergoing radiotherapy.

### 2.10.2. $^{64}\text{Cu}$ labelled DOTATATE in staging neuroendocrine tumours

The use of radioactive somatostatin analogues in the detection, staging and treatment of neuroendocrine tumours is well established. The labelling of DOTATATE with  $^{64}\text{Cu}$  for a PET imaging alternative to conventional SPECT agents is a rather straightforward approach (Fig. 30). One group [32] has demonstrated good performance in a first-in-humans trial and is now using this pharmaceutical clinically.

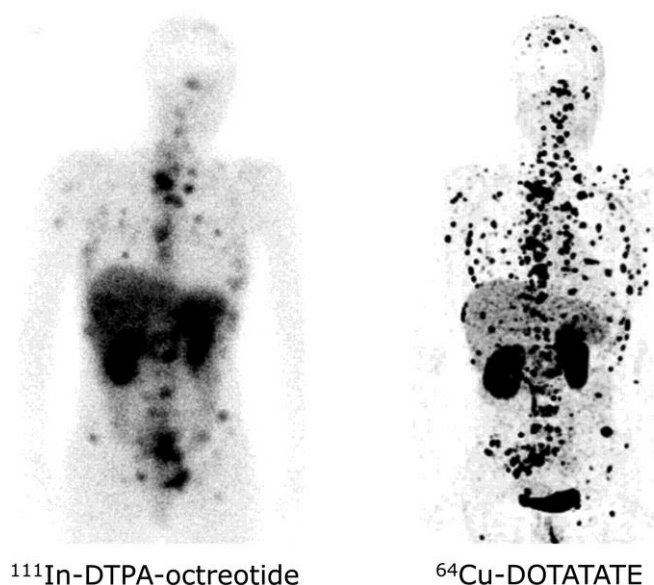


FIG. 30. Comparison of  $^{111}\text{In}$ -DTPA-octreotide and  $^{64}\text{Cu}$ -DOTATATE in same patient with multiple bone and soft-tissue metastases. (Originally published in JNM [32]. Reproduced with permission from the Society of Nuclear Medicine and Molecular Imaging, Inc.)

## 3. PRODUCTION OF $^{124}\text{I}$

### 3.1. SELECTION OF NUCLEAR PRODUCTION ROUTE

Nuclear medicine applications of cyclotron produced radiopharmaceuticals have rapidly increased since the introduction of PET. The accelerating demands of non-standard PET necessitate development and optimization methods and applications for emerging radionuclides, especially  $^{124}\text{I}$ . Ambiguity of target behaviour in terms of yield, tolerable beam current, specific activity and chemical phenomena is still one of the main problems encountered by radiopharmaceuticals producers. This has resulted in an insufficient supply of emerging radionuclides such as  $^{124}\text{I}$  in the required quantities and purities.

For the production of  $^{124}\text{I}$ , several nuclear reactions were suggested. The target production of  $^{124}\text{I}$  is limited to solid targets.

Table 10 shows a selection of production routes and the effective energy level to produce  $^{124}\text{I}$  [33].

TABLE 10. SELECTION OF PUBLISHED DATA ON  $^{124}\text{I}$  PRODUCTION [33]

Nuclear reaction	Effective energy (MeV)	Target material	Enrichment (%)	Yield (MBq/ $\mu\text{A}\cdot\text{h}$ )	Radioiodine impurities (% of I-124)
Te-124(p, n)I-124	13 $\rightarrow$ 9	Te	99.51	20 <sup>a</sup>	I-123 (41)
	12.2 $\rightarrow$ 0	TeO <sub>2</sub>	99.8	13	I-123 (10.039), I-125 (0.018), I-126 (0.041), I-130 (0.379)
	13.5 $\rightarrow$ 9	TeO <sub>2</sub> / 5% Al <sub>2</sub> O <sub>3</sub>	99.8	5.8	I-125 (0.01), I-126 (<0.000 1)
	12.5 $\rightarrow$ 5	TeO <sub>2</sub>	99.3	9.0 $\pm$ 1.0	I-125 (0.053 $\pm$ 0.015)
	11 $\rightarrow$ 2.5	TeO <sub>2</sub> / 6% Al <sub>2</sub> O <sub>3</sub>	99.5	6.40 $\pm$ 0.44	I-125 (<0.02), I-126 (<0.001)
	14 $\rightarrow$ 7	TeO <sub>2</sub> / 5% Al <sub>2</sub> O <sub>3</sub>	99.86	21.1	I-125 (0.03), I-126 (0.007)
Te-125(p, 2n)I-124	20.1 $\rightarrow$ 10.5	TeO <sub>2</sub>	93	43.3	I-123 (8), I-125 (5)
	22 $\rightarrow$ 4	Te	98.3	111 <sup>a</sup>	I-125 (0.89)
	21 $\rightarrow$ 15	Te	98.3	81 <sup>a</sup>	I-123 (7.4), I-125 (0.9)
	22	TeO <sub>2</sub>	98.5	104	I-123 (<1)
Te-126(p, 3n)I-124	36.8 $\rightarrow$ 33.6	Te	Nat	67 <sup>a</sup>	—
	38 $\rightarrow$ 28	Te	>98	148 <sup>a</sup>	I-123 (84), I-125 (1.5), I-126 (1.4)
Te-123(d, n)I-124	11 $\rightarrow$ 6	Te	91.0, 85.4	2.8 <sup>a</sup>	I-123 (3 321 <sup>b</sup> )
Te-124(d, 2n)I-124	15 $\rightarrow$ 0	Te	95	20.4 $\pm$ 2.2	I-126 (0.5)
	15 $\rightarrow$ 8	Te	91.7	18.9	I-125 (0.35 <sup>b</sup> ), I-126 (0.39 <sup>b</sup> ), I-131 (0.08 <sup>b</sup> )
	16 $\rightarrow$ 6	Te	96.7	23.7 <sup>a</sup>	—
	14 $\rightarrow$ 0	TeO <sub>2</sub>	89.6	15	I-123 (1.16), I-125 (1.41), I-126 (1.16), I-130 (7.87), I-131 (0.31)
	14 $\rightarrow$ 10	Te	99.8	17.5 <sup>a</sup>	I-125 (1.7)
Sb-nat( $\alpha$ , xn)I-124	22 $\rightarrow$ 13	Sb	Nat	1.02 <sup>a</sup>	I-123 (892 <sup>b</sup> ), I-125 (13 <sup>b</sup> ), I-126 (0.16 <sup>b</sup> )
Sb-121( $\alpha$ , n)I-124	22 $\rightarrow$ 13	Sb	99.45	2.11 <sup>a</sup>	I-123 (891 <sup>b</sup> ), I-125 (<0.2), I-126 (<0.2)
Sb-nat( $^3\text{He}$ , xn)I-124	35 $\rightarrow$ 13	Sb	Nat	0.95 <sup>a</sup>	I-121 (37 700), I-123 (3 877 <sup>b</sup> ), I-125 (0.6 <sup>b</sup> ), I-126 (0.6)

<sup>a</sup> Based on experimental cross-section data.<sup>b</sup> Percent calculated here from the ratio of the published saturation yield data.

Normally,  $^{124}\text{I}$  production is carried out using  $^{124}\text{TeO}_2$  via the nuclear reaction  $^{124}\text{Te}(p, n)^{124}\text{I}$ . This reaction has the advantages of using cyclotrons with proton energies lower than 14 MeV and providing a very high radionuclidic purity, but yields are rather low. Depending on the effective energy range and target composition, yields range between roughly 6 and 20 MBq/ $\mu\text{A}\cdot\text{h}$  [33]. The scope of this work was to develop a method based on the  $^{125}\text{Te}(p, 2n)^{124}\text{I}$  reaction, which requires a cyclotron capable of providing proton beams of higher energies ( $>20$  MeV). This nuclear reaction also produces a very high radionuclidic purity with higher yields than the (p, n) reaction; depending on the effective energy range and target composition, yields range between 43 and 111 MBq/ $\mu\text{A}\cdot\text{h}$ , between 5 and 7 times more than that resulting from the  $^{124}\text{Te}(p, n)^{124}\text{I}$  reaction [33].

The excitation functions of the two commonly used  $^{124}\text{I}$  reactions are shown in Figs 31 and 32.

There are other nuclear reactions that use  $\alpha$  and  $^3\text{He}$  particles on Sb targets as shown in Table 11, but due to the scarcity of cyclotrons capable of providing  $\alpha$  beams, this route has been less utilized than nuclear reactions based on proton beams.

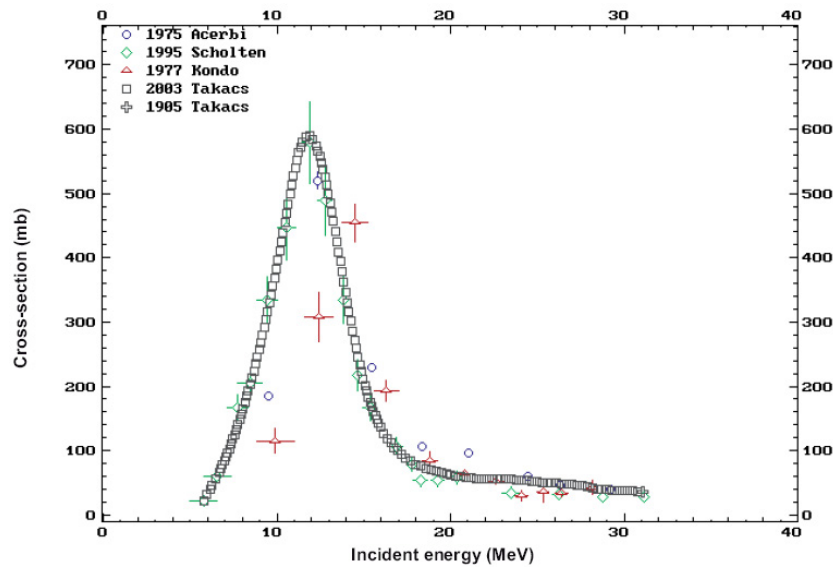


FIG. 31. Excitation function for  $^{124}\text{Te}(p, n)^{124}\text{I}$  reaction (reproduced from Ref. [9]).

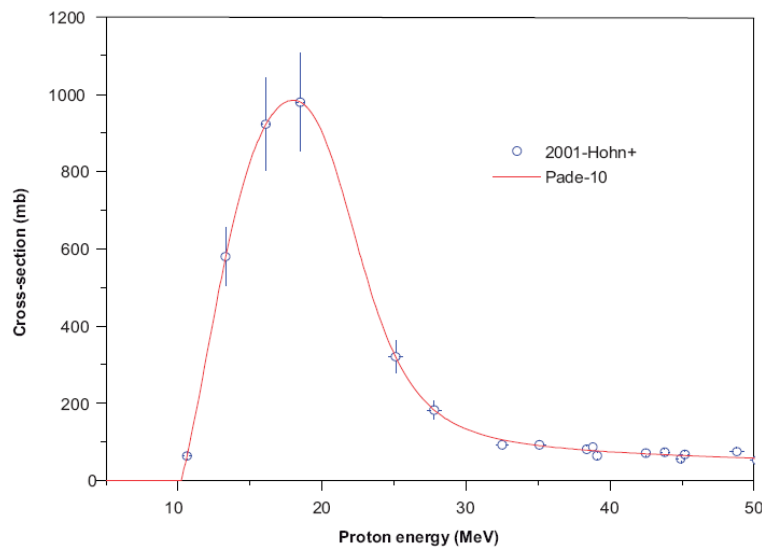


FIG. 32. Excitation function for  $^{125}\text{Te}(p, 2n)^{124}\text{I}$  reaction (reproduced from Ref. [9]).

TABLE 11. PRODUCTION OF  $^{124}\text{I}$  USING  $\alpha$  AND  $^3\text{He}$  PARTICLES ON Sb [34, 35]

Nuclear process	Energy range (MeV)	Thick target yield of I-124 (MBq/ $\mu\text{A}\cdot\text{h}$ )	Radionuclidic impurities (% of I-124)		
			I-123	I-125	I-126
Sb-123( $^3\text{H}$ , 2n)I-124	19–13	0.73	11	0.6	0.6
Sb-121( $\alpha$ , n)I-124	21–14	1.36	534	<0.2	
Sb-123( $\alpha$ , 3n)I-124	45–32	15.5	236	1.19	0.32
Sb-nat( $\alpha$ , xn)I-124	45–32	6.7	537	1.18	0.31
Sb-nat( $\alpha$ , xn)I-124	22–13	1.02	892	13	0.16

Except for the reaction  $^{123}\text{Sb}(\alpha, 3n)^{124}\text{I}$ , with  $\alpha$ -particles in a range of 45–32 MeV, and which produces a yield similar to  $^{124}\text{Te}(\text{p}, \text{n})^{124}\text{I}$ , all the rest of the reactions provide lower yields of  $^{124}\text{I}$ , and almost all produce lower radionuclidic purity, with a very high percentage of  $^{123}\text{I}$ .

A group in Brazil will continue exploring the  $^{121}\text{Sb}(\alpha, \text{n})^{124}\text{I}$  and  $^{\text{nat}}\text{Sb}(\alpha, \text{n})^{124}\text{I}$  reactions on their CV-28 cyclotron and compare with the  $^{125}\text{Te}(\text{p}, 2\text{n})^{124}\text{I}$  reaction, and will decide which one to pursue based on which gives the better economic performance. Unfortunately, the energy range for the only reaction on the Sb target that matches the yield obtained with the  $^{125}\text{Te}$  target,  $^{123}\text{Sb}(\alpha, 3\text{n})^{124}\text{I}$ , is out of the energy range of the CV-28.

Even if all these reactions give lower yields, the decision to explore the  $\alpha$  route will allow Brazil to use its previous experience to go forward quickly and explore the market while working on the set-up of the  $^{125}\text{Te}(\text{p}, 2\text{n})^{124}\text{I}$  reaction. This decision will also expand Brazil's capability in radioisotope production based on cyclotrons. There are several other radioisotopes produced by nuclear reactions using  $\alpha$ -particles that are currently being explored [36]. Probably the most promising is  $^{211}\text{At}$ , an  $\alpha$  emitting therapeutic radioisotope [37–39].

## 3.2. TARGET PREPARATION

### 3.2.1. Target design

#### 3.2.1.1. Irradiation angle

Target designs which set the beam at a small inclination angle allow the beam to be spread over a larger area, thereby reducing power density, leading to higher and easier heat removal. They also reduce the need for beam control techniques like beam wobbling to help increase power dissipation.

If the target is aligned at  $90^\circ$ , the efficiency of the cooling process is a critical parameter to avoid the possibility of target overheating. This can lead to target stressing and also increases the possibility of releasing I during the irradiation process [40].

#### 3.2.1.2. Cooling

In order to prevent hot spots, several groups have implemented different front cooling systems. One example includes a laminar flow of cold water, all protected by a thin Al window, with the least possible energy degradation from the incident beam. Alternatively, chilled He may be used.

Front water cooling has been also tried by other groups [40], but was found to be unsuitable for a target system design where the target was perpendicular to the proton beam. Relatively high losses of  $^{124}\text{I}$  to the cooling water directly in contact with the target were observed, which became a serious problem during extended irradiations. As a consequence, this group decided to use chilled He cooling in the front of the target, finding that with this



technique losses of  $^{124}\text{I}$  were reduced to a negligible amount. It was experimentally checked by measuring the activity collected on a Ag filter (Millipore support) placed over the exit of the He gas.

Also related to the cooling efficiency, Cu is a good target carrier material for the electrodeposition of Sb over Cu in the target for the ( $\alpha$ , n) reaction and for the electrodeposition of Te as well; in this last case, the Cu is coated with a thin Ni layer to ensure good adhesion.

Copper has two properties that make it a good choice for cyclotron targetry: it is a metal with a high melting point ( $1084.62^\circ\text{C}$ ), and it also has one of the highest thermal conductivity rates ( $401\text{ W}\cdot\text{m}^{-1}\cdot\text{K}^{-1}$ ). Its high thermal conductivity allows a high rate of heat removal for easier target cooling.

### 3.2.1.3. Target backing material

Copper, as stated above, is a suitable backing material due to its high thermal conductivity and the fact that its melting point is much higher than the temperature necessary for  $^{124}\text{I}$  dry distillation [40, 41]. However, a drawback is its activation during the irradiation, which yields high radiation doses during operation.

Natural Cu consists of 30.83%  $^{65}\text{Cu}$  and 69.17%  $^{63}\text{Cu}$ , and when irradiated with protons produces different isotopes of Zn:  $^{65}\text{Cu}(\text{p}, \text{n})^{65}\text{Zn}$ ,  $^{65}\text{Cu}(\text{p}, 2\text{n})^{64}\text{Zn}$ ,  $^{63}\text{Cu}(\text{p}, \text{n})^{63}\text{Zn}$  and  $^{63}\text{Cu}(\text{p}, 2\text{n})^{62}\text{Zn}$ . Between them,  $^{65}\text{Zn}$  (half-life = 244 d) has the longest half-life and decays by electron capture to the 1115 keV excited level and by electron capture and beta plus emission to the ground state level of  $^{65}\text{Cu}$ . The maximum cross-section for the reaction  $^{65}\text{Cu}(\text{p}, \text{n})^{65}\text{Zn}$  is around 11 MeV; at the incident energies used for the  $^{125}\text{Te}(\text{p}, 2\text{n})^{124}\text{I}$ , and depending on the target thickness, the cross-section for the  $^{65}\text{Cu}(\text{p}, \text{n})^{65}\text{Zn}$  will be high enough to produce  $^{65}\text{Zn}$ . This radioisotope will produce high radiation doses for a longer period of time; therefore, there are safety concerns that require careful design of operations for target processing.

Natural Ag may be used as a backing material composed of 48.17%  $^{109}\text{Ag}$  and 51.83%  $^{107}\text{Ag}$ , and when irradiated with protons produces different isotopes of Cd:  $^{109}\text{Ag}(\text{p}, \text{n})^{109}\text{Cd}$ ,  $^{109}\text{Ag}(\text{p}, 2\text{n})^{108}\text{Cd}$ ,  $^{107}\text{Ag}(\text{p}, \text{n})^{107}\text{Cd}$  and  $^{107}\text{Ag}(\text{p}, 2\text{n})^{106}\text{Cd}$ . Cadmium-108 and 106 are stable isotopes. At the energy range used to produce  $^{124}\text{I}$  using a Te target, the nuclear reactions on the Ag backing will produce  $^{107}\text{Cd}$  and  $^{109}\text{Cd}$ . Cadmium-107 has a short half-life of 6.5 h, whereas  $^{109}\text{Cd}$  has a long half-life of 453 d, but has no gamma emission and decays by electron capture to the isomeric state (88 keV) of  $^{109}\text{Ag}$ , which has an extremely short half-life of 39.6 s. Therefore, safety concerns for operations with irradiated targets are lower for Ag than for Cu. Silver also has a higher thermal conductivity than Cu ( $429\text{ W}\cdot\text{m}^{-1}\cdot\text{K}^{-1}$ ) and a high melting point of  $961.78^\circ\text{C}$ , making Ag suitable from this point of view. But Ag can have a drawback related to the reduction step during Te recovery from the target dissolved solution. The recovery procedure should take into account that the reduction step to be applied to precipitate the Te may also produce  $\text{Ag}^{(+)}$ , which causes low solubility, and  $\text{AgCl}$  could precipitate to some extent together with the elemental Te, requiring an additional operation for its separation.

An additional possibility is to use Pt as carrier material for a Te target [41]. This material has the advantage that it is not dissolved during the chemical operations to recover Te; therefore, it is not necessary to make one target per irradiation. Additionally, the recovered Te may have a higher chemical purity. Platinum also has a melting point of  $1768^\circ\text{C}$ , which makes it suitable for I dry distillation. But it also has some disadvantages: it is more expensive than Cu and it has a much lower thermal conductivity ( $71.6\text{ W}\cdot\text{m}^{-1}\cdot\text{K}^{-1}$ ).

### 3.2.2. Te targets

Electroplating and sintering can be used to prepare targets. For the latter,  $\text{TeO}_2$  as target material has better thermal characteristics than Te metal, and both are used in combination with  $\text{Al}_2\text{O}_3$ , which offers an effective binding agent and results in the formation of the glassy solid target matrix [41]. Another method reported by Sheh et al. [41] involves preparing the target by heating the  $\text{TeO}_2/\text{Al}_2\text{O}_3$  mixture, but to a temperature higher than the melting point; hence, it is not a sintering process. The solid solution produced because of the melting may also increase the conductive heat transfer path, leading to an enhancement of the thermal conductivity.

Both techniques have advantages and disadvantages. Electroplating might be more expensive and requires more work and a precise set-up of the chemical preparation, but it might also produce higher yields. On the other hand, the sintering process is experimentally simpler and produces targets that can be reused several times.



Sintering, a process whereby a powder is heated to a temperature below the melting point, is effective as it reduces the porosity [42]. It is widely proven that sintering provides thermal conductivity for the sintered porous media which is much higher than for non-sintered porous media due to the improved thermal contact caused by the decreased porosity resulting from the sintering process. The heat transfer mechanism between the target matrix and the target carrier is a combination of conduction and convection. Since a lower porosity means more solid phase, it causes conductive heat transfer to be dominant, which enhances the thermal performance, leading to higher heat transfers [42–44]. This explains why the sintering technique provides targets with good thermal properties.

### 3.2.2.1. Preparation of Te targets using electroplating

Figure 33 shows two types of electroplated targets used for  $^{124}\text{I}$  production. The two typical methods for separating  $^{124}\text{I}$  from the irradiated Te target are through dry distillation, in which the target is heated under gas flow in a quartz tube and then collected in different vessels, and wet chemical processing, in which the target is dissolved chemically. Although the first technique is much simpler and allows the target to be reused as many as five times, the second technique produces higher yield.

#### (a) Preparation of target carrier

Figure 34 shows a target preparation assembly for electroplating. The set-up is capable of making four targets at a time. To ensure good adhesion of the target material to the target carrier, the latter is coated with a 50  $\mu\text{m}$  Ni layer before Te plating. Five hundred grams of  $\text{NiSO}_4 \cdot 6\text{H}_2\text{O}$  is dissolved in 1000 mL of deionized water. The Cu carrier is then cleaned by rubbing with sandpaper (320–500 mesh grade), followed by rinsing with deionized water. The Cu plate (cathode) and a Pt wire (anode) are immersed in a 1000 mL beaker containing the Ni plating solution. The electrode, connected to a DC power supply, is adjusted to deliver a current of 400–800 mA. The Ni is plated out for 3 min, and then the electrode is removed from the solution. Finally, the target carrier is rinsed with water and air dried.

#### (b) Electroplating

The plating solution is prepared from enriched  $^{125}\text{TeO}_2$  by dissolving it in alkaline solution. In a 500 mL flask,  $^{125}\text{TeO}_2$  is added, followed by addition of potassium hydroxide (KOH) and deionized water. Then KBr is added to the stirred solution. The homogenized solution is filtered through a fine glass filter (0.45  $\mu\text{m}$ ) to remove any residual particles, if necessary. The final concentration is 18 mg/mL of Te. The freshly prepared solution of  $^{125}\text{TeO}_2$  is poured into the plating vessel. A current booster is connected to the cathodes by introducing the rotational speed stirrer in such a way that the central Pt anode wire fits into the hollow stirring cylinder. The electrolysis starts by introducing the common output plug of the booster into the bottom of the deposition vessel with a voltage of 6–12 V and 35 mA current per target (it is preferable to apply low current as this results in a homogeneous



FIG. 33. Typical targets used for  $^{124}\text{I}$  production.

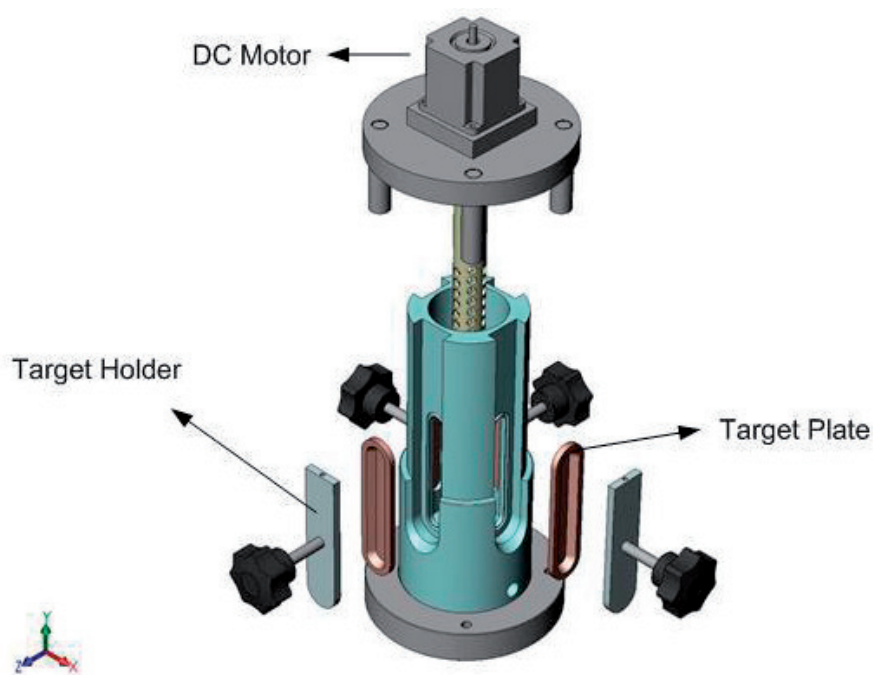


FIG. 34. Motor driven Ni plated target vessel.

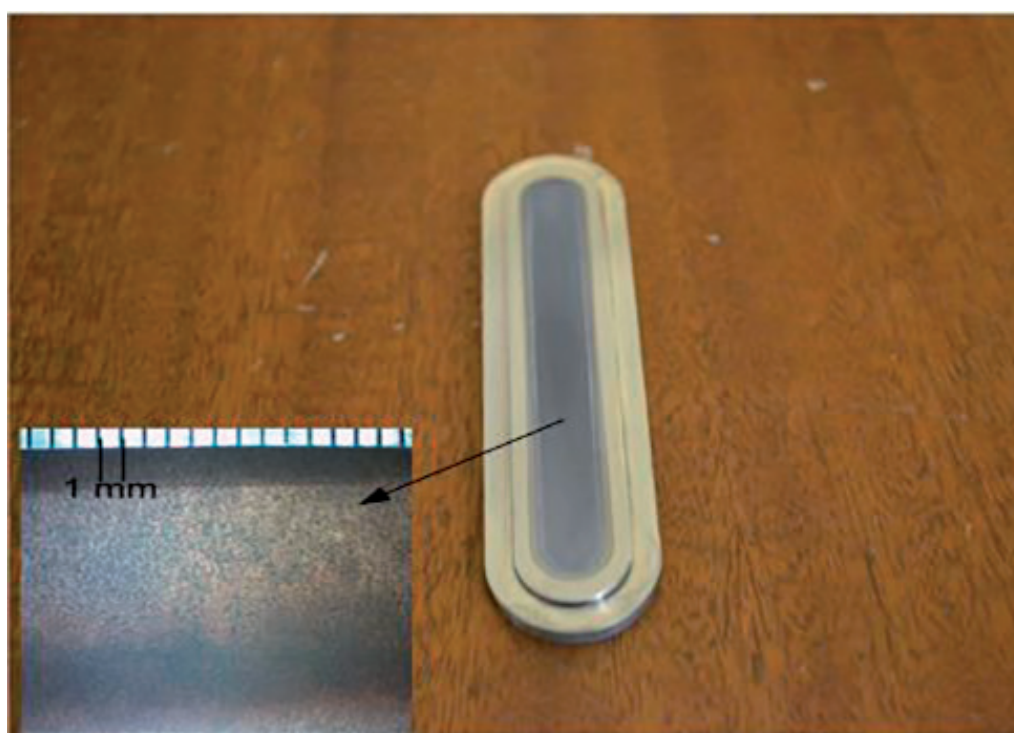


FIG. 35. The target and optical micrograph of the electroplated surface.

surface and smooth shiny metallic tincture). At the end of electrolysis, the stirring motor is stopped and the plate is removed and rinsed extensively with deionized water. Then it is dried in an oven at 100°C and weighed. Figure 35 shows a Ni plated target.

(c) Recovery of the electroplated target

As an example of a typical production technique, the electroplated  $^{125}\text{Te}$  can be recovered as follows. The Te from the irradiated target is dissolved in a mixture of HCl and  $\text{H}_2\text{O}_2$  in a ratio of 3:1 (100 mL). The solution is filtered during warming through 0.45  $\mu\text{m}$  glass fritted funnel. Hydrobromic acid (48%, 40 mL) and deionized water are added, followed by the addition of  $\text{NH}_2\cdot 2\text{HCl}$  and  $\text{Na}_2\text{SO}_3$  until the Te has precipitated. The mixture is then filtered through a 0.45  $\mu\text{m}$  glass fritted filter and the precipitate washed thoroughly with deionized water and acetone. The solution is dried at 100°C for 1 h. The gross weight is then measured and the material stored as enriched Te metal.

This method will ensure above 95% recovery, which is cost effective.

3.2.2.2. Preparation of Te target using sintering

The sintering process for Te is chosen by many institutions because of the increased strength of the oxide, which prevents breakage during irradiation. Sintered grains also show internal porosities that are convenient to the adsorption of I. In a prototype experiment, commercial  $\text{TeO}_2$  is pressed at 7 MPa into a cylindrical shape with a diameter of 11.2 mm and a thickness of 2 mm. The grain bodies are sintered in air at a temperature of 650°C for 2, 4 or 6 h. All particulate samples are analysed by X ray diffraction with  $\text{Cu K}_\alpha$  radiation at 40 kV and 30 mA, with a time constant of 0.5 s and with graphite crystal monochromator. High resolution SEM (Quanta 200 FEG) is used to investigate the morphology of the sintered bodies. The grain size is measured using ImageJ Java software developed by the National Institutes of Health. A He pycnometer is used to assess the relative density of the grains. The images in Fig. 36 show the morphology of samples of  $\text{TeO}_2$  sintered at 650°C for 2, 4 and 6 h. The materials exhibit well-defined grains and many intergranular pores. With increasing sintering time there is an increase of particle size and a reduction in the intergranular pores. With 6 h of heat treatment the densification process is at an advanced stage, resulting in a material more resistant to beam irradiation, but that still has pores that can adsorb the I formed in the nuclear reaction.

The average sizes of the  $\text{TeO}_2$  particles are listed in Table 12.

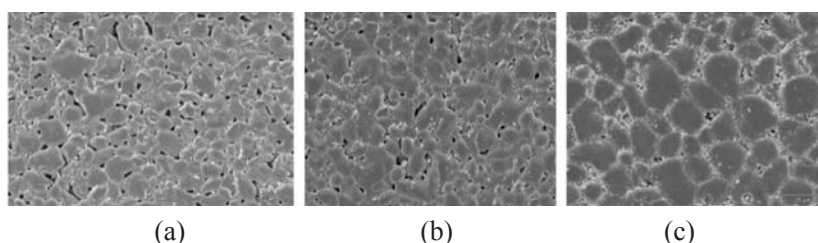


FIG. 36. SEM images of the  $\text{TeO}_2$  pellets sintered for (a) 2 h, (b) 4 h and (c) 6 h.

TABLE 12. TEXTURAL CHARACTERISTICS OF  $\text{TeO}_2$  THERMALLY TREATED AT 650°C

$\text{TeO}_2$		
Calcination time (h)	Density (%)	Grain size by SEM ( $\mu\text{m}$ )
No sinterization	93	—
2	96	11–13
4	97	17
6	99	25

### 3.2.3. Sb targets

In the framework of this CRP, a similar sintering process for preparation of Sb targets used for the ( $\alpha$ , n) nuclear route was carried out using the oxide of Sb. In the X ray diffraction pattern, the presence of a single crystalline phase related to  $\text{Sb}_2\text{O}_3$  was observed. It was found that the commercial material had smaller particle sizes (Table 13), and even with treatment at  $550^\circ\text{C}$  running for 6 h, sintering did not occur fully. Figure 37 shows SEM images of powder  $\text{Sb}_2\text{O}_3$ . The density of the material increases significantly with heat treatment; however, even after 6 h of sintering the assessed density was 96% compared with the theoretical density, indicating that the sintering process was not complete.

Antimony targets can be also prepared by electrodeposition of Sb on Cu. This method for Sb target preparation presents some challenges related to adhesion of the Sb over the backing material, which might require special preparation of the Cu surface to add microgrooves.

TABLE 13. TEXTURAL CHARACTERISTICS OF  $\text{Sb}_2\text{O}_3$  THERMALLY TREATED AT  $550^\circ\text{C}$

$\text{Sb}_2\text{O}_3$		
Calcination time (h)	Density (%)	Grain size by SEM ( $\mu\text{m}$ )
No sinterization	81	
2	88	0.9
4	93	2.0
6	96	2.4

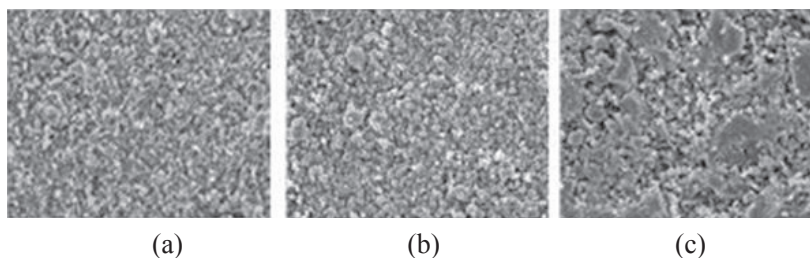


FIG. 37. SEM image of  $\text{Sb}_2\text{O}_3$  pellets sintered for (a) 2 h, (b) 4 h and (c) 6 h.

## 3.3. DEVELOPMENT OF RADIOIODINATED SYNTHONS

### 3.3.1. $^{124}\text{I}$ properties, chemistry and labelling methods

Labelling procedures for  $^{124}\text{I}$  rely on the well known labelling methods used in the past for  $^{131}\text{I}$ . These are completely applicable for labelling with  $^{124}\text{I}$ , as well as for quality control [45]. Therefore, most of the preclinical research for  $^{124}\text{I}$  can be done using the surrogate  $^{131}\text{I}$ , which has a much lower cost and is easily available.

The longer half-life of  $^{124}\text{I}$ , its radiochemical properties and the high energy of its emissions add new hurdles in comparison with  $^{123}\text{I}$  (which is used for SPECT imaging), underscoring the importance of enhancing the in vivo biological stability of the labelled radiopharmaceuticals. The stability issue for  $^{124}\text{I}$  radiopharmaceuticals is more critical than for  $^{123}\text{I}$  not only due to the longer half-life of 4.18 d but also due to the higher radiation dose delivered ( $282 \times 10^{-9}$  Sv/Bq for  $^{124}\text{I}$  versus  $4.42 \times 10^{-9}$  Sv/Bq for  $^{123}\text{I}$ , thyroid ingested).

Radioiodination chemistry is very well known; it is basically the same chemistry as that used for non-radioactive I adapted to the special conditions for use at trace scale concentration. Radioiodination chemistry can be divided in two routes: the nucleophilic and electrophilic synthesis methods. The latter has been the most frequently used radioiodination method, because of the ease of oxidizing iodide into an electrophilic positively charged I ( $I^+$ ) species. Depending on the molecule to be labelled, there are a variety of methods which have been used for a long time [45]. For biomolecules, there are also many possible methods that can be used in different scenarios [46], including direct labelling using oxidants such as chloramine T or iodogen. While it is simple, direct labelling has many very well known problems; thus there arose the necessity of finding methods that allow for more site specific labelling while preserving the biological activity of the biomolecule. Conjugation labelling methods using bifunctional organometallics as labelling precursors fulfil both conditions using a two step strategy [46]. The first step is the radioiodination itself, where the oxidant is used. In the second step, after purification, the radioiodinated molecule is then conjugated to the biomolecule using mild reaction conditions. In this way the biological activity of the biomolecule may be better preserved because it is not exposed to the oxidant.

Using organometallics allows for site specific labelling based on the electronegativity and percentage of ionic character of the carbon–metal bond, which makes the electrophilic attack of the  $I^+$  much more specific. Among the organometallic compounds, the organostannanes have been studied extensively and provide one of the most effective and convenient radioiodination methods [47]. This technology offers an additional and very important advantage: the product formation proceeds with high specific activity.

The in vivo stability issue of radioiodinated compounds can be tackled as a two compartment problem: the first compartment considers all the metabolization processes that might happen to the radioiodinated compound before cell binding or cell trapping; and the second compartment is related to cell metabolization. Each one presents different challenges. For the first one, a very well known key factor is to avoid structural similarity between our template and thyroid hormones — compounds that are broken down into deiodinases. For the second compartment, the problem is a bit more complicated because the cell is a formidable metabolizing machine thanks to lysosomal enzymes.

Several strategies were tried to achieve higher in vivo stability and standardization of labelling. Early approaches used: (a) non-metabolizable carbohydrate conjugates of tyramine including tyramine cellobiose and dilactitol tyramine [48, 49], and (b) labelled templates that are inert to lysosomal digestion and not transported across lysosomal or cell membranes.

Neither of these methods worked for several reasons, including: modest coupling efficiencies and specific activities [50], MAb cross-linking [48, 51] and pronounced retention of activity in spleen, liver and kidneys [50, 52].

More recent approaches were more successful; these involved not trying to avoid metabolization but instead making use of it by designing templates that after lysosomal catabolism will result in charged structures being trapped inside the cell. With this strategy, there were two different approaches, one using organic carriers containing basic functionalities that would be protonated at lysosomal pH and thus trapped within the cells [53–55], the other using poly-D-amino acid containing positively charged amino acids at lysosomal pH [56].

Immuno-PET, which uses intact MAbs, is the area likely to benefit the most from the relatively long half-life of  $^{124}I$  [57], providing additional reasons to find methods to increase in vivo stability. An example where improving stability and cellular internalization might be very helpful is the field of molecular imaging of therapeutic strategies based on epidermal growth factor receptor (EGFR) blockade. EGFR overexpression is documented in several malignant tumours, such as carcinomas of the breast, urinary bladder and lung, and is associated with poor prognosis [58–60]. The problem of detecting in vivo EGFR with a non-invasive approach by means of labelled MAb against the EGFR is very challenging, mainly for two reasons: the extensive lysosomal metabolization that internalized antibodies suffer, which can lead to rapid loss of radioactivity from the target cell; and the slow pharmacokinetics of intact MAb, which typically needs 2–4 d to achieve optimal tumour to non-tumour ratios. Therefore for  $^{124}I$  to be useful, in vivo stability is a key issue.

In order to achieve this goal, a possible approach is to use bifunctional active esters as labelling precursors, which, once reacted, will create a labelled template on the MAb that is positively charged at lysosomal pH. The rationale of this approach was based on successful experience with the retention of positively charged dyes such as chloroquine in the lysosomal compartment [61] and their use for the radioiodination of antibodies [57].



In the framework of this CRP, a proposal was made for the synthesis of two different labelling precursors to be used as model compounds for improving in vivo stability in order to test the concept on biological models: N-succinimidyl 3-radioiodo-benzoate (SIB) and (for improving stability and internalization) N-succinimidyl 5-radioiodo-pyridine-3-carboxylate (SIPC) (Fig. 38).

Iodine-124 also has advantages and disadvantages related to its chemistry and biological stability. Its longer half-life makes  $^{124}\text{I}$  suitable for commercial distribution and also for radiopharmaceuticals requiring longer times for optimal accumulation (MAb). But at the same time, it could increase the possibility of exposing non-target tissues to higher levels and longer periods of activity due to deiodination, which, along with the high energy of its emissions, will produce higher radiation doses, raising dosimetry concerns.

Iodine-124 emits  $\beta$  (1532 keV (11%), 2135 keV (11%)),  $\gamma$  and X rays (511 keV (46%), 603 keV (61%), 1691 keV (11%)), producing higher levels of radiation dose (almost 64 times higher) in comparison with  $^{123}\text{I}$ :  $282 \times 10^{-9}$  Sv/Bq for  $^{124}\text{I}$  (thyroid, ingested), and  $4.42 \times 10^{-9}$  Sv/Bq for  $^{123}\text{I}$  (thyroid, ingested). It might also require restrictions on the level of activity being injected, and because of that it might not be suitable for radiopharmaceuticals with low percentage of accumulation.

In addition to the dosimetry concern, the high energy level of its emissions might also produce poorer image quality than for pure positron emitters like  $^{18}\text{F}$ . In this regard,  $^{124}\text{I}$  presents an additional challenge because of two major features of its radioactive decay: the high energy of the positrons and the high fraction of non-positron decay of single photon emission in the same energy window as the annihilation photons, which may lead to degradation of image quality but also make the numerical data obtained from the images less quantitative [62, 63].

However, on current state of the art PET scanners the inherent disadvantages seen in the context of pharmacological studies seem to be rectified; on these scanners, the image quality with  $^{124}\text{I}$  differs only marginally from that obtained with other isotopes like  $^{18}\text{F}$  and  $^{89}\text{Zr}$  due to the ability of the sophisticated hardware and software to correct the data and compensate for the higher energy positrons [64].

Another consequence of the high energy emissions of  $^{124}\text{I}$  is added radiation safety concerns for the operators involved in the production process. The higher half-value layer (Pb) in comparison with  $^{123}\text{I}$  (8 mm for  $^{124}\text{I}$  versus 1 mm for  $^{123}\text{I}$ ), indicates that  $^{124}\text{I}$  requires more shielding, which might impose restrictions during labelling procedures and might require automation.

The chemical properties of I are completely different from those of radiometals used for PET imaging such as  $^{68}\text{Ga}$ . In contrast with radiometals, which require using chelators, I forms covalent bonds, which yield a chemical stability for the labelling, independent of pH, and allow more complex design while producing lower structural change than coupling chelating agents. These differences give I a wider spectrum of potential molecules — even wider than  $^{18}\text{F}$  due to its longer half-life. However, they also add some problems due to an increase in lipophilicity in comparison with fluoride. It is important to note that, considering the low level of structural change, covalent bonding allows complex design of templates, for example transporting charges without affecting chemical stability of the labelling, that are not possible for chelates/radiometals.

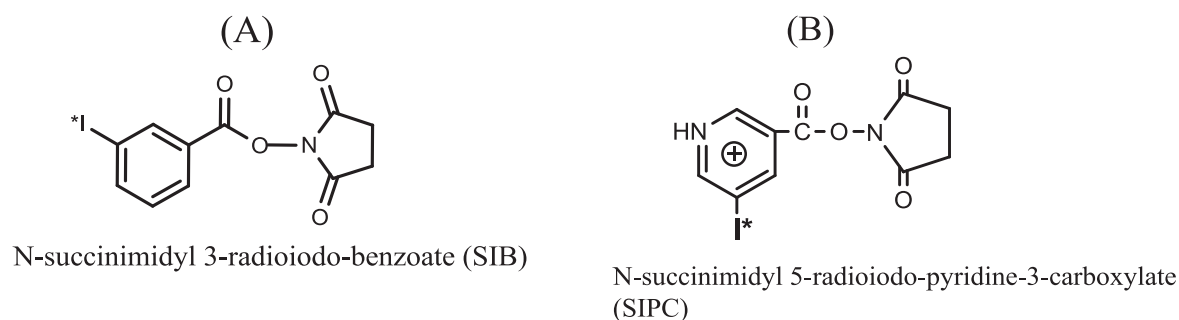


FIG. 38. Model compounds for use with  $^{124}\text{I}$  labelling.

### 3.4. POTENTIAL APPLICATIONS OF $^{124}\text{I}$

Iodine-124 is a radioisotope with a very strong potential in nuclear medicine; being a positron emitter, it offers a superior quality of detection in comparison with  $\gamma$  emitters such as  $^{123}\text{I}$ .

Several areas of molecular imaging may take advantage of this radioisotope, but considering its relatively long half-life, immuno-PET may benefit the most. For a positron emitter to be appropriate for immuno-PET, several aspects must be considered, of which the two most important are the availability of methods to obtain sufficient amounts of pure isotope and the availability of procedures for its stable coupling to the MAb with maintenance of the antibody's *in vivo* biodistribution characteristics.

A predominant factor for determining a positron emitter's suitability for immuno-PET is its physical half-life; the 4.18 d  $^{124}\text{I}$  half-life makes it compatible with the time needed for a MAb or MAb fragment to achieve optimal tumour to non-tumour ratios (typically 2–4 d for intact MAbs and 2–6 h for MAb fragments). Thus far, radiolabelled intact MAbs have been used in tumour detection and treatment planning, as well as in radioimmunotherapy (RIT), whereas the application of MAb fragments has been restricted for the most part to tumour detection. Although the use of shorter lived positron emitters (with half-lives of hours) for immuno-PET with MAb fragments is an option, the kinetics of intact MAbs demand the use of long lived positron emitters (half-lives of days) to allow imaging at later time points to obtain maximum information. The two positron emitters that are suitable for imaging of both intact MAbs and MAb fragments are  $^{124}\text{I}$  and  $^{89}\text{Zr}$  [57, 65–67].

A potential area of  $^{124}\text{I}$  application is for quantitative PET in combination with RIT. For this purpose, the radioimmunoconjugates used for immuno-PET and RIT should demonstrate a similar biodistribution, and therefore radionuclides with comparable chemical properties must be chosen. Iodine-124 can be useful in two different immuno-PET/RIT approaches: the radioisotope pair  $^{124}\text{I}/^{131}\text{I}$  can be used for therapy with the  $\beta$  emitter  $^{131}\text{I}$ , and considering the similarities between I and the radiohalogen At, the PET/RIT surrogate pair  $^{124}\text{I}/^{211}\text{At}$  can be used for therapy with the  $\alpha$  emitter  $^{211}\text{At}$ .

The time needed for intact MAb to achieve optimal tumour to non-tumour ratios (typically 2–4 d) adds an additional hurdle to overcome related to the *in vivo* stability of the labelled compounds. While the *in vivo* dehalogenation of radioiodinated radiopharmaceuticals is a well known challenge, an additional source of problems arises for internalized antibodies. MAbs that bind to the cell membrane associated molecules are often internalized into the cell, thereby exposing the MAb to intracellular catabolic processes including lysosomal proteolysis. For radiolabelled MAbs, intracellular processing can result in loss of label from the target cell, with the magnitude of this effect dependent on the nature of the radionuclide and the labelling method. After lysosomal catabolism, radioactivity from radiometalated MAbs is generally trapped in the cell, in contrast to activity from directly radioiodinated MAbs, which escapes from the cell in the form of monoiodotyrosine. To overcome this problem, two strategies are mainly used: residualizing labelling methods that involve labelled templates that are inert to lysosomal digestion and not transported across lysosomal or cell membranes, or templates that after lysosomal catabolism leave charged structures trapped inside the cell. The first strategy, tried in the 1980s and early 1990s with non-metabolizable carbohydrate residues (tyramine-cellobiose and inulin-tyramine), failed for several reasons. The other strategy for residualization of activity within tumour cells has attempted to exploit the fact that exocytosis of catabolites by passive transport across the membrane can be minimized if they are charged species. Lysosomal pH is  $\sim 5$ , and molecules containing basic functionalities would be protonated under these conditions and thus should be trapped within the cells. The feasibility of increasing the tumour retention of MAbs by labelling them with positively charged templates has been demonstrated using the acylating agent [ $^{131}\text{I}$ ]SIPC, which contains a basic N in its structure and was shown to be protonated at lysosomal pH [53]. Several papers with *in vivo* studies were later published [55, 68, 69]. Even if this compound proved the concept and can be considered a model compound for this approach, new molecules based in guanidine structures were later designed in order to improve the intracellular retention. Guanidines have a logarithmic scale of acidity (pKa) of about 13 and thus a substantially higher proportion of these molecules should be protonated than those based on basic pyridine moieties such as SIPC. Biological studies made with the MAb L8A4 labelled with a compound based in guanidine structure, N-succinimidyl 4-guanidinomethyl-3-[\*I] iodobenzoate (SGMIB), showed an intracellular activity 3–4 times higher than the iodogen labelled MAb [70].



This approach for improving stability and cellular internalization might prove very helpful in the molecular imaging of therapeutic strategies based on EGFR blockade. EGFR is a transmembrane tyrosine kinase receptor that regulates cell proliferation, motility and suppression of apoptosis [71]. Its overexpression has been documented in several malignant tumours, such as carcinomas of the breast, urinary bladder and lung, and is associated with poor prognosis [58]. Disruption of EGFR signaling, either by blocking EGFR binding sites on the extracellular domain or by inhibiting intracellular tyrosine kinase activity, can efficiently impede growth of EGFR expressing tumours [72]. MABs that block ligand engagement with the extracellular domain of EGFR and small molecules that block the catalytic domain of EGFR tyrosine kinase were used for that purpose. At clinical level, the MABs cetuximab (C225, Erbitux) and panitumumab (Vectibix) were used for this purpose in patients with metastatic colorectal cancer, and h-R3 (Nimotuzumab) in patients with high grade glioma.

The problem of detecting *in vivo* EGFR with a non-invasive approach by means of labelled MAB against the EGFR is very challenging for two reasons. The first challenge is that the extensive lysosomal metabolism that internalized antibodies suffer can lead to rapid loss of radioactivity from the target cell; the second challenge relates to the slow pharmacokinetics of intact MAB, which typically needs 2–4 d to achieve optimal tumour to non-tumour ratios.

PET tracers would provide very high quality *in vivo* information, in contrast to *ex vivo* molecular techniques, and would also make it possible to obtain global information on all metastatic sites. To achieve this, it is necessary to overcome both problems mentioned above. Using bifunctional active esters as labelling precursors that once reacted will create a labelled template on the MAB that is positively charged at lysosomal pH (improving stability) — like the ones described above labelled with the long half-life positron emitter  $^{124}\text{I}$  — seems to be a very promising strategy for this purpose.

Therefore, a future aim will be development of labelling methods to increase the *in vivo* stability of the radiohalogenated antibody, where the radiohalogen atom is protected in a chemical environment which is much more stable towards *in vivo* metabolism, and also to enhance the retention of the radioisotope in the intracellular compartment of the cell.

The labelling of biomolecules like MABs which undergo a receptor mediated internalization process, such as those specific for EGFR variant III, can lead to rapid loss of radioactivity from the target cell. The development of a labelling method that improves the *in vivo* stability and retention of the radioisotope for internalizing antibodies will further strengthen the application of  $^{124}\text{I}$  labelled biomolecules in diagnosis and molecular imaging and  $^{131}\text{I}$  labelled biomolecules for radiotherapy as well.

## 4. CONCLUSIONS

### 4.1. $^{64}\text{Cu}$ OUTLOOK

Copper-64 is one of several Cu isotopes of interest to nuclear medicine. With a half-life of 12.7 h, it is an important radionuclide for the investigation of biological processes occurring on the timescale of hours to days and for bridging the gap between diagnostic imaging and therapy. Other Cu radioisotopes supplement these capabilities in such a way that the fundamental labelling chemistry can be applied for a range of half-lives and decay characteristics.

The preferred production routes for  $^{64}\text{Cu}$  are well explored and allow for high radionuclidic purity, high yields and, most importantly, high specific activity. High specific activity and the absence of contaminant metals in the  $^{64}\text{Cu}$  formulation are mandatory for most current biomedical applications. Guidance is given in this publication concerning methods to reduce and qualify the cold metal contamination.

The radiochemistry of Cu and its chelation allow late state incorporation of the radioactive tracer in complicated biomolecules. Recently developed chelators allow the use of mild labelling conditions suitable even for large peptides or proteins, while still maintaining sufficient stability *in vivo*.

The optimized production, purification and separation methods have enabled the development of several new agents and preclinical and clinical trials with these compounds are very promising. Future studies will likely involve the further use of very specific molecularly targeted imaging agents to add to the arsenal of tools for the staging, evaluation and assessment of treatment response in many disease areas.

While  $^{64}\text{Cu}$  is not the only longer lived PET radioisotope, it is certainly the most well explored, and can be seen as a good starting point for solid targetry and transition metal radiochemical separations. As such,  $^{64}\text{Cu}$  can make a good research topic even in fairly new PET cyclotron facilities. The primary production route based on (p, n) reactions on  $^{64}\text{Ni}$  requires only very modest particle energy, allowing all medical cyclotrons to obtain clinically applicable yields in a short time.

There is presently rapid development of other radiometals for PET imaging, spanning half-life ranges similar to or longer than the Cu isotopes. It is still too early to decide if some of these isotopes, and most notably  $^{89}\text{Zr}$ , will in the end replace  $^{64}\text{Cu}$  for antibody and other protein imaging. For now,  $^{64}\text{Cu}$  is the most explored and best documented choice for PET applications with half-life requirements beyond 2–3 h.

The biological role of Cu and its very interesting redox behaviour open possibilities for future uses of  $^{64}\text{Cu}$  in the field of tumour hypoxia as a possible imaging marker and perhaps also in direct therapy. The present PET research on  $^{64}\text{Cu}$  imaging is a start to this kind of tumour research.

## 4.2. $^{124}\text{I}$ OUTLOOK

The rationale of using  $^{124}\text{I}$  as a potential radioisotope for PET imaging is based on its long half-life, the well known radiochemistry of I and the variety of radiopharmaceuticals already developed for other radioiodines ( $^{131}\text{I}$  and  $^{123}\text{I}$ ), combined with the superior imaging provided by the PET–CT modality. In particular, there are three main areas that seem to be appropriate for  $^{124}\text{I}$ : immuno-PET, dosimetry where  $^{124}\text{I}$  is used as surrogate of  $^{131}\text{I}$  and/or  $^{211}\text{At}$ , and better imaging with synthetic radiopharmaceuticals already developed and well established for diagnostics, such as m-iodobenzylguanidine (MIBG).

Although PET is a powerful tool for quantitative in vivo tracking of molecules labelled with positron emitting radionuclides,  $^{124}\text{I}$  presents additional challenges in this regard due to its high positron energy and mixed decay, also involving  $\gamma$  radiation. Current generation PET scanners can to a large degree correct for the additional  $\gamma$  and compensate for the higher energy positrons.

Many different types of  $^{124}\text{I}$  radiopharmaceuticals have been developed from synthetic peptides and proteins (MAb) and tested. Some examples of these synthetic radiopharmaceuticals are  $^{124}\text{I}$ -MIBG used in diagnosis of neuroblastoma and pheochromocytoma, hypoxia imaging agents such as  $^{124}\text{I}$ -IAZA (1- $\alpha$ -D-(5-deoxy-5-[ $^{124}\text{I}$ ]iodo-arabinofuranosyl)-2-nitroimidazole), agents for functional imaging of cell proliferation such as  $^{124}\text{I}$ -IUdR (5-[ $^{124}\text{I}$ ]iodo-2'-deoxyuridine), and m- $^{124}\text{I}$ -IPPM (m-[ $^{124}\text{I}$ ]iodophenylpyrrolomorphinan) as a radiotracer for molecular imaging. Some examples of imaging targets for labelled peptides and proteins (MAb) are ovarian cancer, colon cancer, gliomas, HER2 positive tumours and anti-carcinoembryonic antigen (anti-CEA).

In order to strengthen further application of  $^{124}\text{I}$ , two main hurdles must be surmounted: the development of radioiodinated synthons to increase the in vivo stability of  $^{124}\text{I}$  labelled compounds and the development of methods to produce  $^{124}\text{I}$  in large quantities. Considering the likely requirements for use of this radionuclide, the IAEA has identified both problems as potential areas for investigation and, in the framework of this CRP, is promoting development in both areas.

Current methods use the  $^{124}\text{Te}(\text{p}, \text{n})$  reaction, which produces  $^{124}\text{I}$  with very high radionuclidic purity. It can be carried out using a small cyclotron; however, the yields are rather low. Larger amounts of  $^{124}\text{I}$  can be produced via the  $^{125}\text{Te}(\text{p}, 2\text{n})$  reaction, which has been shown to produce a yield five times higher. However, considering the cross-section, this reaction requires an incident energy of at least 21 MeV, which only medium sized cyclotrons can provide. This method of production requires developing high current  $\text{TeO}_2$  targets and optimizing the procedure with respect to minimizing the  $^{125}\text{I}$  impurity level. Other production routes are also available, some based on  $\alpha$ -particles and Sb target material, and this may be a route of choice for a number of medium sized cyclotrons.

The future role of  $^{124}\text{I}$  in nuclear medicine is still somewhat uncertain. However, the basic principles of its use are well established, and it has the tremendous advantage that it can be shipped regionally and even internationally without prohibitive decay losses. The routine availability of  $^{124}\text{I}$  in the future could still drive the development of new applications. However, it should be remembered that this isotope has a special radiotoxicity profile of importance both to the working environment and to patients. It is therefore suggested that production of pure  $^{124}\text{I}$  for exploration and exploitation be pursued only at experienced research facilities with well established radiochemical practices.

## REFERENCES

- [1] LEDERER, C.M., SHIRLEY, V.S., BROWNE, E., Table of Isotopes, 7th ed, Wiley, New York (1978).
- [2] NATIONAL NUCLEAR DATA CENTRE, NuDat2 database (2015), <http://www.nndc.bnl.gov/nudat2/>
- [3] McCARTHY, D.W., et al, Efficient production of high specific activity  $^{64}\text{Cu}$  using a biomedical cyclotron, *Nucl. Med. Biol.* **24** (1997) 35–43.
- [4] OBATA, A., et al., Production of therapeutic quantities of  $^{64}\text{Cu}$  using a 12 MeV cyclotron, *Nucl. Med. Biol.* **30** (2003) 535–539.
- [5] HETHERINGTON, E.L., SORBY, P.J., CAMAKARIS, J., The preparation of high specific activity copper-64 for medical diagnosis, *Int. J. Rad. Appl. Instrum. A* **37** (1986) 1242–1243.
- [6] KOZEMPEL, J., et al., A novel method for n.c.a.  $^{64}\text{Cu}$  production by the  $^{64}\text{Zn}(\text{d},2\text{p})^{64}\text{Cu}$  reaction and dual ion-exchange column chromatography, *Radiochim. Acta* **95** (2007) 75–80.
- [7] NICKLES, R.J., Production of a broad range of radionuclides with an 11 MeV proton cyclotron, *J. Label. Compd. Radiopharm.* **30** (1991) 120–121.
- [8] ZWEIT, J., SMITH, A.M., DOWNEY, S., SHARMA, H.L., Excitation functions for deuteron induced reactions in natural nickel: Production of no carrier added  $^{64}\text{Cu}$  from enriched  $^{64}\text{Ni}$  target for positron emission tomography, *Appl. Radiat. Isot.* **42** (1991) 193–197.
- [9] INTERNATIONAL ATOMIC ENERGY AGENCY, Cyclotron Produced Radionuclides: Physical Characteristics and Production Methods, Technical Report Series No. 468, IAEA, Vienna, (2009).
- [10] SZELECSENYI, F., et al., Investigation of the  $^{66}\text{Zn}(\text{p},2\text{pn})^{64}\text{Cu}$  and  $^{68}\text{Zn}(\text{p},\text{x})^{64}\text{Cu}$  nuclear processes up to 100 MeV: Production of  $^{64}\text{Cu}$ , *Nucl. Instrum. Methods in Phys. Res. B* **240** (2005) 625.
- [11] LE VAN SO, PELLEGRINI, P., KATSIFIS, A., HOWSE, J., GREGURIC, I., Radiochemical separation and quality assessment for the  $^{68}\text{Zn}$  target based  $^{64}\text{Cu}$  radioisotope production, *J. Radioanal. Nucl. Chem.* **277** (2008) 451–466.
- [12] AVILA-RODRIGUEZ, M.A., Low Energy Cyclotron Production of Multivalent Transition Metals for PET Imaging and Therapy, PhD Thesis, Univ. of Wisconsin (2007).
- [13] INTERNATIONAL ATOMIC ENERGY AGENCY, Standardized High Current Solid Targets for Cyclotron Production of Diagnostic and Therapeutic Radionuclides, Technical Report Series No. 432, IAEA, Vienna (2004).
- [14] AVILA-RODRIGUEZ, M.A., NYE, J.A., NICKLES, R.J., Simultaneous production of high specific activity  $^{64}\text{Cu}$  and  $^{61}\text{Co}$  with 11.4 MeV protons on enriched  $^{64}\text{Ni}$ , *Appl. Radiat. Isot.* **65** (2007) 1115–1120.
- [15] KUME, M., et al., A semi-automated system for the routine production of copper-64, *Appl. Radiat. Isot.* **70** (2012) 1803–1806.
- [16] STRELOW, F.W.E., VICTOR, A.H., VAN ZYL, C.R., ELOFF, C., Distribution coefficients and cation exchange behaviour of elements in hydrochloric acid-acetone, *Anal. Chem.* **43** (1971) 870–876.
- [17] ANDEREGG, G., ARNAUD-NEU, F., DELGADO, R., FELCMAN, J., POPOV, K., Critical evaluation of stability constants of metal complexes of complexones for biomedical and environmental applications, *Pure Appl. Chem.* **77** (2005) 1445–1495.
- [18] TAKAHASHI, N., et al., Evaluation of  $^{62}\text{Cu}$  labeled diacetyl-bis(N4-methylthio-semicarbazone) as a hypoxic tissue tracer in patients with lung cancer, *Ann. Nucl. Med.* **14** 5 (2000) 323–328.
- [19] WADAS, T.J., WONG, E.H., WEISMAN, G.R., ANDERSON, C.J., Coordinating radiometals of copper, gallium, indium, yttrium, and zirconium for PET and SPECT imaging of disease, *Chem. Rev.* **110** (2010) 2858–2902.
- [20] JURISSON, S., CUTLER, C., SMITH, S.V., Radiometal complexes: Characterization and relevant in vitro studies, *Q. J. Nucl. Med. Mol. Imaging* **52** 3 (2008) 222–234.
- [21] WÄNGLER, B., SCHIRRMACHER, R., BARTENSTEIN, P., WÄNGLER, C., Chelating agents and their use in radiopharmaceutical sciences, *Mini Rev. Med. Chem.* **11** (2011) 968–983.
- [22] SHOKEEN, M., WADAS, T.J., The development of copper radiopharmaceuticals for imaging and therapy, *Med. Chem.* **7** 5 (2011) 413–429.
- [23] WADAS, T.J., WONG, E.H., WEISMAN, G.R., ANDERSON, C.J., Copper chelation chemistry and its role in copper radiopharmaceuticals, *Curr. Pharm. Des.* **13** 1 (2007) 316.
- [24] RAMOGIDA, C.F., ORVIG, C., Tumour targeting with radiometals for diagnosis and therapy, *Chem. Commun.* **49** (2013) 4720–4739.
- [25] JIN, Z.H., et al., Noninvasive visualization and quantification of tumor  $\alpha\text{V}\beta 3$  integrin expression using a novel positron emission tomography probe,  $^{64}\text{Cu}$ -cyclam-RAFT-c-(RGDfK)-4, *Nucl. Med. Biol.* **38** (2011) 529–540.
- [26] CHANG, A.J., SOHN, R., LU, Z.H., ARBEIT, J.A., LAPPI, S.E., Detection of rapalog-mediated therapeutic response in renal cancer xenografts using  $^{64}\text{Cu}$ -bevacizumab ImmunoPET, *PLoS One* (2013).
- [27] FUJIBAYASHI, Y., et al., Copper-62-ATSM: A new hypoxia imaging agent with high membrane permeability and low redox potential, *J. Nucl. Med.* **38** (1997) 1155–1160.
- [28] IKAWA, M., et al., PET imaging of redox and energy states in stroke-like episodes of MELAS, *Mitochondrion* **9** 2 (2009) 144–148.

- [29] IKAWA, M., et al., Evaluation of striatal oxidative stress in patients with Parkinson's disease using [ $^{62}\text{Cu}$ ]ATSM PET, *Nucl. Med. Biol.* **38** (2011) 945–951.
- [30] YOSHII, Y., et al., Copper-64-diacetyl-bis (N4-methylthiosemicarbazone) accumulates in rich regions of CD133+ highly tumorigenic cells in mouse colon carcinoma, *Nucl. Med. Biol.* **37** (2010) 395–404.
- [31] YOSHII, Y., et al., Internal radiotherapy with copper-64-diacetyl-bis (N4-methylthiosemicarbazone) reduces CD133+ highly tumorigenic cells and metastatic ability of mouse colon carcinoma, *Nucl. Med. Biol.* **38** (2011) 151–157.
- [32] PFEIFER, A., et al., Clinical PET of neuroendocrine tumors using Cu-64-DOTATATE: First-in-humans study, *J. Nucl. Med.* **53** (2012) 1207–1215.
- [33] KOEHLER, L., GAGNON, K., McQUARRIE, S., WUEST, F., Iodine-124: A promising positron emitter for organic PET chemistry, *Molecules* **15** (2010) 2686–2718.
- [34] ASLAM, M.N., SUDAR, S., HUSSAIN, M., MALIK, A.A., QAIM, S.M., Evaluation of excitation functions of  $^3\text{He}$ - and  $\alpha$ -particle induced reactions on antimony isotopes with special relevance to the production of iodine-124, *Appl. Radiat. Isot.* **69** (2011) 94–104.
- [35] HASSAN, K.F., QAIM, S.M., SALEH, Z.A., COENEN, H.H., Alpha-particle induced reactions on  $^{\text{nat}}\text{Sb}$  and  $^{121}\text{Sb}$  with particular reference to the production of the medically interesting radionuclide  $^{124}\text{I}$ , *Appl. Radiat. Isot.* **64** (2006) 101–109.
- [36] HADDAD, F., et al., ARRONAX a high-energy and high-intensity cyclotron for nuclear medicine, *Eur. J. Nucl. Med. Mol. Imaging* **35** (2008) 1377–1387.
- [37] ZALUTSKY, M.R., POZZI, O.R., Radioimmunotherapy with alpha-particle emitting radionuclides, *Q. J. Nucl. Med. Mol. Imaging* **48** (2004) 289–296.
- [38] ZALUTSKY, M.R., REARDON, D.A., POZZI, O.R., VAIDYANATHAN, G., BIGNER, D.D., Targeted  $\alpha$ -particle radiotherapy with  $^{211}\text{At}$ -labeled monoclonal antibodies, *Nucl. Med. Biol.* **34** (2007) 779–785.
- [39] CHÉREL, M., DAVODEAU, F., KRAEBER-BODÉRE, F., CHATAL, J.F., Current status and perspectives in alpha radioimmunotherapy, *Q. J. Nucl. Med. Mol. Imaging* **50** (2006) 322–329.
- [40] QAIM, S.M., et al., Some optimisation studies relevant to the production of high-purity  $^{124}\text{I}$  and  $^{120}\text{I}_g$  at a small-sized cyclotron, *Appl. Radiat. Isot.* **58** (2003) 69–78.
- [41] SHEH, Y., et al., Low energy cyclotron production and chemical separation of “no carrier added” iodine-124 from a reusable, enriched tellurium-124 dioxide/aluminum oxide solid solution target, *Radiochim. Acta* **88** (2000) 169–173.
- [42] KANG, S.-J.L., Sintering: Densification, Grain Growth and Microstructure, Elsevier Butterworth-Heinemann, Burlington, MA (2005).
- [43] WU-SHUNG FU, HSIN-CHIEN HUANG, Effects of a random porosity model on heat transfer performance of porous media, *Int. J. Heat Mass Trans.* **42** (1999) 13–25.
- [44] PEI-XUE JIANG, MENG LI, TIAN-JIAN LU, LEI YU, ZE-PEI REN, Experimental research on convection heat transfer in sintered porous plate channels, *Int. J. Heat Mass Trans.* **47** (2004) 2085–2096.
- [45] DEWANJEE, M.K., Radioiodination: Theory, Practice, and Biomedical Applications, 1st edn, Kluwer Academic Publishers, Dordrecht (1992).
- [46] SCOTT WILBUR, D., Radiohalogenation of proteins: An overview of radionuclides, labeling methods and reagents for conjugate labeling, *Bioconjugate Chem.* **3** (1992) 433–470.
- [47] VÉRTES, A., NAGY, S., KLENCSÁR, Z., “Radioiodination chemistry and radioiodinated compounds”, *Handbook of Nuclear Chemistry, Vol. 4: Radiochemistry and Radiopharmaceutical Chemistry in Life Sciences*, 1st edn, Springer, New York (2003) 257–277.
- [48] REIST, C.J., et al., Tumor-specific anti-epidermal growth factor receptor variant III monoclonal antibodies: Use of the tyramine-cellobiose radioiodination method enhances cellular retention and uptake in tumor xenografts, *Cancer Res.* **55** (1995) 4375–4382.
- [49] ALI, S.A., et al., Improving the tumor retention of radioiodinated antibody: Aryl carbohydrate adducts, *Cancer Res.* **50** (1990) 783s–788s.
- [50] STEIN, R., GOLDENBERG, D.M., THORPE, S.R., BASU, A., JULES MATTES, M., Effects of radiolabeling monoclonal antibodies with a residualizing iodine radiolabel on the accretion of radioisotope in tumors, *Cancer Res.* **55** (1995) 3132–3139.
- [51] PITTMAN, R.C., et al., A radioiodinated, intracellularly trapped ligand for determining the sites of plasma protein degradation in vivo, *Biochem. J.* **212** (1983) 791–800.
- [52] SCHILLINGA, U., et al., Design of compounds having enhanced tumour uptake, using serum albumin as a carrier — part II. In vivo studies, *Int. J. Rad. Appl. Instrum. B* **19** (1992) 685–695.
- [53] GARG, S., GARG, P.K., ZALUTSKY, M.R., N-succinimidyl 5-(trialkylstannyl)-3-pyridinecarboxylates: A new class of reagents for protein radioiodination, *Bioconjugate Chem.* **2** (1991) 50–56.
- [54] REIST, C.J., GARG, P.K., ALSTON, K.L., BIGNER, D.D., ZALUTSKY, M.R., Radioiodination of internalizing monoclonal antibodies using N-succinimidyl 5-iodo-3-pyridinecarboxylate, *Cancer Res.* **56** (1996) 4970–4977.
- [55] REIST, C.J., ARCHER, G.E., WIKSTRAND, C.J., BIGNER, D.D., ZALUTSKY, M.R., Improved targeting of an antiepidermal growth factor receptor variant III monoclonal antibody in tumor xenografts after labeling using N-succinimidyl 5-iodo-3-pyridinecarboxylate, *Cancer Res.* **57** (1997) 1510–1515.

- [56] FOULON, C.F., WELSH, P.C., BIGNER, D.D., ZALUTSKY, M.R., Positively charged templates for labeling internalizing antibodies: Comparison of N-succinimidyl 5-iodo-3-pyridinecarboxylate and the D-amino acid peptide KRYRR, *Nucl. Med. Biol.* **28** (2001) 769–777.
- [57] VEREL, I., VISSER, G.W.M., VAN DONGEN, G.A., The promise of immuno-PET in radioimmunotherapy, *J. Nucl. Med.* **46** (2005) 164s–171s.
- [58] NICHOLSON, R.I., GEE, J.M., HARPER, M., EGFR and cancer prognosis, *Eur. J. Cancer* **37** (2001) s9–s15.
- [59] ZHU, Z., Targeted cancer therapies based on antibodies directed against epidermal growth factor receptor: Status and perspective, *Acta Pharmacol. Sin.* **28** (2007) 1476–1493.
- [60] DASSONVILLE, O., BOZEC, A., FISCHER, J.L., MILANO, G., EGFR targeting therapies Monoclonal antibodies versus tyrosine kinase inhibitors: Similarities and differences, *Critical Rev. Oncol./Hematol.* **62** (2007) 53–61.
- [61] HOLTZMAN, E., *Lysosomes*, Plenum Press, New York (1989) 95–100.
- [62] HERZOG, H., TELLMANN, L., SCHOLTEN, B., COENEN, H.H., QAIM, S.M., PET imaging problems with the non-standard positron emitters <sup>86</sup>Y and <sup>124</sup>I, *Q. J. Nucl. Med. Mol. Imaging* **52** (2008) 159–165.
- [63] LAFOREST, R., LIU, X., Image quality with non-standard nuclides in PET, *Q. J. Nucl. Med. Mol. Imaging* **52** (2008) 151–158.
- [64] BELOV, V., et al., Iodine-124 as a label for pharmacological PET imaging, *Mol. Pharm.* **8** (2011) 736–747.
- [65] VAN DONGEN, G.A., VISSER, G.W.M., LUB-DE HOOGE, M.N., DE VRIES, E.G., PERK, L.R., Immuno-PET: A navigator in monoclonal antibody development and applications, *Oncologist* **12** (2007) 1379–1389.
- [66] FISCHER, G., SEIBOLD, U., SCHIRRMACHER, R., WÄNGLER, B., WÄNGLER, C., <sup>89</sup>Zr, a radiometal nuclide with high potential for molecular imaging with PET: Chemistry, applications and remaining challenges, *Molecules* **18** (2013) 6469–6490.
- [67] VAN DONGEN, G.A.M.S., VOSJAN, M.J.W.D., Immuno-positron emission tomography: Shedding light on clinical antibody therapy, *Cancer Biother. Radiopharm.* **25** (2010) 375–385.
- [68] GARG, S., et al., Radioiodination of a monoclonal antibody using N-succinimidyl 5-iodo-3-pyridinecarboxylate, *Nucl. Med. Biol.* **20** (1993) 835–842.
- [69] GARG, P.K., ALSTON, K.L., ZALUTSKY, M.R., Catabolism of radioiodinated murine monoclonal antibody F(ab')<sub>2</sub> fragment labeled using N-succinimidyl 3-iodobenzoate and Iodogen methods, *Bioconjugate Chem.* **6** (1995) 493–501.
- [70] VAIDYANATHAN, G., AFFLECK D.J., LI, J., WELSH, P., ZALUTSKY, M.R., A polar substituent-containing acylation agent for the radioiodination of internalizing monoclonal antibodies: N-succinimidyl 4-guanidinomethyl-3-[<sup>131</sup>I]iodobenzoate ([<sup>131</sup>I]SGMIB), *Bioconjugate Chem.* **12** (2001) 428–438.
- [71] YARDEN, Y., SLIWKOWSKI, M.X., Untangling the ErbB signalling network, *Nat. Rev. Mol. Cell Biol.* **2** (2001) 127–137.
- [72] CASTILLO, L., et al., Pharmacological background of EGFR targeting, *Ann. Oncol.* **15** (2004) 1007–1012.





## Annex

### CONTENTS OF THE ATTACHED CD-ROM

#### SUMMARY

#### REPORTS BY THE PARTICIPANTS OF THE COORDINATED RESEARCH PROJECT

Development of the Process for Routine Production of  $^{64}\text{Cu}$  by Two Different Methods: Simultaneous Production of  $^{64}\text{Cu}$ - $^{67}\text{Ga}$  Using  $^{68}\text{Zn}$  Target at 27–16 MeV of Protons and From Natural-Zinc Target at E-Max  $\leq 34$  MeV and E-Min  $\geq 22$ –24 MeV

*O.R. Pozzi, M. Sanchez, M.C. Fornaciari Iljadica, M.C. Ali Santoro, P.A. Lopez, L.L. Santarén, S.E. Siri, D. Ortega, F. Corral, G. Peña, A. Kolosov, N. Gonzalez, C. Rocco*

A Feasibility Study for Routine Production of  $^{124}\text{I}$  by ( $\alpha$ ,xn) Reactions on  $^{121}\text{Sb}$  and  $^{121}\text{Sb}$  at the IEN's CV-28 Cyclotron  
*G.R. Santos, A.M.S. Braghirolli*

Development of Procedure for  $^{64}\text{Cu}$  Production on Cyclone-30 Cyclotron  
*Jixin Liang, Yuqing Chen, Guang Li, Yijia Shen, Xuesong Deng, Laicheng Qiao, Zhifu Luo*

Preparation and Biodistribution of  $^{64}\text{Cu}$ -ATSM  
*Jixin Liang, Hongyi Luo, Feihu Guo, Yuqing Chen, Chunhui Yang, Xuesong Deng, Zhifu Luo*

Preparation and Biological Evaluation of  $^{64}\text{Cu}$  Labeled Somatostatin Conjugates  
*Jixin Liang, Zhenyi Han, Yuqing Chen, Guang Li, Xuesong Deng, Hongyu Li, Zhifu Luo*

Production and Utilization of Emerging Positron Emitters for Medical Applications with Focus on Copper-64  
*M. Jensen, D.R. Elema, G. Severin*

Production and Utilization of  $^{64}\text{Cu}$  at Turku PET Centre  
*J. Rajander, Cheng-Bin Yim, V.-V. Elomaa, J. Schlesinger, O. Solin*

Production of Copper-64 Using Deuteron Beams and Application to PET Imaging Projects such as Cu-ATSM to Study Hypoxia in Tumor  
*C. Alliot, N. Audouin, J. Barbet, A.C. Bonraisin, V. Bossé, C. Bourdeau, M. Bourgeois, A. Faivre-Chauvet, M. Cherel, J.F. Gestin, S. Gouard, F. Haddad, J. Laizé, P. Le Saëc, N. Michel, M. Mokili, V. Potiron, H. Rajerison, S. Supiot*

Production of  $^{64}\text{Cu}$  and Synthesis of  $^{64}\text{Cu}$ -ATSM  
*G. Cicoria, D. Pancaldi, F. Lodi, C. Malizia, S. Costa, M. Marengo, S. Boschi*

Production and Utilization of  $^{64}\text{Cu}$   
*Y. Fujibayashi*

Production and Utilization of Emerging Positron Emitters for Medical Applications with a Focus on Copper-64 in the Republic of Korea  
*Kyo Chul Lee, Hyun Park, Ho Seung Song, Jong Seo Chai*

Production and Utilization of  $^{124}\text{I}$  for Medical Applications  
*F. Al-Rumayan, S. Al-Yanbawi, J. Schneider, A. Al-Gaith, I. Al-Jammaz*

<sup>64</sup>Cu Production for Medical Application in Syrian Arab Republic

*A.H. Al Rayyes*

Production and Utilisation of Emerging Positron Emitters for Medical Applications with a Focus on Copper-64 and Iodine-124: Eczacıbaşı Monrol Experience

*A.A. Soylu*

Production of Orphan Radionuclides at the University of Wisconsin: in Search of a Sustainable, Niche Position

*J.W. Engle, T.E. Barnhart, G.W. Severin, M.A. Avila-Rodrigues, K. Gagnon, J. Silkanen, H.F. Valdovinos, S. Graves, R. Hernandez, R.J. Nickles*

Progress on the Production and Specific Activity Determination of Copper-64

*S.E. Lapi, M.J. Welch*

LIST OF CRP PARTICIPANTS

## ABBREVIATIONS

ATSM	diacetyl-bis(N <sup>4</sup> -methylthiosemicarbazone)
CRP	coordinated research project
CT	computed tomography
EC	electron capture
DOTA	1,4,7,10-tetraazacyclododecane-1,4,7,10-tetraacetic acid
DOTATATE	DOTA-octreotate
EGFR	epidermal growth factor receptor
ESA	effective specific activity
<sup>18</sup> F-FDG	2-[ <sup>18</sup> F]fluoro-2-deoxy-D-glucose
GMP	good manufacturing practices
HPLC	high performance liquid chromatography
ICP-OES	inductively coupled plasma optical emission spectrometry
MAb	monoclonal antibody
NODAGA	1,4,7-triazacyclononane,1-glutaric acid-4,7-acetic acid
NOTA	2,2',2''-(1,4,7-triazanonane-1,4,7-triyl)triacetic acid
PET	positron emission tomography
RIT	radioimmunotherapy
SEM	scanning electron microscopy
SIPC	N-succinimidyl 5-radioiodo-pyridine-3-carboxylate
SPECT	single photon emission computed tomography
SRIM	Stopping and Range of Ions in Matter
TETA	2,2',2'',2'''-(1,4,8,11-tetraazacyclotetradecane-1,4,8,11-tetrayl)tetraacetic acid
TLC	thin-layer chromatography
VEGF	vascular endothelial growth factor



## CONTRIBUTORS TO DRAFTING AND REVIEW

Al Rayyes, A.H.	Atomic Energy Commission of Syria, Syrian Arab Republic
Al-Rumayan, F.	King Faisal Specialist Hospital & Research Centre, Saudi Arabia
Barbet, J.	Cancer Research Center Nantes-Angers, France
Chai, Jong-Seo	Sungkyunkwan University, Republic of Korea
Cicoria, G.	Sant'Orsola-Malpighi Polyclinic, Italy
Fujibayashi, Y.	National Institute of Radiological Sciences, Japan
Haji-Saied, M.	International Atomic Energy Agency
Jensen, M.	Hevesy Laboratory, Technical University of Denmark, Denmark
Lapi, S.	Washington University School of Medicine, United States of America
Liang, Jixin	China Institute of Atomic Energy, China
Nickles, R.J.	University of Wisconsin, Madison, United States of America
Pozzi, O.	National Atomic Energy Commission, Argentina
Rajander, J.	Turku PET Centre, Finland
Santos, G.R.	National Nuclear Energy Commission, Brazil
Soylu, A.	Eczacıbaşı-Monrol Nuclear Products Co., Turkey
Wuest, F.	Cross Cancer Institute, Canada

### Research Coordination Meetings

Vienna, Austria: 31 May–4 June 2010, 1–5 July 2013  
Istanbul, Turkey: 31 October–4 November 2011





# IAEA

International Atomic Energy Agency

No. 24

## ORDERING LOCALLY

In the following countries, IAEA priced publications may be purchased from the sources listed below or from major local booksellers.

Orders for unpriced publications should be made directly to the IAEA. The contact details are given at the end of this list.

### BELGIUM

#### ***Jean de Lannoy***

Avenue du Roi 202, 1190 Brussels, BELGIUM

Telephone: +32 2 5384 308 • Fax: +32 2 5380 841

Email: [jean.de.lannoy@euronet.be](mailto:jean.de.lannoy@euronet.be) • Web site: <http://www.jean-de-lannoy.be>

### CANADA

#### ***Renouf Publishing Co. Ltd.***

22-1010 Polytek Street, Ottawa, ON K1J 9J1, CANADA

Telephone: +1 613 745 2665 • Fax: +1 643 745 7660

Email: [order@renoufbooks.com](mailto:order@renoufbooks.com) • Web site: <http://www.renoufbooks.com>

#### ***Bernan Associates***

4501 Forbes Blvd., Suite 200, Lanham, MD 20706-4391, USA

Telephone: +1 800 865 3457 • Fax: +1 800 865 3450

Email: [orders@bernana.com](mailto:orders@bernana.com) • Web site: <http://www.bernana.com>

### CZECH REPUBLIC

#### ***Suweco CZ, s.r.o.***

SESTUPNÁ 153/11, 162 00 Prague 6, CZECH REPUBLIC

Telephone: +420 242 459 205 • Fax: +420 284 821 646

Email: [nakup@suweco.cz](mailto:nakup@suweco.cz) • Web site: <http://www.suweco.cz>

### FRANCE

#### ***Form-Edit***

5 rue Janssen, PO Box 25, 75921 Paris CEDEX, FRANCE

Telephone: +33 1 42 01 49 49 • Fax: +33 1 42 01 90 90

Email: [fabien.boucard@formedit.fr](mailto:fabien.boucard@formedit.fr) • Web site: <http://www.formedit.fr>

#### ***Lavoisier SAS***

14 rue de Provigny, 94236 Cachan CEDEX, FRANCE

Telephone: +33 1 47 40 67 00 • Fax: +33 1 47 40 67 02

Email: [livres@lavoisier.fr](mailto:livres@lavoisier.fr) • Web site: <http://www.lavoisier.fr>

#### ***L'Appel du livre***

99 rue de Charonne, 75011 Paris, FRANCE

Telephone: +33 1 43 07 43 43 • Fax: +33 1 43 07 50 80

Email: [livres@appeldulivre.fr](mailto:livres@appeldulivre.fr) • Web site: <http://www.appeldulivre.fr>

### GERMANY

#### ***Goethe Buchhandlung Teubig GmbH***

Schweitzer Fachinformationen

Willstätterstrasse 15, 40549 Düsseldorf, GERMANY

Telephone: +49 (0) 211 49 874 015 • Fax: +49 (0) 211 49 874 28

Email: [s.dehaan@schweitzer-online.de](mailto:s.dehaan@schweitzer-online.de) • Web site: <http://www.goethebuch.de>



## HUNGARY

### ***Librotrade Ltd., Book Import***

Pesti ut 237. 1173 Budapest, HUNGARY

Telephone: +36 1 254-0-269 • Fax: +36 1 254-0-274

Email: books@librotrade.hu • Web site: <http://www.librotrade.hu>

## INDIA

### ***Allied Publishers***

1<sup>st</sup> Floor, Dubash House, 15, J.N. Heredi Marg, Ballard Estate, Mumbai 400001, INDIA

Telephone: +91 22 4212 6930/31/69 • Fax: +91 22 2261 7928

Email: alliedpl@vsnl.com • Web site: <http://www.alliedpublishers.com>

### ***Bookwell***

3/79 Nirankari, Delhi 110009, INDIA

Telephone: +91 11 2760 1283/4536

Email: bkwell@nde.vsnl.net.in • Web site: <http://www.bookwellindia.com>

## ITALY

### ***Libreria Scientifica "AEIOU"***

Via Vincenzo Maria Coronelli 6, 20146 Milan, ITALY

Telephone: +39 02 48 95 45 52 • Fax: +39 02 48 95 45 48

Email: info@libreriaaeiou.eu • Web site: <http://www.libreriaaeiou.eu>

## JAPAN

### ***Maruzen Co., Ltd.***

1-9-18 Kaigan, Minato-ku, Tokyo 105-0022, JAPAN

Telephone: +81 3 6367 6047 • Fax: +81 3 6367 6160

Email: journal@maruzen.co.jp • Web site: <http://maruzen.co.jp>

## RUSSIAN FEDERATION

### ***Scientific and Engineering Centre for Nuclear and Radiation Safety***

107140, Moscow, Malaya Krasnoselskaya st. 2/8, bld. 5, RUSSIAN FEDERATION

Telephone: +7 499 264 00 03 • Fax: +7 499 264 28 59

Email: secnrs@secnrs.ru • Web site: <http://www.secnrs.ru>

## UNITED KINGDOM

### ***The Stationery Office Ltd. (TSO)***

St. Crispins House, Duke Street, Norwich, NR3 1PD, UNITED KINGDOM

Telephone: +44 (0) 333 202 5070

Email: customer.services@tso.co.uk • Web site: <http://www.tso.co.uk>

## UNITED STATES OF AMERICA

### ***Bernan Associates***

4501 Forbes Blvd., Suite 200, Lanham, MD 20706-4391, USA

Telephone: +1 800 865 3457 • Fax: +1 800 865 3450

Email: orders@bernan.com • Web site: <http://www.bernan.com>

### ***Renouf Publishing Co. Ltd.***

812 Proctor Avenue, Ogdensburg, NY 13669-2205, USA

Telephone: +1 888 551 7470 • Fax: +1 888 551 7471

Email: orders@renoufbooks.com • Web site: <http://www.renoufbooks.com>

## **Orders for both priced and unpriced publications may be addressed directly to:**

IAEA Publishing Section, Marketing and Sales Unit

International Atomic Energy Agency

Vienna International Centre, PO Box 100, 1400 Vienna, Austria

Telephone: +43 1 2600 22529 or 22530 • Fax: +43 1 2600 29302

Email: sales.publications@iaea.org • Web site: <http://www.iaea.org/books>





INTERNATIONAL ATOMIC ENERGY AGENCY  
VIENNA  
ISBN 978-92-0-109615-9  
ISSN 2413-9556